SCUOLA NORMALE SUPERIORE

Academic Year 2015-2016

PhD Course in Neurobiology

Studying and modulating post-stroke neuroplasticity to improve motor recovery

Author

Claudia Alia

Advisor

Prof. Matteo Caleo, PhD

Internal Supervisor

Prof. Antonino Cattaneo, PhD

Abstract

Limited restoration of motor function occurs spontaneously during a plastic time window after stroke. A deeper understanding of post-stroke plasticity is critical to devise more effective pharmacological and rehabilitative treatments.

Here, I have characterized the spontaneous evolution after a photothrombotic lesion in mice, both in terms of motor deficit and plasticity in the perilesional cortex. In generalized motor tasks such as the Gridwalk and Schallert Cylinder test, motor deficits were stable for at least 30 days after photothrombotic stroke in the Caudal Forelimb Area (CFA). The skilled reaching test, performed once a week, showed a trend for spontaneous improvement over time in the number of correct graspings. However, kinematic analysis, evaluated by means of an innovative semi-automated tool, revealed a persistent alterations in grasping movements, pointing to the development of compensatory strategies.

The perilesional cortex has been proposed as the area mediating functional recovery. I found a reorganization of the motor maps in sensorimotor cortex around to the lesion. Particularly, I observed a significant shrinkage of the forelimb area, in favour of hindlimb representation using Intracortical Microstimulation (ICMS). Moreover, neuroanatomical markers, previously characterized in the literature as “neuroplasticity brakes” (i.e. Perineuronal nets, Parvalbumin- and Somatostatin-positive cells) spontaneously decrease after stroke, suggesting an enhancement of the potential for plastic rearrangements. Altogether these results, suggest a spontaneous attempt to reopen a critical period characterized by sprouting and plasticity phenomena, that needs to be amplified and properly guided for maximizing recovery.

The GABAergic system is one of the key modulators of plasticity in the brain, and its role has been amply studied in relation to opening and closure of the “critical period” in sensory cortices during development. To test whether reductions in GABAergic signalling were causally involved in motor improvements, we treated animals during an early post-stroke period with a benzodiazepine inverse agonist, which impairs $GABA_A$ receptor function. We found that hampering $GABA_A$ signalling led to significant restoration of function in general motor tests such as the gridwalk and the pellet reaching tasks, with no significant impact on the kinematics of reaching movements. Improvements were persistent as they remained detectable about three weeks after treatment.

Using electrophysiological recordings I found an electrical imbalance between the two hemispheres. In particular, contralesional motor cortex was found to exert an enhanced transcallosal inhibition over the spared, perilesional tissue. Silencing the healthy hemisphere

using cortical infusion of Botulinum Neurotoxin E, partially improved motor recovery in the gridwalk test.

We then established a rehabilitation protocol that combined intensive and highly repeatable exercise of the mouse forelimb with a robotic platform with reversible inactivation of the healthy, contralesional motor cortex. We found that such treatment promoted recovery in both Gridwalk and Schallert Cylinder tests and in end point measures during Skilled reaching test. Remarkably, the combined therapy also restores pre-lesion movement patterns during reaching movement, as evaluated by kinematic analysis. Furthermore, such rehabilitated animals showed a more plastic perilesional cortex, with an additional significant decrease in plasticity brakes.

Introduction

1. Stroke in Humans

1.1 General definitions

Stroke is the term to indicate a sudden cerebrovascular dysfunction leading to symptoms related to focal deficits and/or global brain function and lasting more than 24 hours (Mackay and Mensah, 2004).

Brain function, in fact, is strictly dependent on a constant supply of oxygen and glucose, normally assured by blood circulation. A sudden block of such supply determines suppression of neural function within 20-60 seconds, primarily due to interference with synaptic functions (Hofmeijer and Van Putten, 2012). If the event is limited in time, blood deprivation can cause only reversible damage but when the circulation is not promptly restored, the damage becomes permanent (Krnjević, 2008).

The insufficiency of blood supply to an organ is called *ischemia*, a term which indicates not only a lack of oxygen (*anoxia*) and glucose but also a block of removal of potentially toxic metabolites.

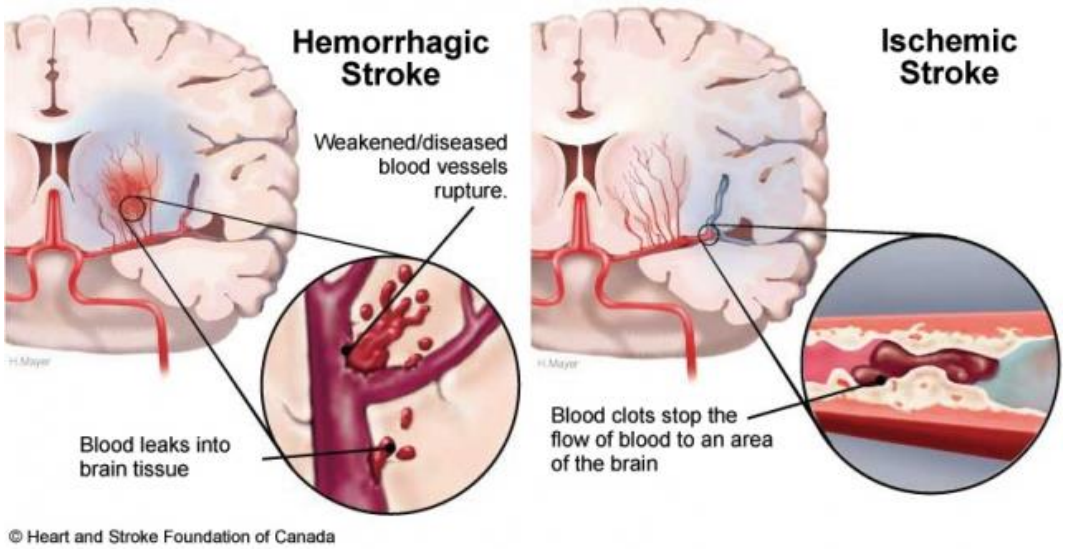

Figure 1 Schematic representation of the two principal types of stroke. Hemorrhagic stroke (left) is caused by a vessel rupture while ischemic stroke (right) is the consequence of blood vessel occlusion. Taken from http://heart.arizona.edu/

When a brain ischemia is so prolonged to cause the death of neurons and other cells, it is called *cerebral infarction* or *ischemic stroke* and it represents about 80% of strokes (American Heart Association. *Heart disease and stroke statistics)*.

There are also other subtypes of stroke as *hemorrhagic stroke*, that is due to a rupture of a cerebral blood vessel (**Figure 1**), and Transient ischemic attack (TIA), a short duration event (few minutes) that represents an important risk factor because in the 33% of cases it is followed by ischemic stroke event.

However, *ischemic stroke* remains the most frequent and it represents the second single most common cause of death in Europe, with almost 1.1 million deaths in Europe each year ("World Heart Day: New European statistics released on heart disease and stroke," n.d., European Heart Network, www.escardio.org) and up to now, an estimated 6.6 million Americans ≥20 years of age have had a stroke (extrapolated to 2012 by use of NHANES 2009–2012 data); moreover, projections show that by 2030, an additional 3.4 million people aged ≥18 years will have had a stroke (Mozaffarian et al., 2014).

1.2 The Ischemic Penumbra

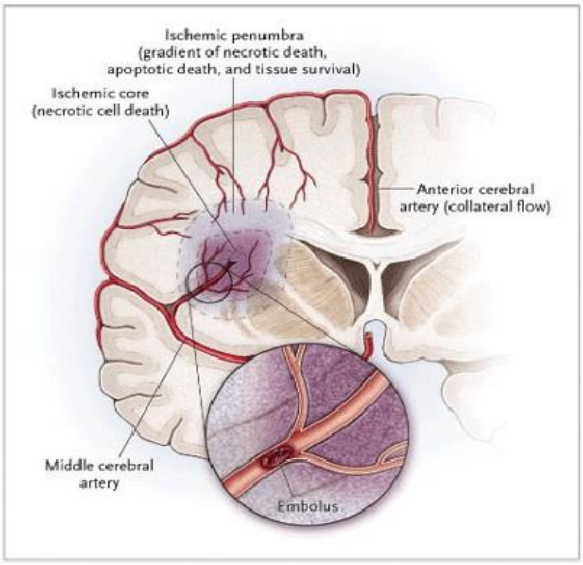

Figure 2. A representative drawing of a human ischemic brain. The ischemic core is colored in dark purple while the surrounding light purple zone represents the penumbra. Taken from https://haudee2011.wordpress.com

An ischemic event is characterized, generally, by the presence of two main areas: a central ischemic zone (*Core*) and a surrounding area known as *ischemic penumbra* (**Figure 2**). The core is affected by severe ischemia, with largely decreased blood flow that results in lack of nutrients and oxygen and, therefore, necrosis of neurons and glial cells.

Among the tissues normally perfused and those involved in the ischemic phenomenon, however, there is usually the presence of a defined area, the penumbra, which is the subject

of several studies, both clinically and in basic research. This phenomenon has been described for the first time in 1981 by Astrup and refers to an area of brain tissue in which the reduction of blood flow is severe enough to cause hypoxia and physiological deficits but not so severe to cause an irreversible arrest of cellular energy metabolism and subsequent tissue necrosis (Paciaroni et al., 2009). It is, therefore, a zone not yet irreversibly damaged, and thus a target for acute therapies (Fisher, 1997).

Studies on a mouse model of stroke induced by middle cerebral artery occlusion (MCAO) followed by 2-photon imaging investigations in vivo, have shown that in the ischemic penumbra reperfusion of tissues can lead to recovery of dendritic structures in neurons damaged by ischemia (Murphy et al., 2008), even when ischemia lasts up to 60 minutes (Li and Murphy, 2008). However the ischemic core does not show any recovery of dendritic structures; the authors therefore suggest that, even if reperfusion could prevent cell death of neurons in the core, there, the efficacy of synaptic transmission would be hopelessly compromised.

The ischemic penumbra is, therefore, a very dynamic region. The tolerance of penumbra tissues to ischemic damage, is closely linked to residual blood flow and duration of vascular dysfunction: if it persists for an excessive period, the penumbra will lose its vitality. This important fact has to be taken in great consideration because it creates a precise and restricted time window for possible interventions of reperfusion over this zone. Therefore it is essential to accurately identify the location and extent of penumbra.

1.3 Clinical outcome

If an ischemic insult occurs in the motor cortex, one or more body parts contralateral to the infarct result impaired or paretic. The degree of the motor impairment depends on many factors, such as the extent of the infarct, the identity of the damaged region and the effectiveness of the initial neuroprotective interventions. In the first weeks after stroke, limited spontaneous recovery can occur. About 26% of stroke survivors are able to carry on everyday activities (Activity of Daily Living or ADLs, i.e. eating, drinking, walking, dressing, bathing, cooking, writing) without any help, but another 26% is forced to shelter in a nursing home (Carmichael, 2005). Impairments of upper and lower limbs, are particularly disabling as they make very hard to have a sufficient degree of independence in ADLs.

To perform a better diagnosis and design the best therapy for each patient is important to know with high precision the location and extension of the ischemic damage. For this purpose many techniques have been developed in the last years.

1.4 Tools for neurological investigations

1.4.1 Brain imaging techniques

The modern diagnostic tests are able to show structure and functionality of the human brain and are able to identify with high precision the affected area. Development and improvements of modern imaging techniques such as Computerized Axial Tomography (CAT) and Magnetic Resonance Imaging (MRI) have facilitated, in recent years, the localization of bleeding even in small and restricted areas of affected tissue. The technique originally used for the identification of the ischemic borders and identification of penumbra is the "Positron Emission Tomography" (PET), which provides data on the cerebral blood flow (CBF) and cerebral volume (CV). This technique is extremely accurate but also complex and expensive, so often it cannot be applied in time for the patient. Today, many health centres use magnetic resonance imaging (MRI) to study perfusion (Perfusion-Weighted or PW) and diffusion phenomena (Diffusion-Weighted or DW). However, even this technique is rather approximate because data are variable and not strictly quantitative; studies of PW / DW Imaging, therefore, are only a first approach of the application of modern techniques of MRI for the identification of ischemic penumbra and it is necessary to apply a more accurate method of data acquisition (Fisher, 1997). Currently, the diagnostic method most widely used on stroke patients is the Perfusion Computed Tomography (CT), which can be used not only as a tool to distinguish between various types of stroke or between an ischemic phenomenon and a brain tumour but also to study changes that characterize the ischemic area in the early post-stroke period. In particular, the "Dynamic Perfusion CT" consists in the acquisition of sequential images using a contrast medium previously administered to the patient, allowing to estimate measures for CBF, CBV, and the mean transit time (MTT). A prolonged MTT and increased CBV indicates that a brain region is compromised at hemodynamic level. Often there are regions that show vasodilatation and recruitment of collateral vessels, meaning they have preserved a certain level of self-regulation and are considered "Tissue at risk" (Paciaroni et al., 2009).

The improvement of these techniques is critical to reduce as much as possible the time interval that precedes the application of the treatment; in fact, one of the key elements for the success of a clinical therapy in acute stroke, is the precise timing of the intervention.

1.4.2 Quantitative electroencephalography

In addition to imaging techniques, stroke diagnosis can be supported by measures of brain electrical activity by Electroencephalography (EEG), Magnetoencephalography (MEG) and

recording of evoked potentials. In many respects, the temporal resolution (milliseconds) of these techniques is optimal for non-invasively capturing the precise timing of stroke-related activity: changes in the electromagnetic field related to neuronal activity can be acquired over a broad frequency spectrum and spectrally decomposed into distinct frequency bands. EEG acquisition allows detecting the signal originating mainly from extracellular currents resulting from the integration of excitatory and inhibitory post-synaptic signals in dendrites of cortical pyramidal cells. Synaptic transmission impairments due to neuronal loss after ischemic stroke generate electrical alterations in neural signals that could be detected by a quantitative EEG (QEEG). After initial conflicting results (De Weerd et al., 1988) this technique has been widely evaluated and adjusted and, in the last few years, it has shown a good predictive potentiality for ischemic stroke pathophysiology (Murri et al., 1998; Luu et al., 2001; Finnigan et al., 2004, 2007). In particular, very specific EEG abnormalities have been detected after ischemic stroke at different time points from injury (Finnigan and van Putten, 2013). Such alterations seem to be also long lasting and detectable even in a chronic phase. Quantitative EEG can detect changes in brain activity a thousand times faster than most biochemical indices, and they are not measures of cell metabolism but the summation of cortical postsynaptic potentials themselves.

Modern EEG and QEEG techniques are considered powerful and promising tools for identification of synaptic alterations after stroke. One of the most relevant parameters that have been seen to correlate with imaging outcomes is the power of EEG signal. This index represent signal intensity and is very informative, especially if it is computed for specific bands of frequency isolated by Fourier transform.

Various indexes using band power ratios or global power measures revealed by EEG have been correlated with lesion volume (Zappasodi et al., 2007), stroke severity and evolution (Finnigan et al., 2004), early treatment effects (i.e. injection of plasminogen tissue activator), and functional outcomes (Sheorajpanday et al., 2011).

1.4.3 Evoked Potentials

Several recent studies have assessed also the potentialities of evoked potentials (EP) as a useful, objective prognostic test in terms of predicting post-stroke functional recovery. The evaluation of motor and sensory evoked potentials (MEP and SEP) allows, indeed, assessing the integrities of cortico-spinal and somatosensory pathways (Tzvetanov et al., 2005).

SEPs are recorded from the somatosensory cortex and consist of a series of waves that reflect sequential activation of neural structures along the somatosensory pathways. SEPs can be elicited by mechanical stimulation of sensory receptors or electrical stimulation of peripheral nerves, which gives larger and more robust responses.

MEPs recording are acquired at the muscular level and requires a safely, not invasive stimulation of the brain cortex, specifically of the motor area. Transcranial magnetic stimulation (TMS), developed by Barker et al. in 1985 (Barker et al., 1985), is a painless (Merton and Morton, 1980), non-invasive technique that uses magnetic fields to stimulate motor cortex. Nowadays, TMS is amply used to obtain information about the function of motor pathways (Theodore, 2002; Bembenek et al., 2012). Parameters obtained from MEPs, such as latency or amplitude, in the limb contralateral to the motor cortex stimulation have been shown to represent good mirrors of the integrity and functionality of the corticomotor pathway, as SEPs are for sensory motor system (Ziemann et al., 1999; Lai et al., 2015a). These findings have encouraged several studies about the use of MEPs as an index of motor function and recovery after stroke (Binkofski et al., 1996; Escudero et al., 1998; Stinear et al., 2007).

Single-pulse MEPs have resulted useful in investigating the presence of movement disorders; when the muscle is under contraction, in fact, a single TMS pulse in the contralateral hemisphere results in an interruption of the electromyography signal for a short time interval, called “silent period”. In hemiparetic post-stroke patients, the affected side can show a longer silent-period when the infarct is located not in M1 (Classen et al., 1997), or a shortened silent period, when the infarct involves M1 (Currà et al., 2002).

TMS delivered when muscle is in a rest condition, produces a MEP of different intensities depending on the motor threshold (i.e. the lowest TMS intensity necessary to evoke the MEP). After stroke, MEP is often not present, and it is related with a bad outcome. When MEP is still visible (predicting a good outcome) the motor threshold increases in the affected hemisphere, but it is decreased in the contralateral one (Currà et al., 2002; Pino et al., 2014), suggesting an imbalance between hemispheres.

Paired-Pulse TMS evoked MEPs (Figure 1.3, B) have also been associated to motor dysfunction. In this approach a conditioning stimulus is followed by a test stimulus that can be given in the same hemisphere or in the contralateral one with different Inter Stimulus intervals (ISIs). The conditioning stimulus be delivered at higher or lower amplitude of the motor threshold (i.e. the lowest TMS intensity necessary to evoke the MEP). After a suprathreshold conditioning pulse there is a strong inhibition of responses to the test stimulus (given in the same hemisphere) if the ISI is longer than 30 ms. The duration and extent of the inhibitory effect depends on the intensity of stimulation (Wassermann et al., 1996). Since stroke often induces plastic changes in motor cortical representation and alterations in neural excitability not only in the affected hemisphere but also in the contralesional one (Cramer et al., 1997; Cao et al., 1998), the study of interhemispheric connection with paired-pulse protocol has been applied on post-stroke patients as an index of motor dysfunction (Buchkremer-Ratzmann and Witte, 1997; Shimizu, 2002).

Unfortunately, not all studies on humans, investigating the prognostic value of MEPs have been successful and this can depend on the heterogeneous methodologies used (Barker et al., 1985; Nascimbeni et al., 2005). Therefore, further investigation about electrophysiological mechanisms underlying MEPs parameters modifications could be useful to validate this tool as a guide for post-stroke motor diagnosis and rehabilitation.

2. Treatment Strategies in the acute phase

The improvement of the techniques mentioned above is essential to reduce as much as possible the time interval that precedes the application of the treatment; one of the key elements for the success of a clinical intervention in acute stroke, in fact, is the timeliness of treatment. Treatment strategies vary depending on the type of stroke; stroke bleeding should usually be treated with surgery aimed at repairing the damaged vessel while thrombotic occlusions are dissolved through the activation of human tissue plasminogen activator (recombinant tissue Plasminogen Activator or rt PA), a potent thrombolytic agent.

Currently, this is done within three hours from the ischemic episode, while, within six hours of the attack, interventions of intra-arterial (IA) thrombolysis are usually performed. In fact, a recent randomized trial by Berkhemer's group demonstrated that in patients with acute ischemic stroke functional recovery could be obtained with surgical intra-arterial treatment when performed within 6 hours after stroke onset (Berkhemer et al., 2014). Continued improvements in radiology and in the design of more effective tools, including clot retrievers and stents, have allowed increasingly applicable interventions of intra-arterial recanalization, allowing secure access to main intracranial blood vessels (Saletti et al., 2011).

2.3 Neuroprotective Treatments

Recently, new drug therapies have been developed to limit the neuronal damage in brain areas affected by stroke.

Despite the above-mentioned actions of thrombolytic therapy, indeed, the percentage of deaths and the development of disability following ischemic events remains very high. Therefore, scientific research continues to focus on increasing the functional recovery following ischemic attack. One of the approaches that have received much interest in this field is the study of the neuroprotective factors. In particular, the potentiality of these substances to preserve neurons affected by the ischemic event from an irreversible functional damage is currently subject of study. This treatment could be particularly important if applied to the tissues included in the ischemic penumbra that, although interested by the

hypoperfusion, are still potentially viable and subject to phenomena of structural and functional recovery after reperfusion, as demonstrated in animal models (Murphy et al., 2008). Also in this case, the timing of intervention is decisive because these tissues are highly dynamic and always at high risk of apoptosis and tissue necrosis. In animal studies, many of these substances have been applied to interfere with these adverse biochemical changes. Preclinical studies indicate a period of at least 4 hours after onset of complete ischemia in which many potentially viable neurons exist in the ischemic penumbra. In humans, the time window may be longer, depending on the severity of the infarct.

The increase in knowledge on the complex pathophysiology of ischemic events has led to the development of various neuroprotective strategies involving several agents. Neurotrophic factors, anti-apoptotic agents, inhibitors of excitotoxicity, hyperpolarizing agents, anti-inflammatory drugs and cytokine inhibitors are only some examples of neuroprotective factors that have been tested in the last years. However, although many neuroprotective agents have produced good results in animal models of stroke, the application on humans is not free of risks and they are used, in some cases, as an attempt to save ischemic neurons in the brain from irreversible injury (Green, 2004).

In its acute phase, the ischemic attack induces a great release of glutamate from neurons and its increase in the extracellular environment determines, in still functionally active neurons, an excessive increase of intracellular calcium, resulting in the activation of apoptosis cascades (Lai et al., 2014). The role of an excessive release of glutamate in early post-stroke damage has been demonstrated in various pre-clinical studies. The block of vesicular release in excitatory neurons via application of Botulinum Neurotoxin E (BoNT/E) in animal models of hippocampal stroke, for example, reduces considerably the loss of hippocampal pyramidal neurons in the 24 hours post-injury. These results lead to suppose that the blockade of synaptic release can prevents neuronal death due to focal cerebral ischemia (Antonucci et al., 2010).

So, one of the most common approaches related to neuroprotection is to reduce phenomena of excitotoxicity in the damaged areas. For this, the effect of antagonists of N-Methyl-D-aspartate (NMDA), glutamatergic receptor, responsible of the excessive entry of calcium into cells, is subject of several studies. Moreover, the application of these antagonists on animal models seems to be effective in reducing neuronal damage following stroke (Davis et al., 2000). However, clinical studies have shown that some NMDA antagonists are poorly tolerated and determine the occurrence of side effects such as hypertension, sedation, hallucinations, until catatonia. Many of these trials have been discontinued for lack of evidence about a satisfactory relationship between risks and benefits (Lees, 1997).

Another, complementary, experimental approach to decrease excitotoxicity is to reinforce the main inhibitory neurotransmitter in the central nervous system (CNS), the γ-amino-butyric acid (GABA). Pre-clinical studies using a GABA agonist, Clomethiazol, have demonstrated its protective effect that is, however, strictly dependent on a prompt intervention, not later than 1 hour after occlusion. However, in the clinical trial of acute stroke involving this strategy, it has been possible to apply the treatment only 12 hours from the onset of symptoms, so it is not surprising that these studies have had negative results (Ginsberg, 2008). Another clinical trial have tested the effect of diazepam (Valium), another GABA agonist also able to inhibit the formation of nitric oxide (NO), within 12 hours after acute ischemic stroke. The data collected in this study, however, did not confirm the effectiveness of the drug in cases of acute ischemic stroke (Lodder et al., 2006). Conversely providing a benzodiazepine inverse agonist immediately after the ischemia induction, determines an increase of the lesion volume (Clarkson 2010).

Therapeutic hypothermia appears to be a promising technique for the treatment of ischemic stroke whose effectiveness as a neuroprotective factor has already been established in animal models of stroke but also of patients suffering from cardiac arrest (Shintani et al., 2010). However, this therapeutic strategy is obviously quite complex to apply in humans. The management of the patient must be highly accurate and sedation, tremor and intubation can lead to adverse effects such as respiratory problems, arrhythmias and clotting disorders. Thanks to recent advances in instrumentation and application techniques, this therapy may become accessible to clinical application in the future (Ginsberg, 2008; Froehler and Ovbiagele, 2010; Hong et al., 2014).

All these approaches might help to limit the functional deficit and to increase neuronal survival but despite this, the full recovery is not assured and the consequences of stroke can be severely disabling, anyway. In fact, even if a recovery of synaptic function can be obtained in the ischemic penumbra following reperfusion, the areas that suffer the major vascular damage (Core) does not show this kind of recovery (Li and Murphy, 2008). And however, even if it were possible to facilitate the survival of the cell bodies of neurons in spared tissues using neuroprotective factors, the functional recovery of the circuits might be hindered by a lack of recovery of dendritic arborisation.

Therefore, complete recovery of the functionality of the brain areas involved in stroke is quite difficult and trying to increase cell survival in the acute phase to limit neurodegeneration in the penumbra could be not enough.

3. Targeting neuroplasticity

In the long-term post stroke recovery, many studies concentrated on stimulation of neuroplasticity, as functional recovery likely results from changes in structure and function of undamaged neurons in the perilesional area and contralateral hemisphere. Plasticity can be enhanced by physical rehabilitation but also by pharmacological treatments. As an example, some drugs as erythropoietin, fluoxetine and neurotrophic factors have been successfully tested on animals and are used to aid the post-stroke recovery of neural injuries, both through neuroprotective and neuroplastic effects. However their systemic administration in humans is often related to side effects (Saver, 2010).

3.1 General concepts

The term "plasticity" has been coined to include all those phenomena of change in the organization of neural components of the CNS. Such changes are thought to be highly involved in mechanisms of aging, adaptation to environment and learning. Moreover, neuronal plastic phenomena are likely to be the basis of adaptive modifications in response to anatomical or functional deficit or brain damage.

Several studies on both animals and humans have been conducted on this topic showing that, during the entire lifespan of an individual, there is a constant turnover of synapses, as shown by studies of two-photon microscopy in vivo (Holtmaat et al., 2005; Huber et al., 2012).

New dendritic spines branch out and proliferate, and effectiveness of synaptic contacts is modulated through a complex network of intracortical and intercortical connections changes (Nudo, 2007). These changes are detectable on different levels, starting from molecular mechanisms at the dendritic spines level continuing with axonal sprouting, involving, finally, the entire neural networks. Through these mechanisms, responsiveness and connectivity of each neuron is continuously modulated by processes of maturation, learning and experience.

In humans, the plastic potential of the brain is not constant throughout the individual life but seems to continue after birth until 18-20 years. However, during life there are periods of maximum plasticity, during which some crucial experiences reach the peak of their effectiveness in promoting proper behavioural development (Mundkur, 2005). This time window is called “critical period” and appears to be different in onset and duration and fundamental for basic visual functions, language and social behaviour. The importance of these periods has been extensively documented by the devastating effects of deprivation of sensory or social experiences in children (Fagiolini and Leblanc, 2011) or in visual deprivation in rodents and cats (Wiesel and Hubel, 1963; Gordon and Stryker, 1996). It has

been extensively demonstrated in fact, that a short period of monocular deprivation during the critical period, is sufficient to induce a chronical shift in the ocular dominance in the visual cortex. Monocular deprivation have no effect if performed later in the adulthood. This experimental paradigm has been widely used to study the critical period in particular determining factor implicated in the opening and closure of this plastic window. In particular it has been shown that many molecular factors such as serotonin, GABA and BDNF play an important role in drawing the limits of the critical period (Baroncelli et al., 2010). These findings could be of great interest, if used to reopen the critical period late in the adulthood or after a brain lesion in order to potentiate the recovery.

However, even if at the end of this time window, the plastic capacity of the brain progressively decreases, it does not disappear completely: in some cases, plastic events can occur also in the adult brain if appropriately stimulated.

In fact, in the adult brain it is still possible to observe phenomena of structural plasticity (Altman, 1962): axonal elongation and pre-/post synaptic modifications could be induced by learning and experience or in response to injury (Gage, 2002).

Environmental enrichment, (including exercise and cognitive stimulation) and the action of neurotrophic molecules (BDNF) have been demonstrated to elicit constructive effects on the architecture of dendritic spines in the hippocampus (Berlucchi, 2011). In addition, several studies, have shown that the maps of topographic motor, somatosensory, tonotopic and retinotopic organization are subject to size and location changes induced by use (physiological plasticity) or injury (pathological plasticity) during the entire life of the individual (Nudo, 2006).

Despite the various mechanisms involved, the behavioural experience seems to be the main modulator of cortical structure. For example, the execution of complex movements, requires several repetitions in order to create motor modules in cortical networks. In these modules, the joint activity of all the muscle involved is conceived as a single, fluent set (Nudo, 2007).

3.2 Neuroplasticity after stroke

A structural brain damage inevitably causes a drastic alteration of the entire complex neural network that characterizes the interested area. However, it has been widely demonstrated, both in animal models and from neuroimaging and neurostimulation studies in humans, that the cerebral cortex exhibits spontaneous phenomena of brain plasticity in response to damage (Gerloff et al., 2006; Nudo, 2007). The destruction of neural networks, in fact, usually stimulates a rewiring and a reorganization of the connections and this plastic

environment is highly sensitive to the experience following the damage (Stroemer et al., 1993; Li and Carmichael, 2006). Particularly such phenomena involve the perilesional tissue and the surrounding brain areas of the injured hemisphere. Nevertheless, plastic phenomena can interest also some portion of the contralateral hemisphere, subcortical and spinal regions.

3.2.1 Neuroplasticity in the perilesional area

The motor cortex (as the sensory cortex) shows a topographical organization. It means that it consists of a map of movement clustered for different body parts. These maps are quite stable, but they can change after experience-dependent plasticity or brain injury.

Remapping of the motor cortical areas have been observed in stroke patients via either functional Magnetic Resonance Imaging (fMRI) or Transcranial Magnetic Stimulation (TMS) (Cicinelli et al., 1997, 2003; Traversa et al., 1997; Liepert et al., 1998; Rossini et al., 2001). In animal models, reorganization of motor maps has been observed using intracortical microstimulation (ICMS) (Nudo and Milliken, 1996; Nishibe et al., 2010) or optogenetic techniques (Harrison et al., 2013).

Studies on primates have demonstrated that following an ischemic injury in the hand area of M1 there is a significant reduction of hand representation if no rehabilitative training is applied. However, if the monkey undergoes rehabilitative exercises, the area of the hand is preserved; it is possible that the training, encouraging the re-acquisition of a degree of motor skills in the injured limb, maintains the effectiveness of the projections of neurons spared to motor neurons of the hand (Nudo, 2007). Other studies confirmed these results in primates and rats (Nudo, 2013; Combs et al., 2015; Nishibe et al., 2015).

Moreover following ischemic injury in M1, secondary motor areas can survive and remain functional and can contribute to the recovery. In fact, in the ventral Premotor area, which receives most of the inputs from M1, not only neural loss was not detected but it was observed phenomena of production and release of Vascular Endothelial Growth Factor (VEGF), which has angiogenic properties and neuroprotective properties (Nudo, 2007). In rodents, many studies on the location and extent of cortical sensory and motor maps, have achieved a good level of knowledge about the anatomy and physiology of these functional representations. These sensory and motor maps can then be used to determine the cellular and anatomical reorganization and possible recovery following stroke (Carmichael, 2005)

Indeed, it is proven that after a small subtotal cortical lesion, peri-infarct areas could actually vicariate lost or damaged functions (Murphy and Corbett, 2009; Dancause and Nudo, 2011).

However, little is known about the cellular mechanisms that lead to these network reorganizations and regain of the lost motor function. It has been proposed that these processes are use-dependent and involve sprouting of new connections as well as the unmasking of pre-existing, normally subthreshold connectivity. The GABAergic system and the extracellular matrix could have an important role in controlling these plastic phenomena. For example, Perineuronal Nets (PNNs), specialized extracellular matrix structures made of condensed chondroitin sulfate proteoglycans, have been correlated with brain plasticity and repair, and preferentially surround the soma of GABAergic neurons, in particular fast-spiking parvalbumin-positive interneurons (Fawcett, 2015). The role of PNNs has been extensively investigated during the maturation of the visual system in relation to the opening and closure of the critical period (Pizzorusso et al., 2002; Deidda et al., 2015). PNNs are thought to stabilize mature connections and downregulate spine motility and functional plasticity. Following CNS injury, the degradation of PNNs, by means of injections of the bacterial enzyme chondroitinase ABC, promotes sensory-motor recovery (Bradbury et al., 2002; Soleman et al., 2012; Gherardini et al., 2015).

The GABAergic system has also been studied in relation to the opening and closure of early “critical periods” in sensory cortices (Hensch, 2005) and in post-stroke motor recovery. Previous works showed that increasing GABAergic signalling after stroke is not effective at improving motor performances (Madden et al., 2003), but rather produces a worsening of recovered function in stroke patients (Lazar et al., 2010). In humans, a reduced GABAergic inhibition is associated with functional recovery (Kim et al., 2014).

Ionotropic $GABA_A$ receptors mainly mediate the inhibitory effect of GABA in the brain (Farrant and Nusser, 2005; Fritschy and Panzanelli, 2014). $GABA_A$ receptors are composed of different subunits and the resulting molecular assembly determines the localization and biological action of the receptor. For instance, $GABA_A$ receptors enriched in α4, α5, α6 and δ subunits are mainly extrasynaptic where they mediate tonic actions of GABA, whereas those enriched in α1, α2, α3 and γ subunits are mainly located in the synaptic cleft and are involved in phasic GABAergic signalling (Cherubini, 2012). However, this subdivision is not strict but it is possible that some receptors subunits, such as alpha1, may exert their role at both synaptic and extrasynaptic level (Che Has et al., 2016). A general downregulation of $GABA_A$ receptors has been found in peri-infarct areas following photothrombosis-induced lesions in rats (Schiene et al., 1996). However, tonic GABAergic signalling appears to be increased in the first two weeks after stroke. In fact, recordings from brain slices showed an increase in GABAA-receptor mediated tonic inhibition in layer 2/3 pyramidal neurons. Experimental reduction of this heightened inhibition using a benzodiazepine inverse agonist, produces significant post-stroke improvements of forelimb function in several behavioral tasks, such as the gridawalk and the Cylinder test. Consistently, transgenic mice lacking α5- or δ-$GABA_A$

receptors showed a lower functional deficit after stroke. (Clarkson et al., 2010; Lake et al., 2015).

Stroke induces the production of various inhibitors of neural regeneration, sprouting and plasticity, such as myelin components (Nogo-A, myelin-associated glycoprotein), and guidance molecules (ephrins, semaphorins). The application of drugs able to neutralize the effect of anti-plastic agents, such as Nogo-A antibodies has been seen to encourage axon regeneration, sprouting and functional recovery in a variety of animal models of cortical and spinal injuries (Freund et al., 2006; García-Alías et al., 2009; Maier et al., 2009; Alilain et al., 2011). Particularly, anti-Nogo-A antibodies treatment (for 2 weeks) delivered before motor training in forelimb reaching (started 2 weeks after stroke) largely improve motor recovery. In this study, a time-dependent effect has been reported, in fact, delivering anti-Nogo-A during motor training is not effective to improve motor deficits (Wahl and Schwab, 2014).

Accordingly, sequential administration of epidermal growth factors, followed by Environmental Enrichment and reaching training accelerates the recovery process in pellet retrieval task (Jeffers et al., 2014).

After stroke, it has been reported a consistent change in terms of “sprouting markers”, for example, GAP43, CAP23, c-Jun, classical axonal growth markers increase in the peri-infarct region. On the other hand, ephrin-A5, chondroitin sulfate proteoglycans (CSPGs) and other growth inhibitory genes, are expressed in proximity of the lesion and at later time points (Carmichael et al., 2001, 2005),

However, even if such spontaneous plastic changes stimulate cortical reorganization, this is insufficient to promote a full functional recovery (Liu and Rouiller, 1999; Frost et al., 2003; Jang et al., 2003; Zemke et al., 2003; Dancause, 2006).

The incapacity of the CNS to spontaneously recover completely from a brain injury, fully exploiting neuroplasticity, could be a protective mechanism: in fact, such regeneration, sprouting and synaptic plasticity, could be also maladaptive if the connections are not re-established in the adequate way and the complexity of the CNS of mammals makes it extremely subject to this kind of errors (Eriksson et al., 1998). This is demonstrated by clinical cases, where maladaptive plastic changes have been associated to the development of serious diseases such as schizophrenia and neuropathy (Glenberg et al., 2010).

3.2.2 Neuroplasticity in contralesional hemisphere

Even in the contralateral hemisphere neuronal connections appear to be altered as a result of cortical damage; it has been seen in adult rat, for example, that after a cortical lesion,

thanks to axonal sprouting, the healthy hemisphere contacts both the ipsilateral and contralateral (ipsilesional) striatum (Napieralski et al., 1996).

Moreover, human functional imaging studies on post-stroke patients, using PET and functional MRI, have identified a role of the healthy hemisphere in recovery. In particular, the reorganization process in the intact hemisphere seems to be important for vicariating the impaired functions of damaged areas, thus promoting the processes of recovery after stroke (Calautti and Baron, 2003). An enhanced activity in the contralesional hemisphere has been reported in patients in the first 10 days post injury, followed by an increase in the ipsilesional one (3-6 months). This sequential activtation was related to improvements in motor performance (Marshall et al., 2000; Ward et al., 2003).

Similarly, in rodents, the activity of the contralesional hemisphere was enhanced immediately after stroke (when the deficit was more pronounced) and was followed by perilesional activation at later stages during the recovery phase (Dijkhuizen et al., 2001)

In the somatosensory cortex (SSC) it has been showed that after focal ischemia, basal metabolism and field potentials after vibrotactile stimuli of the impaired limb, were transiently increased as baseline activity and response-related activity in the healthy hemisphere after somatosensory stimulation of the ipsilateral (impaired) forelimb (Takatsuru et al., 2009). Other studies in SSC showed that the lesion induced changes in the contralesional cortex sensory map, with an increase in dendritic branches of layer V pyramidal cells. These changes appear to be increased if the animal is subjected to early exercises that increase motor skills (Biernaskie et al., 2004; Gonzalez et al., 2004). Moreover, two-photon imaging in vivo studies have highlighted phenomena of structural rearrangements of neurons in the healthy hemisphere, both at the level of individual cells and of whole circuits. In particular, it was highlighted a transient, localized increase in the turn-over of dendritic fungiform spines (mushroom), usually very stable in a healthy brain, in a time period limited to one week post-stroke (Takatsuru et al., 2009).

Pharmacological or electrically silencing of the healthy hemisphere after stroke improves motor function in the late phase (Mansoori et al., 2014).

These results could indicate an involvement of the healthy hemisphere in functional alterations following an injury in the contralateral one. However, whether the healthy hemisphere has a positive or negative impact on the recovery is still controversial. In fact, there are many evidence that in some cases the activity of the healthy hemisphere can worsen motor recovery. For example, a recent QEEG study in stroke survivors showed that the increase of contralesional hemisphere activity, during the acute phase, is related to negative final outcome. In fact, the increase of the contralesional power associates to an interhemispheric communication breakdown (Assenza et al., 2013).

A possible hypothesis takes in consideration the lesion volume: when the lesion is sufficiently small to allow the reorganization of spared adjacent motor areas, the contralesional hemisphere activity would have a negative impact on the recovery; conversely, when the lesion extent is so vast to involve most of motor areas, the healthy hemisphere could be important to vicariate lost functions (Di Pino et al., 2014).

In keeping with this idea, acute inactivation of the healthy hemisphere (via injection of lidocaine), induced different effects in ischemic rats, depending on the lesion size. Animals with large lesions were dramatically affected by lidocaine administration as shown by a worsening of the performance in a reaching task (Biernaskie et al., 2005).

3.2.3 Post-stroke alterations in inter-hemispheric activity

The interaction between the two brain hemispheres before and after stroke is a widely investigated argument. The neural activity in the brain motor areas is functionally coupled between the two hemispheres (Kinsbourne, 1974) and the lateralization of neural activity during movements is likely to be related to interhemispheric inhibition between motor areas exerted via transcallosal connections (Bütefisch et al., 2008). After a cortical injury, the subjects recovering from stroke showed changes in these interhemispheric influences (Kobayashi and Pascual-Leone, 2003; Mohajerani et al., 2011) which are thought to be caused by an imbalance in the mutual interhemispheric inhibition between the two motor cortices (Murase et al., 2004) that could be an obstacle for motor recovery (Dancause et al., 2015). In humans, many studies have been pursued by means of different techniques of recording and analysis of fMRI data. In particular, fMRI recordings are very suitable for measuring the connectivity because they use an indirect measure of the synchronization of neural activity, i.e. BOLD signal. For this reason, this noninvasive technique provides the mapping of wide brain regions (James et al., 2009). A second suitable technique for such investigations is the multichannel EEG recording which is minimally invasive and allows for a measurement of the functional connectivity of different and far cortical regions (Choi et al., 2012). However to directly investigate the local neural activity, Local Field Potentials (LFPs) are more suitable because they are generated by transmembrane current flow in ensembles of neurons close to the site of electrode insertion (Kajikawa and Schroeder, 2011). Studies of EEG coherence have shown that cortico-cortical connections appear weakened in the impaired hemisphere after a capsular stroke even in well recovered chronic patients, but resulted increased in the contralesional hemisphere suggesting a shift of cortical connectivity towards this healthy one (Gerloff et al., 2006). This functional integration between the two hemispheres could have as anatomical substrate the corpus callosum: a bundle of transcallosal fibers connecting homologue areas in the two hemispheres (Wise et al., 1997).

It has been proposed that after unilateral stroke, transcallosal connections could vehicle an excessive inter-hemispheric inhibition so that the unaffected hemisphere takes advantage of the other one. Despite the scarce knowledge about the mechanisms mediating these phenomena, the involvement of transcallosal glutamatergic connections acting on pyramidal tract neurons via GABAergic interneurons is widely accepted (Reis et al., 2008). The role of the corpus callosum in inhibitory interhemispheric mechanisms have been strongly demonstrated on humans through transcranial stimulation studies on patients with agenesis of the callosum (Meyer et al., 1995).

Functional Magnetic Resonance Imaging (fMRI) studies have shown an increased bihemispheric activation during movements of the affected limb in early post-stroke patients (Loubinoux, 2003) and suggest persistent alterations in intracortical and transcallosal connections, despite a good degree of functional recovery of patients (Nair et al., 2007). This is probably due to a decrease of the ipsilesional neuronal activity and an increase of the contralesional one (Murase et al., 2004; Fregni and Pascual-Leone, 2007); the imbalanced activation of the healthy hemisphere causes an increased inhibitory transcallosal signal to the affected one. Thus, as said above, the significance of contralesional activation during execution of a motor task with the affected limb is still uncertain: it could represent an epiphenomenon of recovery, an adaptive neuroplastic process or even a sign of maladaptive modifications that might interfere with the recovery process.

Despite the results from all of these studies, the knowledge about changes in intracortical connections following a focal ischemic injury is still very scarce. It is evident, however, that after cortical infarction, the spared tissues of both hemisphere show reorganization phenomena that could also be very consistent and may represent an adaptive mechanism to facilitate recovery or lead to the development of aberrant connections. Understanding the rules that guide these plastic phenomena represents a major challenge for research, especially with the aim to find a way to drive these amazing plastic capacity of the cerebral cortex toward the recovery following an ischemic injury. In clinical cases of CNS injury, in fact, neuroplastic phenomena appear to be the neural substrate for spontaneous recovery and a more complete knowledge about their mechanisms would probably promote new, more effective rehabilitation approaches.

4. Rehabilitative strategies

When the functional impairment after stroke remains even after the first pharmacological interventions, rehabilitation remains the only effective weapon to increase motor outcomes of patients.

Several studies have been conducted to test the effect of different rehabilitative strategies, often leading to contradictory conclusions. However, a common finding is that the effects of rehabilitation are higher and faster if it is applied in a precise time window after stroke. In particular the maximum recovery has been seen in 80% of cases within 3 weeks and in 95% within 9 weeks since the occurrence of stroke (Nakayama et al., 1994). Thus, timing is essential for functional recovery, indeed many studies are focused on understanding the "critical period" for post stroke plasticity. Ideally rehabilitation should start in conjunction with the opening of this plasticity window.

Since the 90s, numerous clinical trials have been designed starting from therapies developed in animal models, trying to re-scale them for human applications. In particular, different types of rehabilitation strategies have been developed, aimed to obtain a certain degree of motor control after stroke.

Post-stroke rehabilitation techniques must be precisely developed for the purpose of helping patients to regain their independence in everyday activities.

Obviously, the rehabilitation is not able to cancel the effects of stroke but primarily aims to increase strength and effectiveness of parts that were not affected by the damage and also the confidence of patients with their deficits with which often must learn to live and allowing the patient to be autonomous in his activities despite the effects of stroke.

Usually, stroke rehabilitation includes several physical activities, involving the affected body parts, such as exercises that improve strength and coordination or damaged muscle and regain ability of motion.

Over the years, the results of basic research and clinical trials have enriched the spectrum of rehabilitation strategies.

4.1 Standard Rehabilitation

This definition is used to indicate a series of specific exercises, often aimed to give back some degree of motor control to the patient by promoting correct movements and trying to abolish anomalous ones. Some of these exercises are focused on neuromuscular components remained intact to improve their functionality.

Types of exercises and their intensity are not constant or standardized but are chosen case by case, depending on the patient's medical history and status. In general, however, several sessions, usually lasting about 30-60 minutes per day, are necessary in the early phase following a stroke. The time dedicated to rehabilitation, however, tends to decrease with time from injury. The amount of time that patients spend in rehabilitation depends primarily on the degree of dysfunction but usually does not exceed 6 months. For ambulation dysfunction, however, it was observed that, in case of mild or moderate paresis, a good recovery can be obtained in 3 weeks while for severe paresis or paralysis of the lower limbs, functional improvements can be seen at least in 6 weeks (Jørgensen et al., 1995).

The degree of recovery, in general, tends to decrease with the increase of time from the ischemic episode and to reach a plateau in about 6 months (Hendricks et al., 2002). Nevertheless, even after completing the standard rehabilitation protocol, at least 50-60% of patients continue to suffer from some degree of motor deficits (Hendricks et al., 2002) and about 50% reaches only a partial level of independence in ADLs (Gresham GE, Duncan PW, 1995).

This data suggest the importance of research in searching for new and more effective rehabilitation strategies, able to achieve better results.

4.2 Intensive Motor Rehabilitation

Intensity and repeatability of rehabilitative treatments seem to have a key role in recovery of motor functions. Recent studies have shown that repetitive and focused treatments of the upper limbs are effective even after more than a year from the ischemic attack, when the patient is considered chronic (Barreca et al., 2003; Duncan et al., 2005). Moreover, the increase of the intensity of motor therapy have been seen to improve the results in functional recovery of the patients in many clinical cases (Kwakkel et al., 1997; Steultjens et al., 2003; Teasell et al., 2003).

There are several approaches that provide intensive rehabilitation through increased neuromuscular activity. The lower limbs seem to benefit from long-lasting progressive aerobic exercises, resistance exercises and from a cyclic application of them. For the upper limb, however, more fine therapies seem to be necessary to achieve such good results. “Constraint-Induced Movement Therapy” (see below) and the “bilateral arm training”, are both common applied techniques to increase motor outcomes through forced use of paretic limb and the simultaneous use of both limbs, respectively (Taub et al., 1993; Schaechter, 2004; Stewart et al., 2006).

However, it is still very tricky to demonstrate whether these intensive therapies are actually more effective than others, or if the results are confined only to particular subgroups of patients and are therefore not generalizable.

4.2.1 Constraint-Induced Movement Therapy (CIMT)

CIMT is a therapeutic strategy which forces the use of the affected side by tying the healthy one. In this way the patient is obliged to use the impaired limb intensively and repetitively for at least 2 weeks. This therapy was developed by Dr. Edward Taub (University of Alabama, Birmingham) based on the observation that stroke survivors actually try to use the affected side but are immediately discouraged by the inevitable failure (Taub et al., 1993). Other studies on primates have shown that animals tend to avoid the use of the impaired limb even if they are still able to move (Berlucchi, 2011). The limitation of voluntary movements of the impaired limb, in fact, induces the animal to learn to use only the healthy limb, increasing motor disability of the injured one (Taub et al., 2006). In rodents it has been seen that the forced use of the compromised limb, imposed by specific training in skilled behavioral tests like reaching task (where the animal have to grasp a piece of food with the impaired limb), improves motor performances and promotes dendritic plasticity not only in the peri-infarct zone but also in the corresponding areas of the contralateral hemisphere (Biernaskie and Corbett, 2001a). Furthermore, the application of this treatment protocol seems to be more effective when applied early after stroke (Biernaskie et al., 2004). Of note, studies on rats demonstrated that the training of the non-paretic limb can worsen the motor performance of the paretic one and that this effect depends on transcallosal projections (Allred et al., 2010). CIMT have been tested on humans in several clinical trials and patients have obtained a significant improve in many cases. Repeated use of specific neural pathways, or at least their protection from misuse, can be, therefore, beneficial for motor recovery. It remains to assess whether these effects can actually be attributed to brain plasticity related to learning, or they should be attributed to other mechanisms such as phenomena due to neuromuscular potentiation or production of neurotrophic factors (as BDNF) in an activity-dependent manner (Berlucchi, 2011).

4.2.2 Restoration of interhemispheric balance after stroke

The effect of the Constraint Induced Movement Therapy could be due not only to an enhancement of muscular strength of the impaired limb but also acting on the interhemispheric connections between functional cortices of the two hemispheres at the “central” level reestablishing the interhemispheric balance.

Some rehabilitative techniques involving invasive brain stimulation of targeted cortical and subcortical areas through epidural electrodes have been tested (Brown et al., 2003). However, an increasing number of clinical trials continue to test new non-invasive techniques to modulate neuronal activity thus promoting better functional recovery after stroke. These include also the Transcranial Magnetic Stimulation (TMS) and Transcranial Direct Current Stimulation (tDCS). The trials carried out have shown that in the tDCS, which involves the application of weak electric currents (1-2 mA) to modulate neuronal activity, determined detectable phenomena of neuro-rehabilitation (Nitsche et al., 2008).

TMS is a painless technique consisting in the passage of a strong brief electrical current through an insulated wired coil placed on the skull thus generating a transient magnetic field capable to induce electric currents in the cortex, aimed at modulating neuronal excitability at the stimulated sites (Hummel and Cohen, 2006).

Both TMS and tDCS could modulate synaptic activity in the two opposite direction, in inhibitory or excitatory. Anodal tDCS and High Frequency (>5 Hz) Repeated TMS (rTMS) have an excitatory effect on the local cerebral cortex by depolarizing neurons, while cathodal tDCS and Low Frequencies (1 Hz) rTMS cause neuronal hyperpolarization.

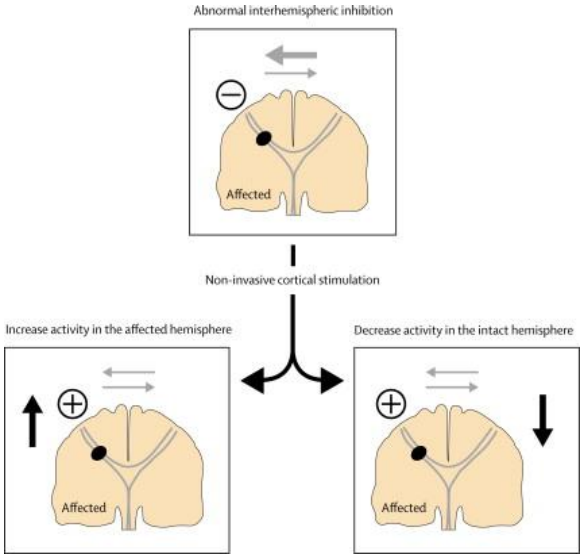

Figure 3. intervention strategies based on neuromodulation of inter-hemispheric activity using Non Invasive Brain stimulation (NIBS) tecniques.

Whether the most effective strategy is enhancing activity in the ipsilesional hemisphere or inhibiting the activity of the contralesional one is still subject of debate (**Figure 3**). Various studies in stroke patients have demonstrated that dampening the unaffected hemisphere decreases the interhemispheric inhibition to the affected one increasing its excitability, thus promoting motor recovery in the paretic hand and plastic modifications of perilesional cortex (Hummel and Cohen, 2006; Zimerman et al., 2012). However, not all the clinical trials involving this intervention have resulted in good motor outcomes (Lotze et al., 2006; Seniow

et al., 2012) and physiological mechanisms underlying the effect of these techniques are still almost unknown. However, a recent study added anodal transcranial direct current stimulation (tDCS) in the ipsilesional cortex to a 9-day motor rehabilitation protocol. They found increased activity during movement of the affected hand in the ipsilesional motor and premotor cortex after the treatment compared to patients that received sham stimulation (Allman et al., 2016).

The potentialities of these techniques are numerous and the variability of their outcomes in clinical practice could be the result of the lack of uniformity of the protocols applied or the groups of patients recruited. Moreover, non-invasive brain stimulation techniques have the great advantage to be easily used simultaneously with the robotic therapy to increase its effectiveness by facilitating neuronal plasticity (Edwards et al., 2009) (see also below).

4.2.3 Technology-assisted physical activities

The continuous improvements in technologies and the successful cooperation of physics, informatics and engineers with doctors and therapists, have led to the introduction of new devices aimed to help and ameliorate the outcomes of rehabilitative strategies.

- **Wireless technology,** which monitors patient activity.
- **Functional electrical stimulation,** based on the use of electricity to induce contraction in weakened muscles in order to re-educate them.
- **Virtual reality,** such as video games and visuo-motor tasks, where patients have to interact with a simulated environment. It is an emerging, strategy that is becoming more and more common and complex thanks to good patient response and to the improvement of computer graphic.
- **Robotic technology,** a more complex rehabilitative technique that uses robotic devices to assist impaired limbs while patient is performing repetitive exercises, helping them regain strength and function (see below). The degree of complexity of these devices is various and in continuous evolution. Moreover, their use can easily be coupled with one or more of the techniques mentioned above.

Unfortunately, the effects of these strategies are quite variable and up to now, an official guideline for post-stroke treatment does not exist. The main problem is that clinical trials aimed at assessing their effects are often applied on chronic patients or small groups of subjects, often involving people with different characteristics of brain lesion, medical history, motor outcomes etc. Recruitment of patients is, indeed, quite complicated and the type of interventions and investigations that is possible to apply on human patients is, obviously, limited. However, basic science in recent years have provide more and more tools to model human injuries, physical deficits and motor pathologies and have opened various pathways

to better investigate physiological mechanisms underlying the effects of all these rehabilitative strategies. With such knowledge, it will be possible to shed light on this complex field and to define the best treatment to apply for each clinical case.

4.2.3 Robot-mediated rehabilitation

As mentioned before, the effectiveness of post-stroke rehabilitation techniques seems to be strictly related to the duration and intensity of the therapy sessions. Timing, repeatability and intensity of treatment are the key words to regain some motor function and to induce a reorganization of neural circuits. This treatment results very complex, tiring (for both the patient and the rehabilitator) and expensive (Posteraro et al., 2010). These are some of the reasons which led the medical research to focus on the effects of using robotic instruments in rehabilitation after damage of the nervous system. The robotic therapy is usually administered by means of a mechatronic device that helps a patient to perform a specific motor task.

The use of robotic devices for post-stroke rehabilitation therapy was firstly introduced in 1997 (Aisen et al., 1997). Since then, numerous works have been published on the use of robotic devices to help provide rehabilitation therapy following neurologic injuries. The goal of robotic therapy is to design and control robotic devices for rehabilitation exercise. There are two main advantages of robotics for rehabilitation compared to traditional physiotherapy: (i) provides an intensive and highly repeatable "dose" of the therapy and (ii) provides an objective and quantitative assessment of the recovery of each patient, characterized by different kinetic parameters and kinematic (e.g. the force exerted by the subject, the smoothness of the movement, etc. that would be unachievable by humans (Prange et al., 2006; Sicuri et al., 2014). A protocol of intensive rehabilitation is able to provide long-term benefits in patients with moderate or severe damage, even years after the onset of a stroke (Lo et al., 2010) and robotic devices seem to be particularly suitable for this purpose. In a recent study, an exoskeleton robot that allows task-specific training in three dimensions has been used on patients having motor impairment for more than 6 months and moderate-to-severe arm paresis. They found that after 8 weeks of treatment, patients assigned to robotic therapy had significantly greater improvements in motor function of the affected arm over the course of the study as measured by Fugl-Meyer assessment (FMA-UE) than those assigned to conventional therapy (Klamroth-Marganska et al., 2014).

Some studies on chronic or sub-acute patients survived from ischemic attack have shown how the use of robotic therapy can actually improve the functionality of the upper limbs thanks to an intensive treatment in both chronic and sub-acute post-stroke populations (Volpe et al., 2000; Fasoli et al., 2003; Brewer et al., 2013; Poli et al., 2013) (**Figure 4**).

In particular, it has been shown that this type of therapeutic approach is able to improve muscle strength and motor coordination in patients with neurological deficits (Barreca et al., 2003; Micera et al., 2005).

Moreover, data on the kinetics and kinematics collected from robotic tools can be useful for implementing new markers of progression in motor recovery.

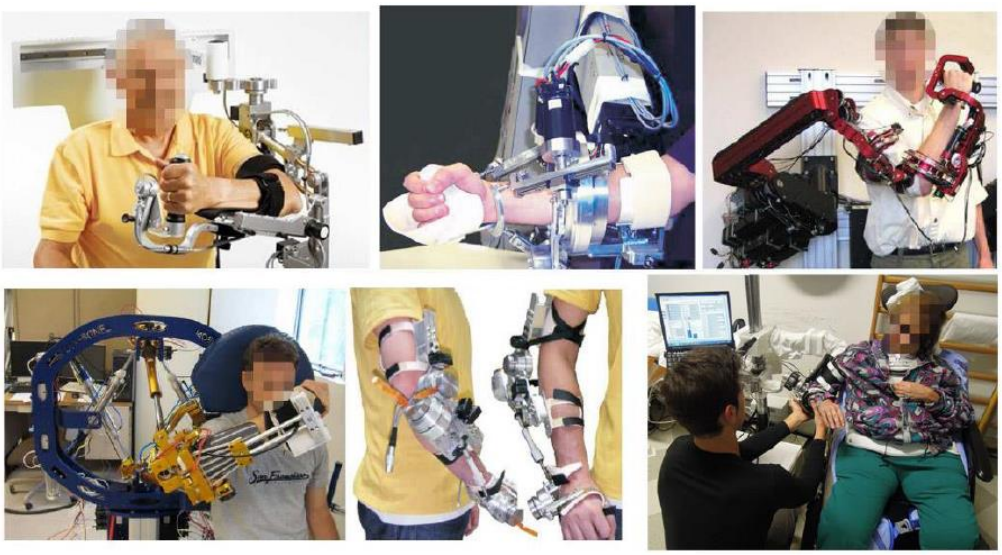

Figure 4. Some examples of upper-limb robots for rehabilitation. from left to right, and up to down, Armeo™, RiceWrist, CADEN-7, BONES, WOTAS,

With robotic devices, in each session the patient can carry up 1000 voluntary finalized movements in about 45 minutes; such amount of treatment would be physically very heavy for a physiotherapist (Posteraro et al., 2009).

Furthermore, the direct interaction between the patient and the machine allows, according to the performance of the patient himself, to adjust exercises in terms of degree of assistance provided by the machine during the training (“assist as needed” approach).

Despite all these findings and potentialities, however, in literature there are not studies that demonstrate without any doubts the efficacy and the actual benefits of these technologies, especially considering their relatively high cost (Dickstein, 2008). It remains also unclear what are the neural mechanisms underlying the possible improvement provided by this therapeutic approach. Clearly, such information would be of great help to further improve the effectiveness of the robotic therapy, allowing an approach "knowledge-based", with which the rehabilitation protocols could be designed to facilitate those changes in the brain that contribute most to an improvement of the motor functionality.

4.3 Combined therapies

In the last few years, a considerable amount of knowledge has been generated by biomedical research about the possible combination of robotic therapy for stroke rehabilitation and pharmacological treatments to improve recovery. As described above, plasticizing treatments have the potentiality to change the neuronal environment into a more permissive terrain for remapping and synaptic adjustments. However, since results both in clinical and basic science studies about the effective benefits of such spontaneous changes on functional recovery are often controversial due to the fact the in some cases plasticity could be unfavorable to recovery (Liu and Rouiller, 1999; Frost et al., 2003; Jang et al., 2003; Zemke et al., 2003; Dancause, 2006). Thus it is important that every plasticizing treatment is well targeted and guided appropriately to achieve the best functional outcome.

Thus, stimulation of plasticity by itself could not be sufficient to fully promote motor recovery: rebuilding appropriate connections during sprouting phenomena should be guided appropriately using training and exercise. Fawcett and collaborators, combined Chondroitinase ABC treatment with focused or general motor exercise after spinal cord injury. They found an improvement of manual dexterity when chondroitinase treatment, inducing sprouting of corticospinal axons, was flanked by specific motor training (García-Alías et al., 2009). On the other hand, another study tested the efficacy of combining transgenic deletion of Nogo66-receptor gene with physical exercise in a mouse model of spinal cord injury. In this case, authors reports an efficacy of the two approaches but without any synergistic effect after combination of them.(Harel et al., 2010). Other examples of combinatorial strategies are reported in Starkey and Schwab, 2012; van den Brand et al., 2012.

Interesting studies have been conducted on the effect of environmental enrichment in rodent models of ischemic stroke in the sensorimotor cortex. It has been shown that the simple exposure to enriched environmental conditions before or after the induction of ischemic event does not appear to improve the motor function of the fingers and front limb (Grabowski et al., 1993a). However, when environmental enrichment is coupled with forelimb training in a skilled reaching task, it is able to promote the recovery of motor function and to induce an increase in number, length and complexity of dendritic branches of pyramidal neurons in the intact hemisphere, even if the treatment is applied after 15 days from stroke (Biernaskie and Corbett, 2001a). When the same protocol, however, was repeated using enriched rehabilitation at earlier stages, it was found a major improvement in motor performance and in the increase of dendritic complexity in pyramidal cells of layer V, in the cortex and striatum intact hemisphere, with respect to later treatment (30 days) (Biernaskie et al., 2004).

It is confirmed, therefore, that the effectiveness of rehabilitation treatment, even if supported by environmental enrichment or other therapeutic strategies, is strictly dependent on the time window during which it is applied and not only on its intensity and duration (Johansson, 2000; Kleim and Jones, 2008; Zhao et al., 2013).

Another possibility is to couple standard motor rehabilitation with neuromuscular plasticity. Functional electrical stimulation (FES) is a commonly used therapy in addition to motor exercise. It provide electrical activation of the muscles during the passive execution of a movement. It has been shown that coupling FES during a cycling movement in post-stroke hemiplegic patients, in addition to standard rehabilitation protocols, significantly improves final motor outcome (Ferrante et al., 2008).

5. Compensation vs. True recovery

The main target of motor rehabilitation is to allow patients to recover the lost function. Rehabilitation therapy trains the affected limb with specific exercises, with the aim of improving also performance of the daily activities where the movement of the limb is needed (i.e., generalization). For example, it is desirable that after a specific goal-directed grasping rehabilitation in a stroke patient, the subject improves the capability in i.e. grasping a glass of water. To evaluate the overall proficiency in this task, the end-point measure would be the number of correctly grasped glasses. However, the motor strategy used to grasp the glass could be changed after post-stroke rehabilitation, compared to the pre-stroke movement. This phenomenon is called compensation (Zangwill, 1947; Kitago et al., 2013) and includes all the changes in motor strategy involving relative joints timing- and spatial coordination. In this context, kinematics is a potent tool to discriminate between post-stroke “true recovery” and compensatory strategies, making it useful also in pre-clinical studies in order to discriminate between maladaptive and adaptive recovery-driven neuroplasticity.

For example, skilled reaching kinematic analysis is an objective and quantitative tool for an accurate evaluation of limb motor performance (Cirstea and Levin, 2000; Alt Murphy et al., 2011). Skilled reaching is a spontaneous and widely conserved behavior in both humans and other mammals. Animals could be easily trained to use their forelimbs to reach a piece of food through a defined aperture and bring it to their mouth and such task could allow multiple and highly repeatable measurements (Klein and Dunnett, 2012). That is why pre-clinical research about post-stroke rehabilitation has shown great interest on rodent skilled reaching models to shad light over mechanisms underlying functional impairments and true recovery (Klein et al., 2012). Despite obvious differences from human motor strategies, rodents skilled

reaching could be compared to humans in various kinetic and kinematic aspects (Sacrey et al., 2009).

The analysis of limb movements in both pre-clinical and clinical studies could be done by means of high-speed video recordings that allow to evaluate motor performances in terms of end-point measurements and kinematic parameters.

For animal studies, the application of markers has been previously used on rats to automatically track hindlimb movements (Dominici et al., 2012). For animal models of smaller dimensions like mice, however, this approach is more challenging because of the limit in reducing markers dimensions. In mouse studies, indeed, measures of kinematic parameters has been extracted, until now, by means of video-based tracking (Alaverdashvili and Whishaw, 2013), i.e. a frame-by-frame manual video analyses to reconstruct the position of the mouse paws. Obviously, this method is very time consuming and not completely objective (Farr and Whishaw, 2002; Klein et al., 2012).

Despite this, several studies have used kinematic analysis to quantify post-stroke impairments in motor execution (Whishaw et al., 1991; Alaverdashvili and Whishaw, 2010) and to identify functional recovery. Of note, these studies have identified various homologies or rodents model with humans as the manifestation of compensatory movements, together with the loss of smoothness in movement execution (Subramanian et al., 2010; Alt Murphy et al., 2011; van Dokkum et al., 2014).

6. Animal models of stroke and motor function rehabilitation

Several animal models have been developed in the recent years to evaluate possible therapeutic approaches for the restoration of function following a focal ischemic insult in the brain (Wittenberg, 2010).

Rodent models allow a coordinated electrophysiological, behavioral, biochemical, and anatomical analysis of post stroke recovery. Mice, in particular, are largely used in this field because of their convenience in terms of costs, reproducibility, manageability and the broad-spectrum of investigations (Ginsberg and Busto, 1989). The highly variability of the consequences of neurological dysfunction associated with stroke among different species makes it difficult to find an animal model which reliably reproduces an episode of stroke human, with all its consequences. Most of the experimental models that have been developed mimic focal ischemia showing, as accurately as possible, phenomena that are typical of a cortical ischemic event. The high levels of knowledge about their anatomy and physiology, the relatively small size which facilitates the physiological and histological

analysis, the low cost, the existence of similarities in movements of the limb in motor components with humans (see above), the possibility to develop complex experimental designs, hardly applicable in experiments on humans or non-human primates, make rodents the most appealing model for research on stroke.

Moreover, despite the differences in the organization of cortical areas and in the distribution of corticospinal neurons, intracortical connections between different areas of the somatosensory cortex are very human-like. This makes the rodents a reasonably good model for understanding the changes in the intracortical communications following a brain injury (Nudo, 2007). Mice (*Mus musculus*), in particular, offer the possibility to carry out various genetic manipulations. Their strong genetic homogeneity allows to make standardized and reproducible modifications at the level of their DNA. The use of these genetically engineered mice as models represents a very powerful tool to study the complex phenomena that characterize the ischemic event. These mechanisms could be investigated by selectively enabling or disabling one or more genes for possible genetic risk factors or protective factors.

Using Knock-out mice is possible, therefore, to carry out studies aimed at identifying the molecules involved in the pathophysiology of stroke and related neuronal events such as neuroprotective phenomena, ischemic tolerance and ischemia-induced neurogenesis (Wang et al., 2007). Moreover, such genetic manipulations could involve photo-activated proteins linked to specific promoters (i.e. targeted to highly selective areas of the brain or even neuronal populations) and able to induce or inhibit neuronal activity, making optogenetic experiments possible. It must be specified that animal models that reproduce human stroke have several limitations, some of which are difficult to overcome. The human clinical stroke is often a result of a number of predisposing factors such as depression, diabetes, obesity and circulatory problems (Nudo, 2007; Pearson-Fuhrhop et al., 2009) while in the animal models reproduce only an ischemic insult in strictly controlled experimental conditions that cannot reproduce the complexity and heterogeneity of a human stroke. In addition, the corticospinal tract is very different in the two species. In mammals, this descending path from the layer V of the motor cortex to the spinal motor neurons is the main motor output. Primates, however, present a higher number of corticospinal neurons than the rodents. Moreover, in primates fibers that cross to the contralateral side of the spinal cord prevail while in rodents the ipsilateral component is greater and represents a potential compensatory pathway. For this reason, rodents often show a better and faster recovery after injury than humans (Nudo, 2006). The possibility to control and standardize factors like age, location of lesion and its extension is a great advantage in terms of experimental results but it also introduces a difference from humans where all those aspects are often variable. The characteristics and the consequences of ischemic damage itself could be different: in humans the extent of the

damage in terms of extension and localization could be highly variable while in animal models we can obtain extremely focused damages that are very useful to obtain specific motor effects but create another difference from humans.

Regarding the recovery therapies, different approaches have been used so far in the two species; in humans these almost always require the presence of a therapist that guides the rehabilitation while in the animal model the recovery was based only on the execution of some motor tasks, without a specific apparatus that assist it, and often representing both a rehabilitation therapy and an output for the evaluation of the motor performance.

6.2 Middle cerebral artery occlusion (MCAo)

Middle cerebral artery occlusion (MCAo) is one of the most widely used procedure to induce cerebral stroke in rodents (Carmichael, 2005). It consists of the intra-arterial occlusion of the middle cerebral artery. The occlusion can be permanent or transient: in the second case reperfusion can usually occur after 60, 90 or 120 minuts. This approach creates an unilateral stroke involving cortical and subcortical regions, but in the 12% of cases subarachnoid hemorrhage is observed, reducing cerebral blod flow bilaterally (Schmid-Elsaesser et al., 1998). MCAo lesions involve primarily striatum and overlying frontal, parietal, temporal, and portions of occipital cortex, but also variable damage in the thalamus, cervicomedullary junction, substantia nigra, and hypothalamus. The resulting deficit presents different motor, sensory and cognitive features, quite variable among animals. The major advantage of this technique is the fact that it mimics well what usually happens in humans. For example, this model in characterized by a wide penumbra, making this model particularly useful for neuroprotective studies (Cheng et al., 2004).

6.3 Endothelin-1

One of the most commonly used rodent models of stroke in the literature to cause focal ischemic damage in motor and somatosensory cortex is the local application of Endothelin-1 (ET-1), a potent vasoconstrictor. ET-1 is a 21 amino acids peptide produced by the vascular endothelium that binds to two receptor subtypes, ETA and ETB, both coupled to Gq proteins and localized to the endothelium and smooth muscle of blood vessels. Their activation causes the production of Inositol trisphosphate (IP3) and the resulting release of calcium ions from the sarcoplasmic reticulum (SR). The latter leads to an increase in the contraction of smooth muscles of the vessels thus inducing a vasoconstriction. Some of ETB receptors located in the endothelium also stimulate the formation of nitric oxide (NO) which, in the

absence of the activation of ETA and ETB of the smooth muscles of the vessels, produces vasodilatation.

The distribution of receptors suggests that the activity of ET-1 may cause a transient vasodilation - for initial activation of endothelial receptors - and hypotension, followed by a prolonged period of vasoconstriction and hypertension for ETA and ETB receptor activation on the smooth muscles. If injected directly into the brain tissue, therefore, ET-1 is able to reduce blood flow thus producing an extremely localized ischemic event (Kleim et al., 2007). The reduction of the blood flow is very rapid but not immediate, and after a few hours from the surgery reperfusion often occurs (Macrae et al., 1993). These effects make the model of ischemic induction by injection of ET-1 one of the most representatives of human stroke. Furthermore, the intracerebral injection of ET-1 produces a localized and dose-dependent injury and rarely leads to the formation of edema (Kleim et al., 2007); this allows to target the ischemic damage in a specific cortical or subcortical region, something difficult to achieve using methods of physical occlusion of blood vessels such as the middle cerebral artery occlusion (MCAO). However, the ET-1, its converting enzyme and both its receptor subtypes are not found exclusively at the level of endothelial cells but also at the level of the cell membrane of neurons and glial cells. This means that endothelin is able to activate a cascade of receptor-mediated signals between astrocytes and neurons that might interfere with the interpretation of the ischemic outputs (Carmichael, 2005). Moreover, the mechanisms of the interaction between ET-1 and its receptors are not completely understood (Kleim et al., 2007)

6.4 Photothrombosis

Another ischemic model for rodents that has become more and more diffuse in the scientific field is the phototrombotic stroke. Photothrombosis is a technique that allows to induce a cortical infarct by means of systemic injection of a photosensitive dye and the subsequent irradiation of a specific cortical area with a light beam (Watson et al., 1985). The most used dye used for this purpose is the Rose Bengal that could be administered directly in the tail vein or with an intraperitoneal injection. Rose Bengal has its peak of absorption in the green part of the spectrum (560 nm) and the size of the infarct volume induced (with the same concentration of the dye) could be adjusted by regulating the field aperture of the light source (Wang et al., 2010). The illumination can be delivered directly from the skull, so that this technique is not only quick, precise and reproducible but also minimally invasive. The local activation of the dye induces the generation of singlet oxygen that leads to focal endothelial damage and aggregation of platelets in all the brain vessels of the targeted area. The coagulation cascade determines the occlusion of the small vessels but not the generation of

a penumbra because of the rapid induction of edema and breakdown of the blood brain barrier (Dietrich et al., 1986). The lack of penumbra could be disadvantageous for preclinical studies of reperfusion or early interventions aimed at preserving the survival of the instable tissue. On the contrary, for investigations involving cortical plasticity and remapping induced by ischemic injury, restorative drugs and neuronal repair, phototrombotic ischemic model is highly useful (Durukan and Tatlisumak, 2007). Based on the original protocol for rats introduced by Watson et al. (1985), the phototrombotic model has been simplified and adapted for mice by Schroeter et al. (2002). The main advantage introduced by this work is the validation of irradiation parameters with a conventional cold white light source that simplifies the application of this technique (Schroeter et al., 2002).

Aim of the thesis

The aim of my PhD project was studying post-stroke functional plasticity in order to implement innovative therapies, taking advantage of some robotic tools for the training and assessment of the motor function, in a mouse model of stroke. I chose the photothrombotic model because it is a non-invasive procedure and allows an high reproducibility among animals, producing a well confined focal cortical stroke in the Caudal Forelimb Area.

The first part of the project regarded the assessment of the spontaneous evolution of the post-stroke neuropathophysiology. Firstly, I characterized the post-stroke motor deficit both in terms of general coordination (using Gridwalk and Schallert cylinder test) and during more skilled task (Single pellet reaching task) evaluating the motor features during the spontaneous recovery. Moreover, I implemented a semi-automatic system to extract the paw trajectory during a skilled reaching movement, with the final goal to evaluate in a detailed and objective way, the quality of the movement, therefore, distinguishing between true recovery and compensation during the healing process in my model.

Then, I focused my attention on the neuroplastic changes occurring spontaneously, and triggered by the ischemic lesion, in the perilesional area and in more distant cortical district in the injured hemisphere. For this purpose, I used neuroanatomical investigations of the perilesional tissue to evaluate changes in number of inhibitory interneurons populations as Somatostatin-, and Parvalbumin-positive cells, Perineuronal nets, and excitatory/inhibitory synapses. I also used electrophysiological investigations (Intracortical Microstimulation) to study the remapping of the injured motor and premotor cortex, taking into consideration also quantitative parameters such as responsive area and activation threshold of forelimb, hindlimb and tail maps.

The second part of the project concerned the implementation of novel therapeutic treatments based on focused motor training and stimulating neuroplasticity. Briefly, I modulated the GABA system using an inverse agonist of the $GABA_A$ receptor and evaluated the effectiveness during motor recovery. I also used a different approach, reversibly inhibiting the healthy hemisphere in the first weeks after stroke by means of Botulinum Neurotoxin injections.

In parallel I set up and characterized a robotic platform for the rehabilitation of the mouse forelimb, integrated with built-in sensors for an objective and quantitative feedback of the mouse performance.

I evaluated the effectiveness of all these strategies applied separately and then I combined them in order to gauge synergic effect when more therapies were employed at the same time.

Finally I started to explore the possibility to treat cortical stroke using transplants of in vitro differentiated neurons, reporting here some preliminary results.

Materials and Methods

Animals

All procedures were performed in compliance with the EU Council Directive 2010/63/EU on the protection of animals used for scientific purposes, and were approved by the Italian Ministry of Health. Every effort was made to minimize the number of animals used and their suffering. Adult male and female C57BL/6J mice - 2-6 months old, 28 ±5 g body weight - were used for the main part of the project.

For optogenetic experiments, transgenic mice B6.Cg-Tg (Thy1-ChR2/EYFP) 18Cfng/J (Jackson Laboratories, USA) were used (Lim et al., 2012).

All animals were housed in groups in standard cages with a 12-hour/12 hour light/dark cycle, 20°C and 40% RH. When not trained or subjected to behavioural tests, animals had food (Pellet Diet Standard, Mucedola S.r.l.) and water available ad libitum.

Photothrombotic lesion

The photothrombotic lesion was induced as previously described (Lai et al., 2015b). Briefly, animals were anesthetized with Avertin (20ml/kg, 2,2,2 tribromoethanol 1.25%; Sigma-Aldrich, USA) and placed in a stereotaxic apparatus. After a midline scalp incision, the bone was carefully dried and cleaned. Rose Bengal (0.2 ml of a 10mg/ml solution in PBS; Sigma Aldrich) was injected intraperitoneally. After 5 min, the brain was illuminated through the intact skull for 15 min using a cold light source (ZEISS CL 6000) linked to a 20X objective that was positioned 0.5 mm anterior and 1.75 mm lateral from Bregma (i.e. in correspondence with the caudal forelimb area; Tennant et al. 2011; Vallone et al. 2016). Sham animals underwent scalp incision and Rose Bengal injection but no light irradiation. At the end of the surgery, the skin was sutured and mice were allowed to awaken from anaesthesia.

ET-1 induced lesion

For the characterization of the robotic platform, the ischemic cortical lesion was induced by intracortical delivery of Endothelin-1 (ET-1, Sigma, Italy). Mice were anesthetized with Avertin, placed in a stereotaxic apparatus and body temperature was maintained at 37°C. Injections were performed within the Caudal Forelimb Area (CFA) of the right hemisphere.

The stereotaxic coordinates were defined according to the mouse atlas by Paxinos and Franklin. I used 3 sites, where ET-1 (1 µg/µl in sterile saline, 200 nl per site) were injected, to target the core of CFA. The coordinates for injection, all in mm and relative to bregma were: (i) +0.5 antero-posterior, +1.7 medio-lateral; (ii) –0.25 antero-posterior, +1.7 medio-lateral; (iii) 0.0 antero-posterior, +1.25 medio-lateral. The solution was injected by means of heat-pulled glass micropipettes (Harvard Apparatus, USA) at 700 µm cortical depth.

Motor tests

Gridwalk Test

Animals were allowed to walk freely for 5 minutes on an elevated grid (32 x 20 cm, with 11 x 11 mm-large openings) and the task was video-recorded. The video recordings were analyzed off-line by means of a custom-designed Graphical User Interface implemented in Matlab (Lai et al., 2015b) by an experimenter blinded to the experimental group. Correct steps and foot-faults, i.e. steps not providing body support, with the foot falling into grid hole were assessed and the percentage of foot faults for each limb was then calculated, as previously described (Lai et al., 2015b).

Schallert **Cylinder Test**

Animals were placed in a Plexiglas cylinder (8 cm diameter, 15 cm height) and recorded for 5 minutes by a video-camera placed below the cylinder. Videos were analyzed frame by frame and the spontaneous use of both forelimbs was assessed during exploration of the walls, by counting the number of contacts performed by the paws of the animal. The experimenter was blinded to the experimental group. For each wall exploration, the last paw that left and the first paw that contacted the wall or the ground were assessed. In order to quantify forelimb-use asymmetry displayed by the animal, an Asymmetry Index was computed, according to Lai et al. (2015).

Skilled Reaching Test

The percentage of correct movements and the kinematic analysis of the whole reaching movements were performed as previously described (Lai et al., 2015b). Briefly, animals (food deprived for 15 hours) were placed in a testing chamber with transparent walls and trained to

perform a skilled reaching task with their preferred paw, which had to pass through a small frontal rectangular aperture (0.5 x 1.3 cm) to grasp and retrieve food pellets. The task was recorded by a high frame-rate video camera (Hero 3, GO-Pro, USA), placed on the side of the testing chamber thus allowing for a sagittal view of the animal.

The shaping phase consisted in 2 days of habituation, in which a few pellets were placed inside the chamber. During the next phase, animals were trained daily until they reached 30 pellets in a single session (each lasting maximum 20 minutes). Animals were trained for a couple of weeks until they reached a plateau in the performance. Animals that did not reached a good performance (60% of correct grasping per session) were excluded from the study. The baseline value was obtained using the average of the last 3 sessions prior to the stroke. After the ischemic lesion animals were tested once a week without any additional training sessions.

The number of correct (i.e., a reach and grasp movements ending with pellet eating) and incorrect movements (i.e., when the mouse passed by the frontal window and reached the pellet but missed it or dropped the pellet after grasping it) were manually assessed. Then the percentage of incorrect grasping was calculated over the total attempts (i.e. total number of times that the paw crossed the frontal window).

Open Field

Thirty minutes after DMCM treatment, animal were placed in a Plexiglass 60 cm x 60 cm arena with a white background and black walls for 10 minutes. The position of the animal during the test was automatically tracked using EthoVision XT (Noldus, Netherlands) and the total distance travelled was computed at the end of each experimental session.

Kinematic analysis of the reaching movement

Setup

Mice were trained to perform a skilled reaching task in a testing chamber, TC (13.5 x 5 x 9 cm) housed into an U-shaped plastic case (30 x 20 x 21 cm). The TC was made of black plastic (Delrin®, Du Pont™,Wilmington, DE, USA) except for the frontal, bottom and lateral sides, which were made of Plexiglas (5 x 4.7 x 5 cm). The front wall of the TC had a small rectangular aperture (0.5 x 1.3 cm) 3 mm from the floor. During the task, the paw passed through the aperture to reach for a food pellet, placed in a slot 8 mm distant from the

aperture. Below the transparent floor, a 45°-tilted mirror (6 x 3.7 cm) enabled the experimenter to view the animal from the bottom (**Figure 1A**).

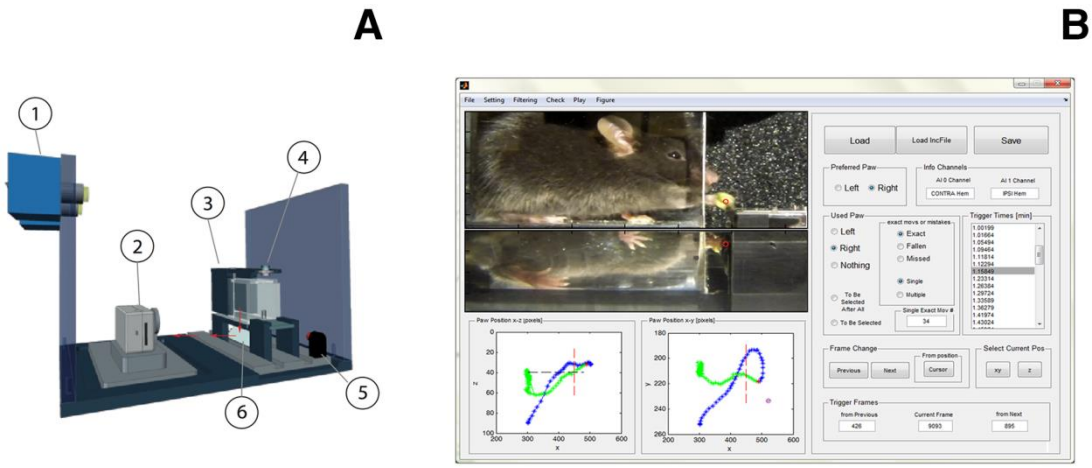

Figure 5. Experimental setup. (A) Schematic representation of the Apparatus, which consists of a cold-light source (1), a digital video camera (2), a testing chamber (3), a photo-cell (4), a red LED (5) and a mirror (6). (B) Snapshot of the Graphical User Interface for the off-line trajectory tracking. The left part allows for visualization of both the recorded video and the reconstructed trajectory on the sagittal (x,y) and coronal (x,z) planes. The right part allows the experimenter to select a specific trial, to navigate across frames, and to mark key features.

A photo-detector, placed on the top of the TC, was aligned with a photo-diode placed under the slot containing the pellet, such that whenever the animal grasped the pellet, the photocell switched a red LED (*Feedback LED*) on. Reaching and grasping movements were recorded at 120 frames/s by a digital video camera (Hero 3, GO-Pro, San Mateo, CA, USA), placed on a fixed support 13 cm from the TC. The camera was equipped with a macro lens (x10) and a Blurfix adapter to correct optical distortions in the acquired images. Appropriate lighting conditions were guaranteed by a cold-light source (CL 6000, ZEISS, Oberkochen, Germany). Before testing, both the palm and the back of the forepaw were painted with a green non-toxic dye (Stabilo Boss, Stabilo, Heroldsberg, Germany), which dried in a few minutes (**Figure 5B**).

Algorithm and Interfaces for offline analysis

Reconstruction of paw trajectories was performed off-line by a semi-automated algorithm based on color contrast analysis. The algorithm only required limited inputs from the experimenter, who interacted via a Graphical User Interface (GUI, **Figure 5B**). Both the tracking algorithm and the GUI were programmed in Matlab® (MathWorks, Natick, MA, USA).

The tracking process consisted of three distinct phases. In phase (i), the algorithm synchronized the recorded video and the photocell signal, which were acquired

independently. Based on the switching times of the photocell, the video was segmented into short clips, each of which demonstrated a grasping attempt by the mouse. To discard clips not related to pellet grasping (e.g., the photocell switched because the experimenter was handling the pellet), the algorithm checked for the presence of the pellet in its slot in selected frames before each switch activation by asking the user to locate the pellet in the first frame via the GUI.

Before extracting the paw trajectory, the algorithm asked the user to select a part of the green area denoting the paw (*Paw area*) in a few (n<5) initial frames. The algorithm used these pixels to define three average values (μ_k), and the corresponding confidence intervals (*gCIs*), of each RGB component of the green dye (k=1, red; k=2, green; k=3, blue), which would be used in phase (ii) to locate the paw in all of the subsequent frames.

In phase (ii), the x (antero-posterior), y (dorso-ventral) and z (medio-lateral) Cartesian coordinates of paw position were automatically extracted from each frame of a grasping attempt. Trajectories were composed of 321 points (i.e., they described a ~3s long paw movement), and the central point (*i*=160) corresponded to the switching time of the photocell. To extract paw position from a frame, the algorithm searched for green spots within the image. The RGB color components of all of the pixels in the frame were compared with the *gCIs,* and the groups of pixels with color levels included in the *gCIs* were selected as possible regions of interest (pROI). In case of multiple pROIs, the algorithm looked for the largest region with the most similar colors with respect to the *Paw Area* selected by the user. A metric *m* assessing both spatial extent (*Area*) and color levels (d_{Col}) was computed for each pROI:

$$m = \frac{Area(pROI)}{d_{Col}}.$$

The parameter d_{Col} is defined as:

$$d_{Col} = \sum_{k=1}^{3} abs\left(\frac{1}{n}\sum_{i=1}^{n} X_{i,k} - \mu_k\right)$$

and weights the difference between the RGB components of all *n* pixels in the pROI, $X_{i,k}$, and the central values of the *gCIs*, μ_k. The pROI with the largest value of *m* was chosen as the best candidate among the pROIs, and the coordinates of its centroid were selected as the new paw position. Although not used in the following analyses, the z-coordinate of the paw could also be detected by applying a similar procedure to the plane (x, z). Once the paw position was extracted for all 321 frames, a 3rd order Savitzky-Golay Filter was applied to smooth the trajectory.

In phase (iii), the user had to perform a quick review of the extracted trajectories, and assign them to three categories: *exact*, i.e., a reach and grasp movement ending with pellet

eating; *missed*, if the mouse reached for the pellet but missed it or knocked the food away; and *fallen*, if the animal dropped the pellet after grasping it.

Analysis of the movement

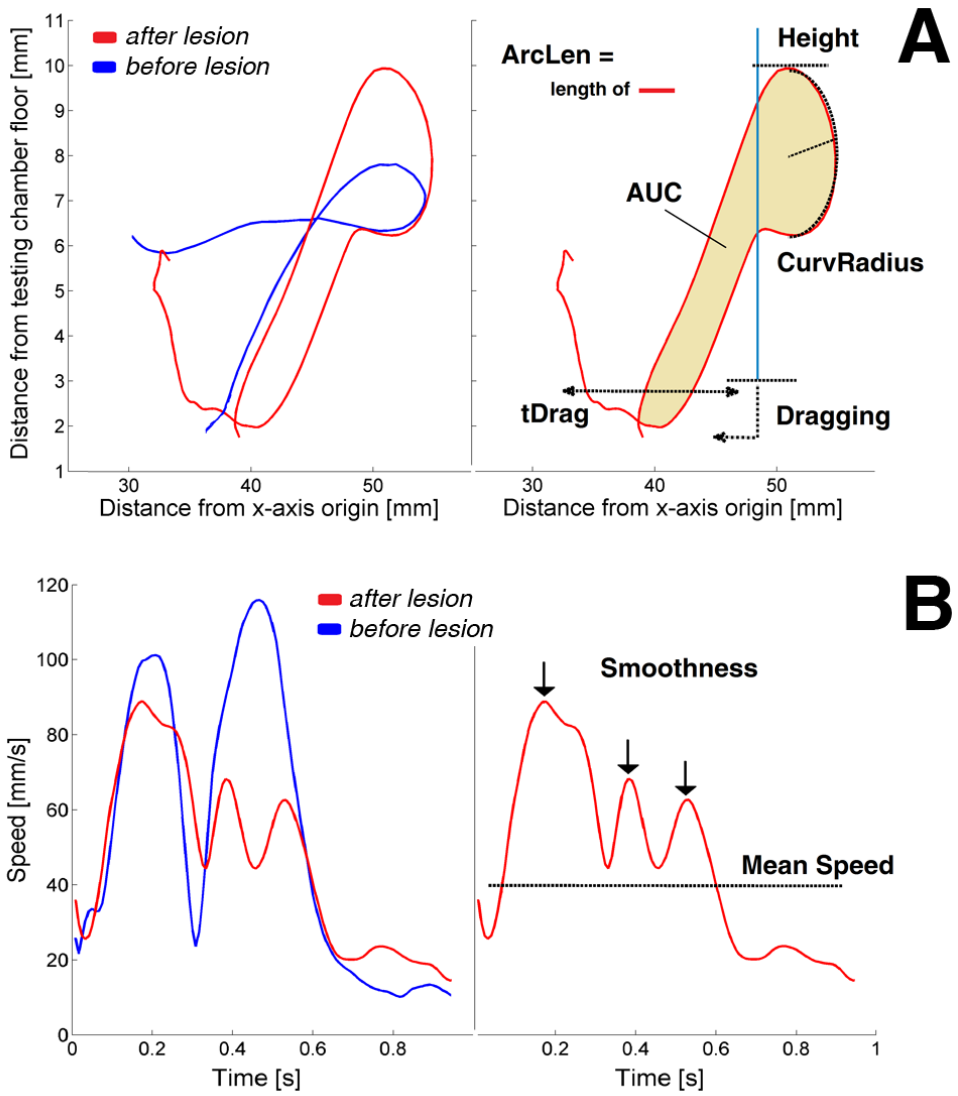

Figure 6 Reaching trajectories and extracted kinematic parameters. (A) On the left, average trajectories recorded before (blue) and after stroke (red) during two experimental sessions of the same mouse. On the right, kinematic parameters extracted from the Cartesian components of the trajectories. The vertical sky blue line symbolizes the position of the aperture the animal has to pass through to reach for pellets. (B) On the left, average tangential velocity profiles measured before (blue) and after stroke (red). On the right, parameters extracted from speed curve.

To ensure consistency, only trajectories from successful (*exact*) trials were considered. Paw positions from non-informative video frames (i.e., those preceding the beginning of the movement or following task completion) were automatically removed from the trajectory. Based on previous studies on the kinematics of post-stroke upper limb movements in

humans (Cirstea and Levin, 2000; Rohrer et al., 2002; Subramanian et al., 2010; Alt Murphy et al., 2011, 2013; Hogan and Krebs, 2011; Panarese et al., 2012; van Dokkum et al., 2014), several kinematic measures were computed to detect overall and local modifications of paw movements before vs. after stroke (**Figure 6**).

Overall changes include variations in the length of the end-point trajectory (*ArcLen*), the area enclosed by the curve (*AUC*), the average tangential velocity (*Mean Speed*) and the movement smoothness, quantified by the number of peaks in the tangential velocity profile (*Smoothness*).

Local curve modifications take into account changes in the maximum height reached by the paw during the movement (*Height*), the curvature of the trajectory when the paw approaches the pellet (*CurvRadius*), the fraction of the total trials during which a dragging movement occurs (*Dragging*) and the duration of dragging (*tDrag*). Dragging was automatically detected when the height of the paw during the retraction phase and upon crossing the aperture in the front wall remained below a threshold, *hT*, for at least a fixed time period, *tT*. The threshold *hT* was set at 3 mm from the floor of the testing chamber (i.e., corresponding with the bottom side of the aperture in the wall), while *tT* was set as 2**tCA*, where *tCA* was the mean time required to retract the paw from the pellet slot to the aperture for each animal. This allowed us to take into account the inter-individual variability in speed of the retraction movement.

Intracortical Microstimulation (ICMS)

Animals were anesthetized using a ketamine (100 mg/kg) and xylazine (10mg/kg) cocktail. A stable level of anaesthesia was maintained delivering 1/10 of the starting dose every 30 minutes. Animals were placed in a stereotaxic apparatus, the skull was exposed and a craniotomy (extending 3 mm and 4mm in the medio-lateral and antero-posterior direction, respectively) was performed in the ipsilesional hemisphere.

The cortex was stimulated through a tungsten microelectrode (1 MΩ, FHC, USA), inserted slowly into the brain at 700 µm depth for each stimulation point, following a grid with nodes spaced 250 µm. The ground electrode was placed under the skin of the neck. As reported in Tennant et al., 2011, at each penetration site, a 40 ms train of 13 cathodic current pulses (0.2 ms duty cycle) was delivered at 350 Hz from an electrically isolated, constant current stimulator (World Precision Instruments Inc., USA) guided by an electronic board (National Instruments Corp, USA). The amplitude of the pulses was increased from a minimum of 20 µA to a maximum of 60 µA (with steps of 10 µA). Movements of several body parts were collected by a second experimenter, blinded to the stimulation coordinates in the grid. At the end of the ICMS procedure, the animal was sacrificed and the brain dissected for histology.

Data Analysis

Data collected during ICMS were analyzed through a custom made algorithm developed in Matlab (Mathworks, USA).

The body part (BP) maps (e.g. the stimulation maps for contralateral forelimb, contralateral hindlimb and tail) were obtained as follows. For each animal a matrix, with the same size of the stimulation grid (240 elements), was created for each BP and different stimulation current. Every element of the matrix indicates the presence/absence of the movement referred to the specific BP. The matrices of the single animals were then averaged into a mean map of 240 squares, each one depicted with a colorimetric index showing the probability to evoke the BP movement (Probability of Activation – *PA*). For each *j-th* site (j=1,..,NS, where NS is the number of stimulated sites*)* the *PA* was computed as follows:

$$PA_j = \frac{Ra_j}{Na}$$

where Ra_j is the number of animals showing the BP movement following the stimulation of the *j-th* site and *Na* is the total number of animals for each experimental group.

To improve the visual resolution, the matrix was 10-fold upsampled and Gaussian filtered.

Since the distance between adjacent sites was 250 μm, the areas of 250 x 250 μm^2 centred at the each site were considered to calculate the *Percentage of Responding Area* (i.e. percentage of stimulated area which elicits the BP movement, for a specific amplitude of stimulation current) of the whole maps:

$$\%\ of\ Responding\ Area = \frac{K \times (250\ \mu m)^2}{Total\ Area} \times 100$$

where *K* is the number of responsive sites and *Total Area* is defined as $NS \times (250\ \mu m)^2$, where *NS* is number of total stimulated sites.

For each animal, the *Minimum Current Threshold* was defined as the mean lowest current amplitude needed to evoke a movement of a specific BP.

Multiple sites analysis was performed taking into consideration 3 BPs: the contralateral forelimb, the contralateral hindlimb and the tail, since I observed a widespread activation of these BPs after stroke. For each stimulation intensity, the analysis was performed by clustering sites into 3 classes: (i) sites evoking movements of a single BP (i.e. only forelimb); sites evoking movements of two (ii) or three (iii) BPs at the same time (i.e. forelimb, hindlimb and tail).

I also quantified how each cortical site changes its forelimb preference after the ischemic injury. I was interested in those sites that maximized the difference in forelimb activation probability in sham and stroke animals, i.e. those sites that had a high (or low) probability to

evoke a forelimb movement in the sham group and a low (or high) probability to elicit forelimb movement after stroke. Thus, I defined a novel parameter, the Transition Index (TI), which shows the sham-stroke difference in forelimb activation probability. In order to quantify the TI amplitude, which shows the extent of the sham-stroke change, the average probability matrices of forelimb activation (*fPA*) and non-activation (*nfPA*) in sham and stroke groups were computed with a stimulation current of 30 µA. The *fPA* matrix is the PA matrix (see previous definition) computed with BP = {forelimb}, whereas *nfPA* is the *PA* matrix with BP = {non-forelimb}. For each *j-th* site (j=1,..,N, where N=240*)*, the amplitude of the TI was defined as an Euclidean distance:

$$TI_j = \sqrt{\left(\Delta P_{(sham)\ j}\right)^2 + \left(\Delta P_{(stroke)\ j}\right)^2}$$

where $\Delta P_{(sham)\ j} = (fPA_j - nfPA_j)$ for sham animals, whereas $\Delta P_{(stroke)\ j} = (fPA_j - nfPA_j)$ for stroke animals. Accordingly to this definition the TI value is defined within a range of $\pm\sqrt{2}$. Since I focused only on sites that inverted their *ΔP* after stroke (i.e. $\Delta P_{(sham)}$ and $\Delta P_{(stroke)}$ have different signs), I did not consider cases with $\Delta P_{(sham)}$ and $\Delta P_{(stroke)}$ with the same sign, thus arbitrarily setting the TI of these sites to zero. In the other cases, the sign of TI (sTI) that shows the direction of the change, was assigned accordingly as follow: (i) when $\Delta P_{(sham)} > 0$ and $\Delta P_{(stroke)} < 0$ then sTI was defined positive (i.e. loss of forelimb movements); (ii) when $\Delta P_{(sham)} < 0$ and $\Delta P_{(stroke)} > 0$ then sTI was defined negative (i.e. gain of forelimb).

Immunohistochemical analysis

At the end of the experiment, all animals were transcardially perfused with 4% paraformaldehyde. Brains were cut using a sliding microtome (Leica, Germany) to obtain 50-µm thick coronal sections that were used for immunostaining of NeuN (1:1,000, Millipore, Germany), Perineuronal Nets (Wisteria floribunda agglutinin, WFA; 1:100, Sigma, USA), Parvalbumin (1:300, Synaptic Systems, Germany), Somatostatin (1:400, Millipore, Germany), MBP (1:500, Millipore, Germany), (1:800, Synaptic Systems, Germany), V-GluT1 (1:1,000, Synaptic Systems, Germany). The number of Perineuronal Nets, Parvalbumin- and Somatostatin-positive neurons, was analyzed using a fluorescence microscope (Zeiss, Germany) with a 10x objective, counting in a 200 µm wide cortical column drawn at the medial and lateral edge of the ischemic tissue by Stereo Investigator software (MBF Bioscience, USA). MBP mean fluorescence was measured only in the lateral 200 µm wide column. Images were acquired using a Zeiss Fluorescence microscope and the mean fluorescence for each column was computed using Image J. Data are reported as number of cells for each columns. For immunohistochemical analysis after the combined therapy

(BoNT/E + Robot) data from lateral and medial column were pooled together so results indicates the number of cells for 400 µm wide columns. For all these analyses three sections per animal were analyzed.

The V-GAT e V-GluT1 signals were acquired using a confocal microscope (Leica, Germany) with a 63x objective and a 2.5 digital zoom, in medial-superficial/deep and lateral-superficial/deep regions in the perilesional tissue (**Figure 7)**.

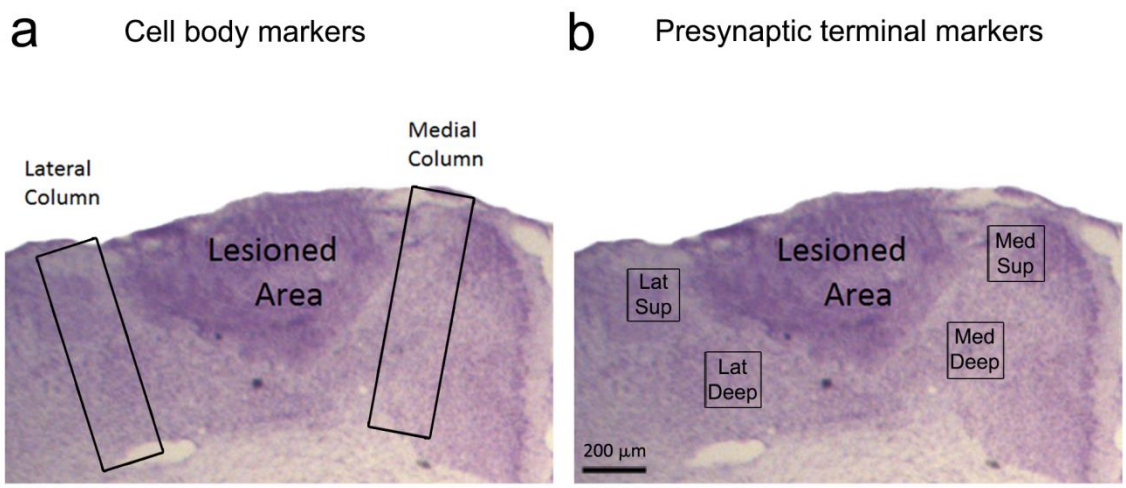

Figure 7 Location of counting boxes for the immunohistochemical analyses. (A) Cell-counting scheme for PNNs, PV-+, SOM-+ cells and MBP signal, superimposed on a representative Nissl staining of a cortical section. Two cortical columns (200µm wide) adjacent to the lesion have been analyzed for each section. (B) Scheme for the fluorescence analysis of the presynaptic terminal markers. Four regions has been taken into consideration: Lateral-superficial layers (Lat Sup), Lateral-deep layers (Lat Deep), Medial-superficial layers (Med Sup) and Medial-deep layers (Med Deep).

Three fields (95 µm x 95 µm) for each location were acquired (three sections per animal). Acquired images were processed using Metamorph software (Molecular devices, USA) to analyze the mean fluorescence in the entire image and in puncta rings regions by an experimenter blinded to the group (Cerri et al., 2011; Restani et al., 2011; Deidda et al., 2015). To minimize variations due to the different quality of the immunostaining in individual mice/sections, fluorescence in perilesional areas was normalized to values calculated in three reference fields taken in the basal cortices of each analyzed coronal section.

To evaluate the effect of BoNT/E injected into the motor cortex, I stained cortical sections with antibodies recognizing either the intact or BoNT/E-truncated forms of SNAP-25 (Caleo et al., 2007; Antonucci et al., 2010). The analysis was performed 3 days after BoNT/E injections.

To quantify the lesion volume, 1 out of every 6 sections was stained with Hoechst 33258 (Sigma-Aldrich, USA). The ischemic region was contoured using a 10x objective and its area measured. The lesion volume for each animal was calculated by summing up all damage

areas and multiplying the number by section thickness and by 6 (the spacing factor). A total infarction volume in mm^3 is given as the mean ± standard error of all analyzed animals.

DMCM treatment

DMCM (methyl-6,7-dimethoxy-4-ethyl-beta-carboline-3-carboxylate) (Tocris, United Kingdom) was reconstituted in sterile water to obtain a concentration of 4 mg/ml. The DMCM treatment started at day 3 post lesion and continued up to day 8. DMCM (1.5 mg/kg) was delivered intraperitoneally under brief isoflurane anaesthesia twice a day, 10 hours apart. Behavioural effects of this dose of DMCM were verified in naïve mice by quantifying total distance travelled in the open field 30 minutes after a single DMCM injection.

Optogenetic recordings

Sham and 30 days injured mice were anesthetized with an initial cocktail of ketamine (100 mg/kg, i.p.) and xylazine (10 mg/kg, i.p.) that was supplemented with additional doses to maintain the plane of anesthesia. Each animal was then placed in a stereotaxic apparatus and a midline incision was made to expose the skull and the sutures.

A 3 x 3 mm craniotomy centered at 2mm anterior and 1.2 mm lateral to Bregma (corresponding to the RFA (Tennant et al., 2011; Vallone et al., 2016)) was performed in both hemispheres of the anesthetized animal. The dura mater was left intact, and a recording chamber of dental cement (Ivoclar Vivadent Inc., New York, USA) was made to preserve and moisten the tissue with saline or for local drugs application. The tip of the optic fiber was positioned stereotactically over the dura mater of the RFA in one hemisphere.

Optogenetic stimulation was delivered by means of PlexBright Optogenetic Stimulation System (Plexon Inc, USA) with a PlexBright LD-1 Single Channel LED Driver (Plexon Inc, USA) and a 456 nm Table-top LED Module connected to a 200 μm Core 0.39 NA optic fiber (Thorlabs Inc, USA). Stimulation parameters were commanded by a custom-made software developed in Matlab (Matlab, Matworks) and a USB DAQ board (NI USB-6212 BNC, National Instruments, USA).

Neuronal activity was recorded in the other hemisphere by means of 16 channels linear probes (NeuroNexus, Michigan, USA), connected to the OmniPlex D Neural Data Acquisition System (Plexon Inc, USA). Signals were acquired at 40.000 Hz and amplified 1K.

Quantification of the first negative and second peaks currents has been made by measuring the amplitude of the peak-baseline amplitude for each component, using a custom-made Matlab Interface. For all animals in each group, the quantification of the FP was performed in

the 13th channel (≈650μm deep from the cortical surface) following stimulation with single light pulses at 3 mW power.

Silencing of the healthy hemisphere with Botulinum Neurotoxin

To validate the hypothesis that loss of the normal inter-hemispheric balance with an excessive inhibition targeted by the healthy hemisphere over the perilesional tissue could impair stroke recovery, I decided to test the effect of transient inhibition of the healthy hemisphere, alone or in association with robotic therapy, on forelimb motor outcomes in our mouse model of phototrombotic stroke.

Toxin injections were performed in the same surgical session of phototrombotic lesions; after 15 minutes of illumination that caused the Rose Bengal activation, the dura mater of animals was exposed in the non-injured hemisphere by means of a dental drill. I injected 500 nl of BoNT/E (80 nM) or vehicle divided in 2 different injections of 250 nl at (i) +0.5 anteroposterior, +1.7 mediolateral and (ii) +0.4 anteroposterior, +1.7 mediolateral by means of heat pulled glass micropipettes (Harvard Apparatus, Holliston, MA) at 700 μm cortical depth. After toxin infusion, the micropipette was left in place for at least 5 minutes. After surgery, animals were sutured and treated with paracetamol (100 mg/kg) in drinking water for 4 post-operation days.

Western blotting

Brains were rapidly removed, and motor cortex were dissected and frozen on dry ice. Proteins were extracted with lysis buffer (20 mM Tris-HCl, pH 7.45, 150 mM NaCl, 10 mM EDTA, 0.1 mM Na3VO4, 1 mM PMSF, 1 μg/ml leupeptin, 1 μg/ml aprotinin, 1% Triton X-100, and 10% glycerol), and total concentration of the samples was assessed with a protein assay kit (Bio-Rad) using a bovine serum albumin-based standard curve. Total proteins loaded per lane were 15 μg and were separated by electrophoresis and blotted; filters were blocked and incubated overnight at 4°C with primary antibodies (anti-cleaved and anti-intact SNAP25 at 1:1000; Sternberger Monoclonals, Lutherville, MD). Filters were also probed with anti-α-tubulin antibody (polyclonal, 1:15,000 dilution; Abcam) as an internal standard for protein quantification. Blots were then rinsed [0.2% Tween 20 added to PBS (TPBS)], incubated with secondary antibodies conjugated with infrared-emitting dyes (anti-rabbit IRDye 680LT at 1:30,000 or anti-rabbit 800CW at 1:20,000; Li-Cor Biosciences), washed in TPBS, and briefly

rinsed in PBS. Filters were scanned using an Odyssey IR scanner (Li-Cor Biosciences), and images were acquired with Image Studio software version 3.1 (Li-Cor Biosciences).

Robotic rehabilitation

The robotic platform

Our robotic system (dimensions 300 x 300 mm) was composed of a linear actuator (Micro Cylinder RCL, IAI, Industrieroboter GmbH, Germany), a 6-axis load cell (Nano 17, ATI Industrial Automation, Garner, NC, USA), a precision linear slide (IKO BWU 25-75), and a custom-designed handle that was fastened to the mouse wrist (Fig. 1A). The handle was composed of two hinged parts, an upper (UC) and a lower (LC) component, which had a semicircular groove (1.15 mm radius) and one magnet stuck near the hinge to help in maintaining the UC and LC juxtaposed. One extremity of the LC was screwed on the load cell for lossless transfer of the forces to the sensor; the other end formed a support for the animal wrist by allowing a comfortable fixing (i.e., no compression) without letting the forepaw slide through.

During the task, the animal was kept in a U-shaped restrainer (interior dimensions 35 x 80 x 30 mm), and its head was fixated by means of a post cemented to the skull and connected to a translation stage (Melles Griot 2493M). In each trial, the linear motor pushed the handle and extended the mouse forelimb (passive phase); then, it quickly decoupled from the slide and retracted, such that the animal had to voluntarily pull back the handle (active phase) to move the slide. Mice pulling attempts resulted on handle displacements whenever the applied force level overcame the static friction resisting to sliding movements (F_s = 20 mN). A Hall effect position sensor (SS495A1, Honeywell International Inc.) and a tone generator were included for detecting and signalling task initiation and completion. A peristaltic pump (80204 Liquid Pump, Campden Instruments Ltd) was used for liquid reward (apple juice or milk) delivery.

Custom-made standard circuitry for Nano17 signal conditioning was developed, achieving a resolution of 2.5 mN RMS (Root Mean Square), in all directions and a bandwidth of 0–1.2 kHz. Force signals were acquired and digitized (16 bits) using a USB DAQ board (USB-M6251, National Instruments Corp., USA). A Programmable Logic Controller (PLC) was used to control the linear actuator (ACON-CG, IAI, Industrieroboter GmbH, Germany). A custom-

made interface circuitry between the PLC and the DAQ board was developed, capable to shift voltage levels and making communication between the two devices possible.

A linear encoder embedded in the actuator monitored the position of the handle during the passive phase of the protocol. The repeatability of the system during this phase was characterized by the Repeatability Standard Deviation (RSD) computed according to ASTM International, 2009. The RSD is the RMS value of the standard deviation (SD) of position signals acquired while imposing the same trajectory repeatedly. The RSD was calculated on 540 repetitions of the passive phase of the protocol performed by two different mice (270 repetitions per mice). The RSD was 0.085 mm on a range of 10 mm.

During the active phase of the protocol, the position of the handle was monitored with a video camera (MVX3i, Canon). A black squared marker (5x5 mm) fixed to the linear slide was used as a reference. The handle was rigid (Young Modulus ≈ 2.5 GPa) and assembled on the linear slide, such that the variation in position for the two components was basically the same. Signals from the video camera were analyzed offline. The video was synchronized with the force signal from the load cell. A custom made Matlab algorithm was used to extract the position values from the recorded video frame by frame. To obtain speed values, a conventional five-point method to compute the first derivative of the position in time was used (Abramowitz and Stegun, 1964).

Head fixation surgery

Mice were anaesthetized with Avertin (2.5% W/V Tri-Br-Ethanol (Sigma, Italy) in 5% V/V Tert-amyl alcohol in water; 0.02 ml/g) and placed in a stereotaxic apparatus. Using a motorized micromanipulator (Sutter Instruments, USA), a metal post (length 8 mm, diameter 2 mm, weight 0.2 g) was placed on the occipital bone and fixed by means of dentistry cement (Paladur, Pala, Germany).

Shaping and training on the platform

Mice were food-deprived for 16 ± 1 h before testing on the robotic platform, which was always performed at the same hour in the morning. At least two consecutive days were devoted to habituate the animals to stay in the test chamber and to associate the reward, provided at regular intervals, with a tone. Then, the animal's wrist was positioned in the handle and the following 2-3 days were needed to let the animal associate the reward with the end of the retraction task.

After the shaping phase, the animals were subjected every day to experimental sessions within the robotic platform. An average of 15 trials per session were performed before the animals become satiated by the liquid reward and lost their motivation, i.e., they stopped licking the milk drop from the gavage needle.

The training protocol consisted of a passive and an active phase. During the first one the actuator extended the mouse forelimb from the resting position (RP) to the maximum extension position (MEP, 10 mm from RP). Then, the actuator was turned off and a tone (Ts1 = 0.50s) informed the mouse about the task initiation. During the active phase, the animal performed the task by flexing the forelimb and pulling back the handle up to the RP. A different tone (Ts2 = 1.00s) signaled task completion and the peristaltic pump automatically supplied a liquid reward (10 µl milk) only when the handle reached the RP. Finally within a fixed time delay (T2 = 5.00 s) the animal could drink the reward before starting a new cycle.

Cell transplants in adult mice

Mice were anesthetized with Avertin (20ml/kg, 2,2,2 tribromoethanol 1.25%; Sigma-Aldrich, USA) and placed in a stereotaxic apparatus. Injections were performed within the right hemisphere. The stereotaxic coordinates were defined according to the mouse atlas by Paxinos and Franklin and previous intracortical mapping studies. For injections in normal animals I targeted the motor cortex (+0.5mm antero-posterior, +1.75mm medio-lateral from Bregma and 750µm cortical depth), or the hippocampus (-2mm antero-posterior to bregma; 1.5mm lateral and 1.7mm from the cortical surface). For post-stroke injections I targeted the core of the ischemic lesion (+0.5mm antero-posterior, +1.75mm medio-lateral from Bregma and 750µm cortical depth) and the perilesional area posterior to the stroke (-1.75mm antero-posterior, +1.75mm medio-lateral from Bregma and 750µm cortical depth).

100,000-150,000 cells/µl were injected per each site using a syringe pump (Legato™ 130, KD Scientific, infusion speed: 0.5µl/min; total volume 1µl). At the end of the surgery, the skin was sutured and mice were allowed to awaken from anaesthesia.

Statistical Analysis

All statistical tests were performed using SigmaPlot 11.0 (Systat Software Inc, USA). For behavioural tests (gridwalk test, Schallert cylinder test, open field and skilled reaching test) a Two Way Repeated Measures ANOVA was used followed by a Tukey's Test. To assess variations between baseline and post-treatment values of the kinematic parameters, all values were normalized to baseline and a Kruskal-Wallis test was used, followed by Tukey's

post-hoc analysis. To compare performance on the robotic platform before and after vehicle injections, the Mann–Whitney rank sum test was used.

For Immunohistochemical analysis t-test, One Way ANOVA was used followed by a Holm-Sidak test, or ANOVA on ranks followed by Dunn's test when the sample failed the normality test. For intracortical microstimulation data a T-test was used. All statistical analyses were performed on raw data (alpha value 0.05).

Results

1. Deficits in forelimb function following stroke

I induced a focal injury in the caudal forelimb area (CFA) of the mouse motor cortex using Rose Bengal-mediated photothrombosis (Lai et al., 2015b). The ischemic lesion was confined to the targeted cortical area of the illuminated hemisphere. The histopathological analysis was conducted 30 days after the ischemic injury and showed that the lesion volume was 1.03±0.18 mm^3. Anteroposterior reconstruction of the lesion showed that the ischemic damage remained confined into the CFA and did not involve the Rostral Forelimb Area (between +1.5 and +2.25mm anterior to bregma suture) and the hindlimb representation (between -0.75 and -1.25mm posterior to bregma) according to average maps obtained by (Tennant et al., 2011) (Figure 1a). Coronal sections of the ischemic brains demonstrated a complete loss of neurons in the core of the infarct, and well-defined boundaries that separate the lesion from the healthy perilesional tissue (**Figure 8b**).

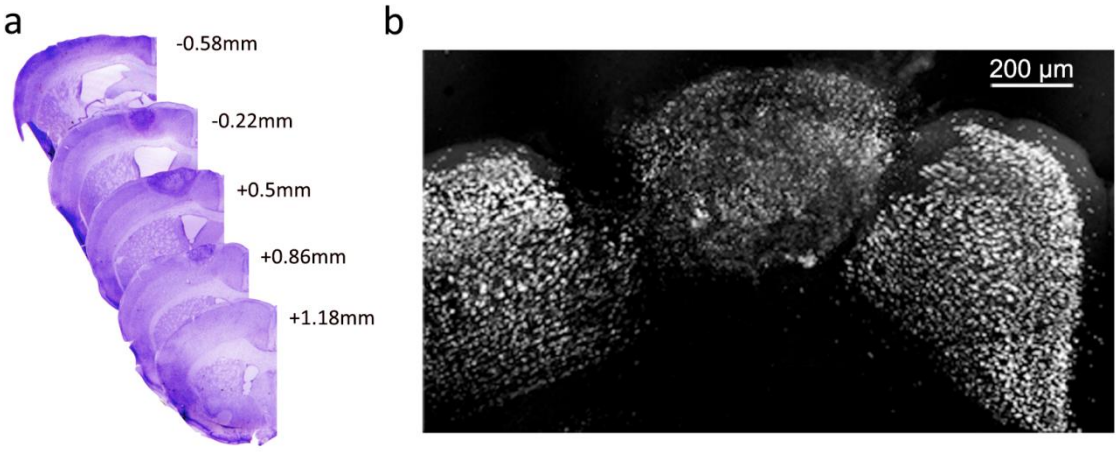

Figure 8. Stroke-induced neuronal damage. (a) anteroposterior reconstruction of the photothrombotic lesion covering the CFA (b) Representative NeuN immunostaining of the phothrombotic lesion in a coronal brain section. The boundaries of the ischemic region are clearly evident and the core of the lesion shows loss of NeuN staining. Scale bar = 200 µm.

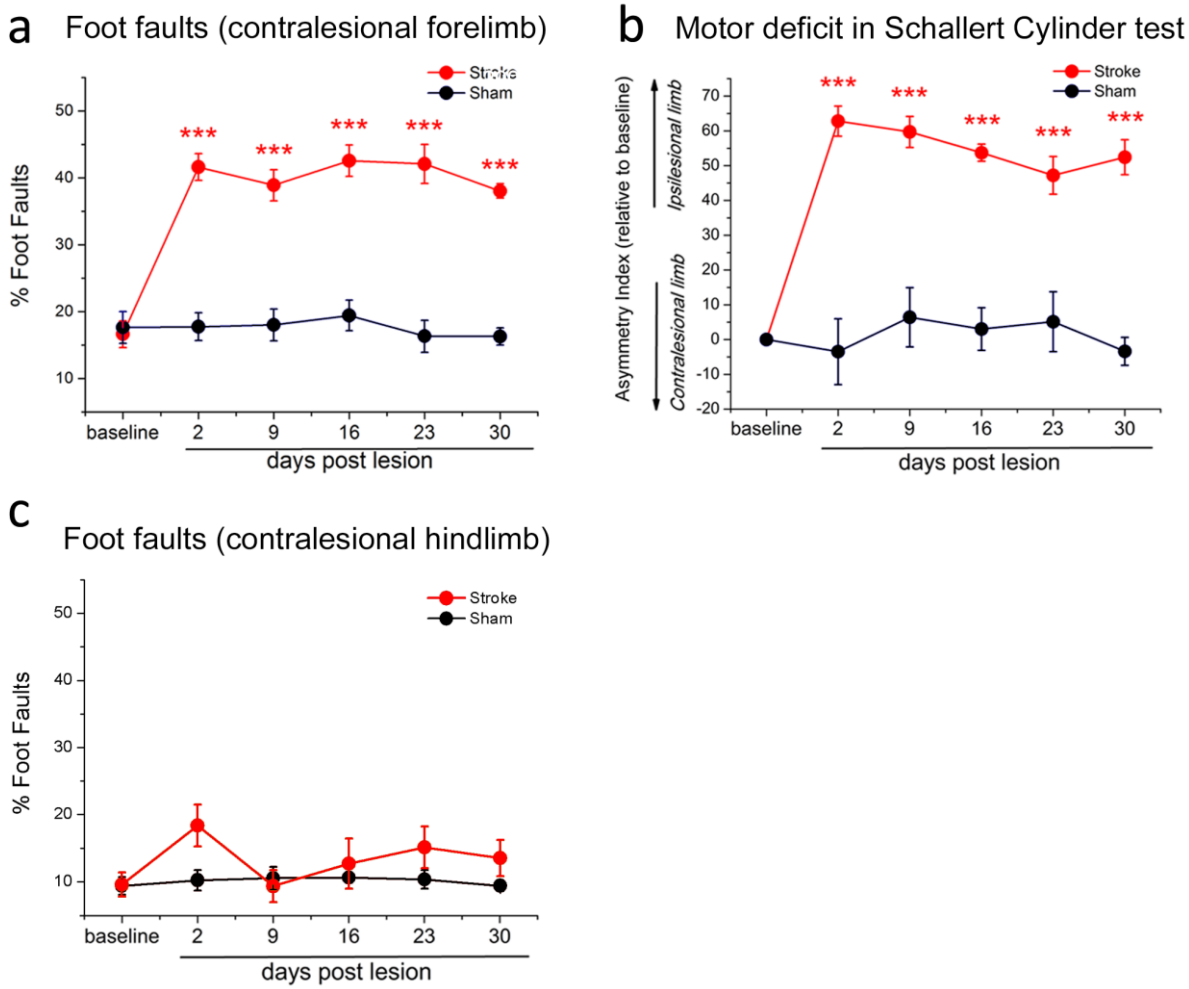

Figure 9 Stroke-associated motor deficits. Pre- and post-lesion performance of the stroke (red, n=11) and sham (black, n=9) groups measured as the percentage of contralesional forelimb foot faults in the gridwalk task (A) and the Asymmetry Index in the Schallert cylinder test (B). Note persistent motor deficits in the stroke mice. The sham animals maintained a low proportion of foot faults and a balanced use of their forelimbs throughout the testing period (A, B). Foot faults in contralesional hindlimb are not different from baseline (C). Data are mean ± SE. Two Way RM ANOVA followed by Tukey test, $p<0.001$ with respect to baseline.

To investigate the time-course of functional motor deficits, animals were tested on two motor tasks (gridwalk, Schallert cylinder) before the injury (baseline) and up to 30 days after the ischemic lesion (once a week starting from day 2). **Figure 9A** reports the percentage of foot faults done with the contralesional forelimb in the gridwalk test. After the ischemic injury, ischemic mice showed a significant and stable increase in foot faults as compared to sham-treated animals. The Asymmetry Index evaluated with the Schallert cylinder test showed increased reliance on the ipsilesional forelimb during exploration of the vertical walls in ischemic mice throughout the testing period (**Figure 9B**). Consistent with the anatomical localization of the lesion within the CFA, the contralesional hindlimb showed no significant motor impairment, confirming that the hindlimb area is not affected by the stroke (**Figure 9C;** for all these tests two way ANOVA followed by Tukey test was used)**.**

1.2 Skilled reaching test and kinematic parameters

In ischemic animals, the percentage of incorrect graspings (i.e. missed and fallen pellets) significantly increased after injury (one way RM ANOVA, p<0.001). End point measure of this test showed a motor deficit with a trend for spontaneous improvement over time, however performance at 4 weeks post stroke was still significantly different from baseline (**Figure 10**).

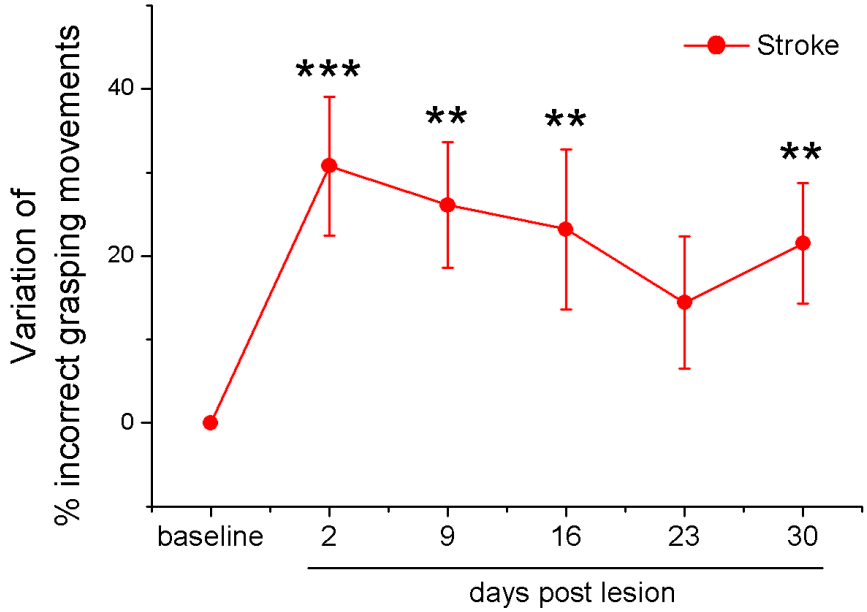

Figure 10. Post-stroke performance in the skilled reaching test. After stroke the performance in the skilled reaching test significantly dropped (n=6). The percentage of incorrect graspings increased after stroke and remained different to baseline with a trend for spontaneous improvement visible up to 30 days after stroke. Data are mean ± SE. One Way RM ANOVA followed by Tukey test, *, p<0.05; **, p<0.01; ***, p<0.001 with respect to baseline.

These data are consistent with limited spontaneous functional restoration after injury (van Meer et al., 2010; Starkey et al., 2012; Kerr et al., 2013; Lai et al., 2015b; Ng et al., 2015).

I was interested in determining whether this spontaneous improvement in performance was due to compensation or restoration of pre-lesion movement patterns. Thus I conducted a kinematic analysis to compare grasping trajectories before and after stroke. For this purpose I used a semi-automated tool to extract the paw trajectory during the reaching movement (Lai et al., 2015b). Animals were video-recorded during the skilled reaching task and then, trajectories of successful graspings were extracted. Baseline values of each kinematic parameter were computed based on pooled trajectories from the three sessions preceding treatment (see Methods).

I found that these measures varied considerably among animals, likely reflecting inter-individual differences in grasping strategies (Gholamrezaei and Whishaw, 2009; O'Bryant et al., 2011). Because I was primarily interested in highlighting differences in performance of

individual animals before vs. after stroke, I hereafter report values observed during post-stroke sessions as changes with respect to baseline.

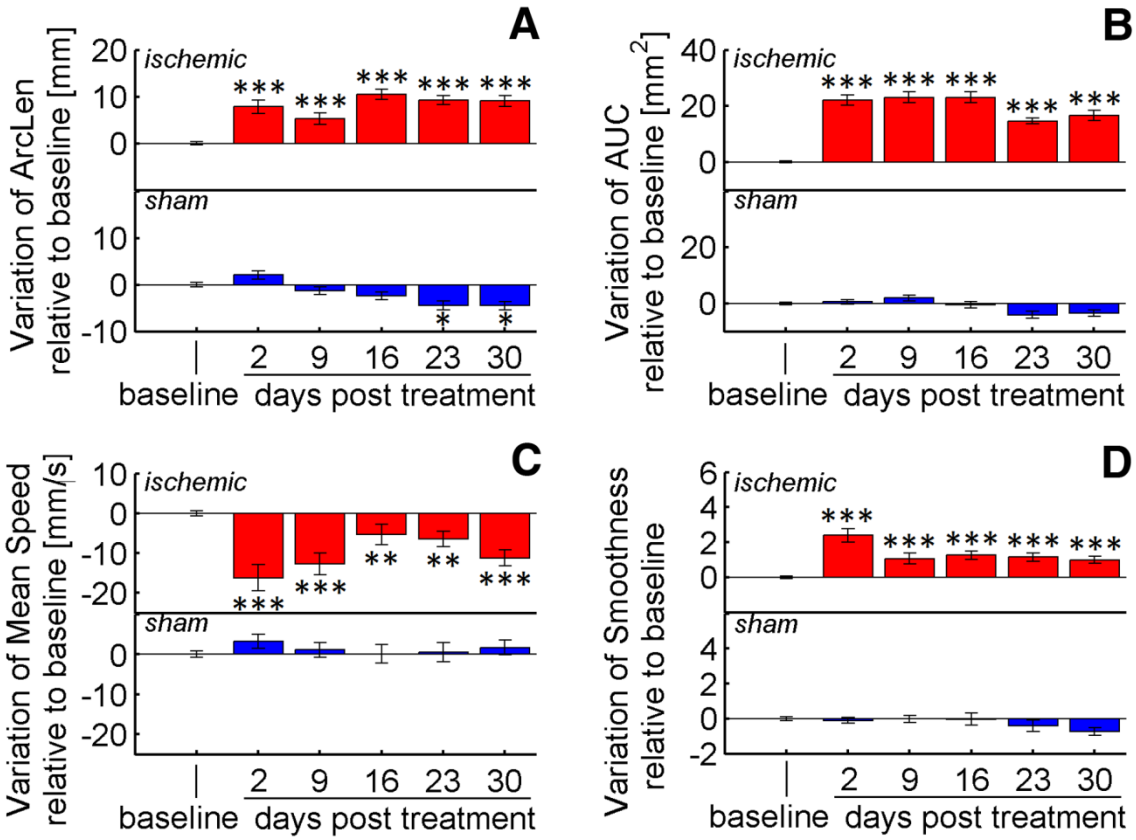

Figure 11. Whole trajectory kinematic modifications. Variation of: (i) *ArcLen*, (ii) *AUC*, (iii) *Mean Speed*, and (iv) *Smoothness* at 2, 9, 16, 23, and 30 days after treatment: stroke (red, n=6) or sham treatment (blue, n=5). Values are normalized by subtracting baselines, and plotted as mean values ± standard error. Kruskal-Wallis test followed by Tukey: ***, p<0.001; **, p<0.01; *, p<0.05 and refers to baseline.

Various kinematic parameters detected differences in reaching performance before vs. after stroke. For the ischemic group, all parameters computed during the first post-stroke session showed significant differences from baseline (p<0.001; **Figure 11** and **Figure 12**).

Movements performed by the *ischemic* group were longer (+8 mm, *ArcLen*), slower (-16 mm/s, *Mean Speed*), had an increased number of trajectory adjustments (+2.7 peaks, *Smoothness*) and spanned a broader workspace (+22 mm^2, *AUC*) than at baseline. When looking at local trajectory modifications, both the reaching and the retraction phases of the task were affected: reaching movements were higher (+0.9 mm, *Height*), and mice approached the pellet with a larger curvature (+1.02 mm, *CurvRadius*) than at baseline. Moreover, dragging after pellet grasping occurred more frequently (+66%, *Dragging*) and lasted for a longer period of time (+0.48 s, *tDrag*) than at baseline.

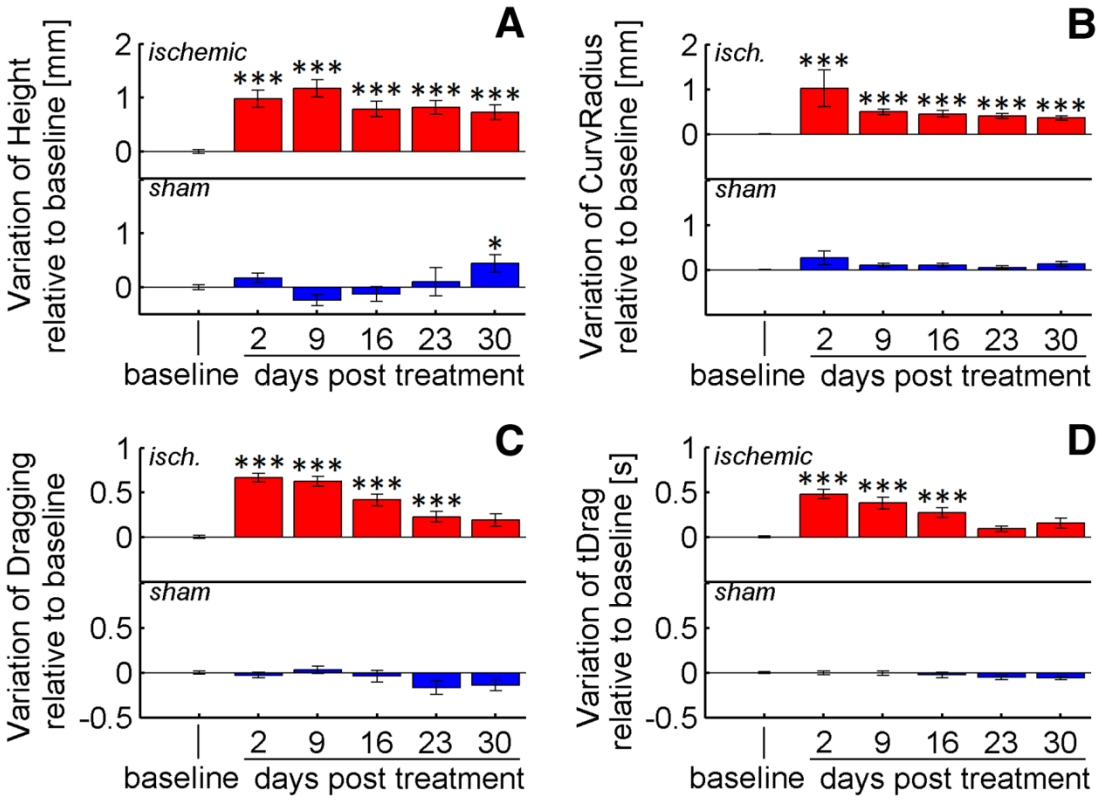

Figure 12. Local kinematic modifications. Variation of: (i) Height, (ii) CurvRadius, (iii) Dragging, and (iv) tDrag at 2, 9, 16, 23, and 30 days after treatment: stroke (red, n=6) or sham injection (blue, n=5). Values are normalized by subtracting baselines, and plotted as mean values ± standard error. Asterisks correspond to the following significance values: ***, p<0.001; **, p<0.01; *, p<0.05 and and refers to baseline.

For four parameters, *AUC*, *ArcLen*, *CurvRadius* and *Height,* differences with respect to baseline values remained significant up to 30 days after lesion (p<0.001), while *tDrag* and *Dragging* recovered to baseline after 3 and 4 weeks, respectively. *Mean Speed* and *Smoothness* yielded less reliable outcomes on weeks 2-5 because differences from baseline became comparable with intrinsic variations due to tracking precision.

Sham treatment did not significantly impact performance, and all of the parameter values remained stable throughout the observation period, except for *ArcLen* and *Height,* which showed small drifts at days 23 and 30 post-treatment (**Figure 11** and **Figure 12**). Taken together, these results reveal that stroke induces persistent (up to 30 days) kinematic modifications on reaching movements, whereas reaching success shows a spontaneous improvement (**Figure 10**). This suggests the application of compensatory strategies rather than a restitution of the original movement patterns.

1.3 Plastic modifications of motor maps after injury

Intracortical microstimulation (ICMS) was used to investigate the spontaneous remapping of motor areas, 30 days after the ischemic lesion. Specifically, I measured the extension and

selectivity of the cortical representation of the affected forelimb in the intact areas surrounding the infarct.

Forelimb motor maps from sham and stroke animals are compared in **Figure 13a-c**. In control animals, the CFA is well defined and extends from approximately -1.0 mm posterior up to 1.25 mm anterior to the bregma suture, consistent with previous reports (Tennant et al., 2011). A second, smaller forelimb representation (Rostral Forelimb Area, RFA) is centred at about 2.5 mm anterior to bregma (**Figure 13a**). This area displays a slightly higher current threshold for evoking limb movements as compared to the CFA (RFA, 36.5±10.9 μA; CFA, 28.9±5.7 μA; t-test, p = 0.08).

After injury, the area corresponding to the infarct (shaded region in **Figure 13a, b**) was no longer effective in triggering forelimb movements. Areas anterior and posterior to the lesion continued to evoke a forelimb response after stroke (**Figure 13b**). However, the quantitative analysis, performed only in the healthy tissue (comprised between -0.75mm and -2mm and between +1.5mm and +2.75mm from Bregma) indicated, a significant shrinkage of the forelimb area in perilesional cortex of ischemic animals as compared to the corresponding regions in controls. In fact, the percentage of responding area in peri-infarct cortex indicated a reduced representation of the contralesional forelimb in ischemic mice (t-test, p=0.03) (**Figure 13c**). The effect was evident and significant across a range of stimulation intensities (20-40 μA; data not shown). It is also worth noting that the current threshold required for eliciting a forelimb movement in perilesional areas significantly increased after stroke (**Figure 14a**; t-test, p=0.003).

During ICMS, I also examined movements of other body parts such as the contralesional hindlimb and tail. In normal animals, the hindlimb and tail representations are smaller than the forelimb and occupy the caudal extent of primary motor cortex (Tennant et al., 2011). Interestingly, I found that the proportion of sites mapping the contralesional hindlimb increased in the perilesional cortex of ischemic mice, thus overrunning forelimb representation (t-test, p=0.04) (**Figure 13d-f**).

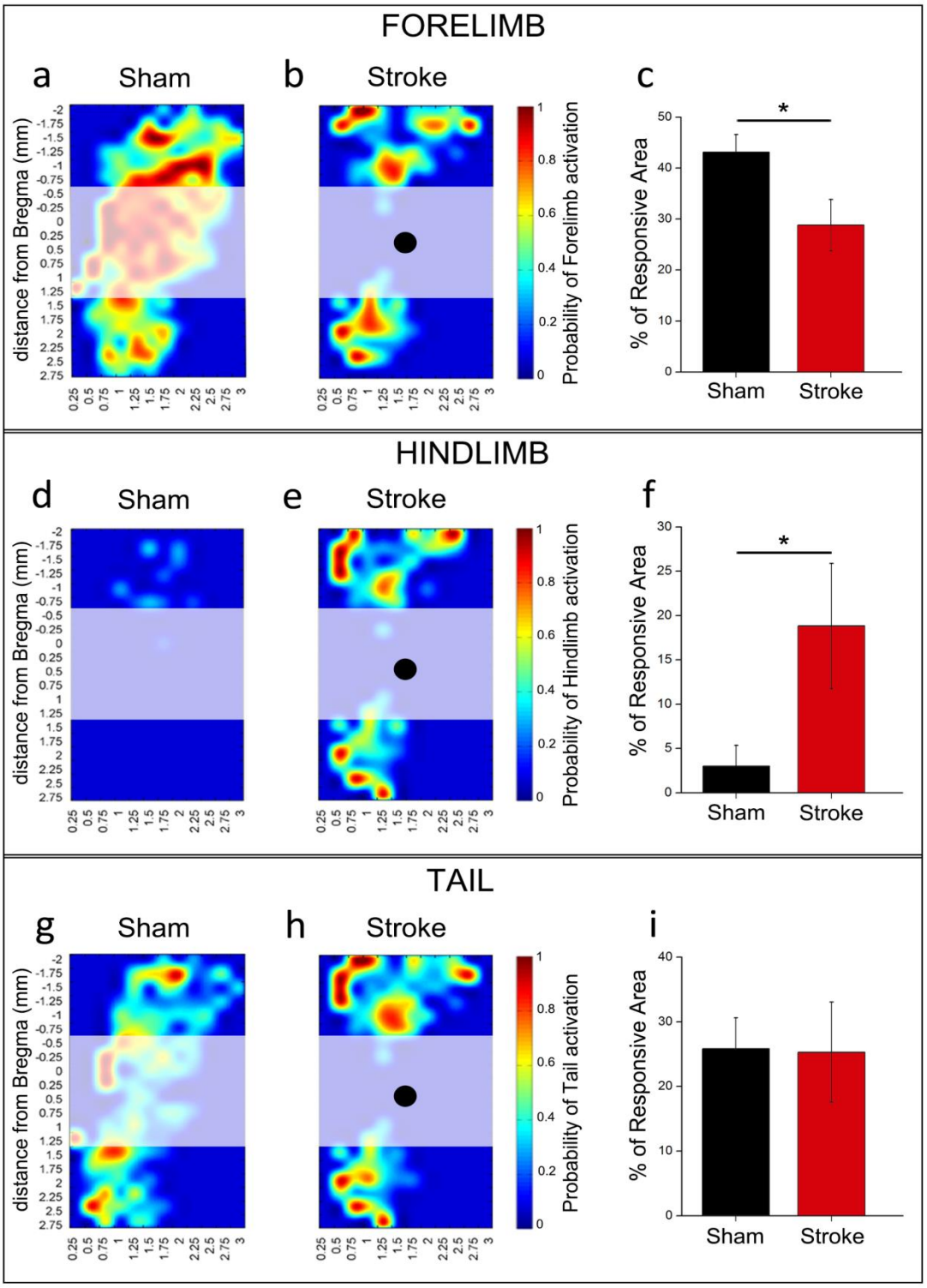

Figure 13 . Plasticity of motor maps after stroke. Average motor maps of sham (n=9) and ischemic animals (n=6) obtained by the intracortical microstimulation (ICMS) technique following a grid of stimulation site of 250 µm (see coordinates from bregma). For each pixel in the maps, a color code indicates the probability (high – red; low – blue) to elicit movement of a body part (contralateral forelimb in a, b; contralateral hindlimb in d, e; tail in g, h) after stimulation with a train of cathodal pulses (current, 30 µA).The quantitative analysis was performed in regions rostral and caudal to the infarct zone, which is indicated by the shaded areas (black dots indicate the coordinates of the lesion). (c, f, i) Quantification of the percentage of perilesional motor areas eliciting forelimb (c), hindlimb (f) and tail responses (i) in sham and stroke animals. After stroke, there is a significant decrease in the cortical area that evokes forelimb responses (t-test, $p<0.05$), with a corresponding expansion of hindlimb motor maps (t-test, $p<0.05$). Tail representations are not altered by the infarct (t-test, $p =0.551$). Data are mean ± SE.

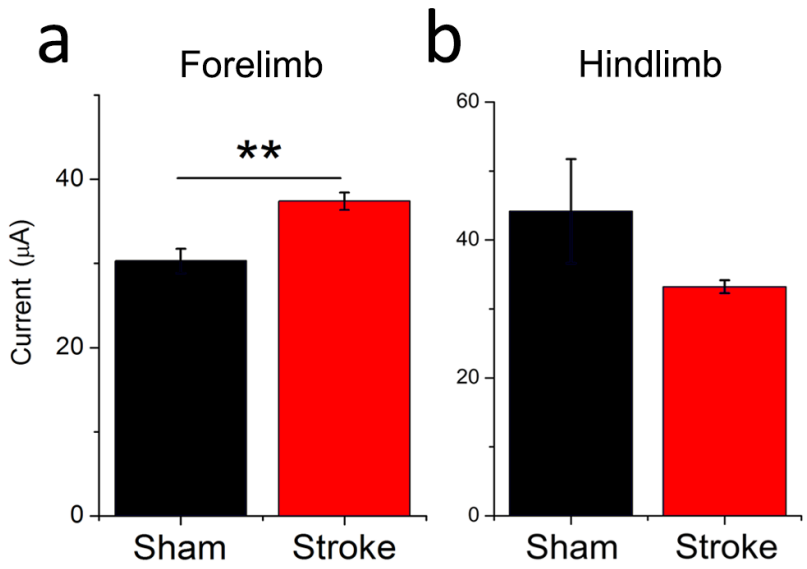

Figure 14 Stroke increases the threshold current required to evoke forelimb movements. Minimum current amplitude required to elicit movement of the contralateral forelimb (A) or hindlimb (B) in the sham (n=9) and stroke group (n=6). The current threshold of the residual forelimb sites in perilesional areas were higher than normal (t-test, $p<0.01$). A tendency for reduction was detected for the current intensities required to evoke hindlimb movements, but this trend only approached statistical significance (t-test, $p=0.148$). Data are mean ± SE.

There was also a non significant trend towards a post-stroke reduction in the current threshold required for eliciting hindlimb movements in forelimb area (**Figure 14b**; t-test, $p=0.148$). Expansion of the hindlimb map was evident and significant at various stimulation currents (20-60 μA). In contrast, the overall dimensions of the tail map did not change significantly in stroke vs. control mice (t-test, $p=0.551$) (**Figure 13g-i**).

Overall, these data indicate a significant reduction of the size of forelimb representations in the intact perilesional tissue, with corresponding expansion and invasion of hindlimb maps. I next investigated whether the functional selectivity of the perilesional tissue was affected in stroke vs. control animals. Selectivity was quantified by counting the proportion of cortical sites evoking movement of 1, 2 or 3 parts of the body (i.e., contralesional forelimb, contralesional hindlimb and tail) using a 30 μA stimulation current. I found that the majority of sites in normal animals evoke the movement of either 1 or 2 body parts, whereas very few sites evoke simultaneous movements of forelimb, hindlimb, and tail (**Figure 15a**). The picture was radically different in ischemic animals, where very few sites were specific for the forelimb (t-test, $p=0.011$), and the majority of cortical locations drove movements of 2 or 3 body parts, even at low current intensities (t-test, $p=0.046$**; Figure 15a**).

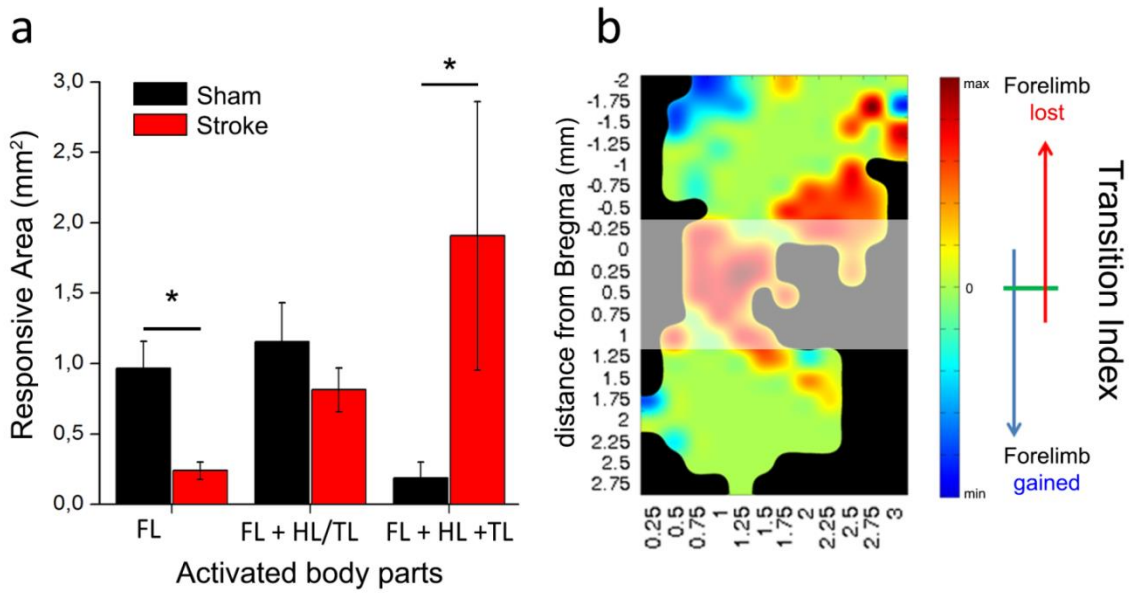

Figure 15 Loss of movement selectivity following a cortical infarct. (a) Surface area eliciting movement of forelimb (FL) alone, forelimb + hindlimb (HL) or tail (TL), or the three body parts together at a stimulation current of 30 µA in sham (black, n=9) and ischemic animals (red, n=6). The quantitative analysis was performed in regions rostral and caudal to the infarct (see Fig. 1). Following stroke, very few sites retain their selectivity for forelimb movements, while most cortical locations elicit simultaneous movement of forelimb, hindlimb and tail (t-test, $p<0.05$). Data are mean ± SE. (b) Map of the Transition Index (TI; see Methods) showing for each pixel the tendency to gain (blue) or lose (red) forelimb movement after stroke in my experimental sample. The colorimetric index is defined within a range of $\pm\sqrt{2}$ (see Methods).

I also investigated whether specific locations in the perilesional cortex consistently lose or gain forelimb preference following a cortical infarct. To this aim, I computed a "Transition Index" (TI) (see Methods) that indicates with a colorimetric scale if each cortical site gains (blue) or loses (red) forelimb movements after stroke (**Figure 15b**). Overall, a robust loss of forelimb sites was evident both anterior and posterior to the infarct, with the exception of a postero-medial area (blue) that appears to gain forelimb responses in stroke vs. sham mice (**Figure 15b**).

1.4 Downregulation of GABAergic markers following stroke

I next used immunostaining to evaluate expression of markers of plasticity (Bavelier et al., 2010; Deidda et al., 2015) in perilesional cortical areas. I performed staining for perineuronal nets (PNNs), somatostatin and parvalbumin-positive (SOM- and PV-positive) inhibitory interneurons, and glutamatergic and GABAergic terminals. Three groups of animals were examined: a sham group with no injury, and ischemic animals at either 7 or 30 days post-lesion.

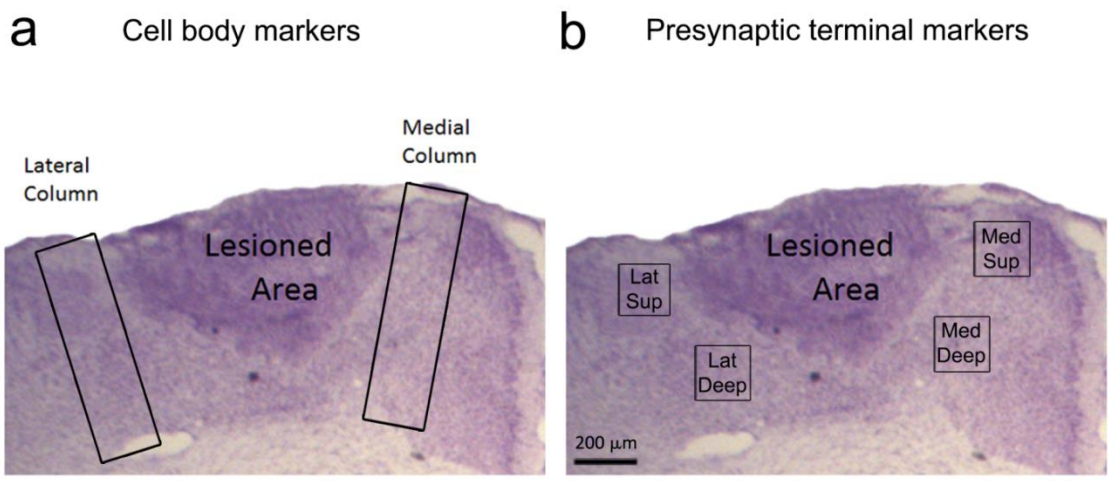

Figure 16 Location of counting boxes for the immunohistochemical analyses. (A) Cell-counting scheme for PNNs, PV-+ and SOM-+ cells superimposed on a representative Nissl staining of a cortical section. Two cortical columns (200µm wide) adjacent to the lesion have been analyzed for each section. (B) Scheme for the fluorescence analysis of the presynaptic terminal markers. Four regions has been taken into consideration: Lateral-superficial layers (Lat Sup), Lateral-deep layers (Lat Deep), Medial-superficial layers (Med Sup) and Medial-deep layers (Med Deep).

To ensure consistency among animals and lesions, I sampled well defined areas in the perilesional region (see **Figure 16**). Specifically, the density of PNNs, PV- and SOM-positive cells was determined in cortical columns (200 µm wide) medial and lateral to the lesion, while glutamatergic and GABAergic synaptic terminals were sampled in counting boxes located in both superficial and deep layers of peri-infarct cortex (**Figure 16**). Homotopic regions of the contralesional hemisphere were examined as well, but I did not detect any significant changes in ischemic animals with respect to sham controls (data not shown).

The density of PNNs was assessed by staining cortical sections with Wisteria Floribunda Agglutinin (WFA). PNNs enwrap specific sub-populations of neurons and are known to play a key role in limiting adult plasticity (Soleman et al., 2012; Deidda et al., 2015; Gherardini et al., 2015). I found that the density of PNNs remained unaltered at day 7 but consistently decreased 30 days after stroke in cortical columns medial and lateral to the infarct (one way ANOVA followed by Holm-Sidak test, medial and lateral, $p<0.001$; **Figure 17**).

Since PNNs mainly surround PV-positive cells (corresponding mainly to fast-spiking inhibitory neurons), I then measured the density of this neural population. PV-positive cells showed the same trend as PNNs, and were significantly downregulated 30 but not 7 days after stroke (one way ANOVA, followed by Holm-Sidak medial $p=0.027$; lateral $p=0.009$; **Figure 18a**).

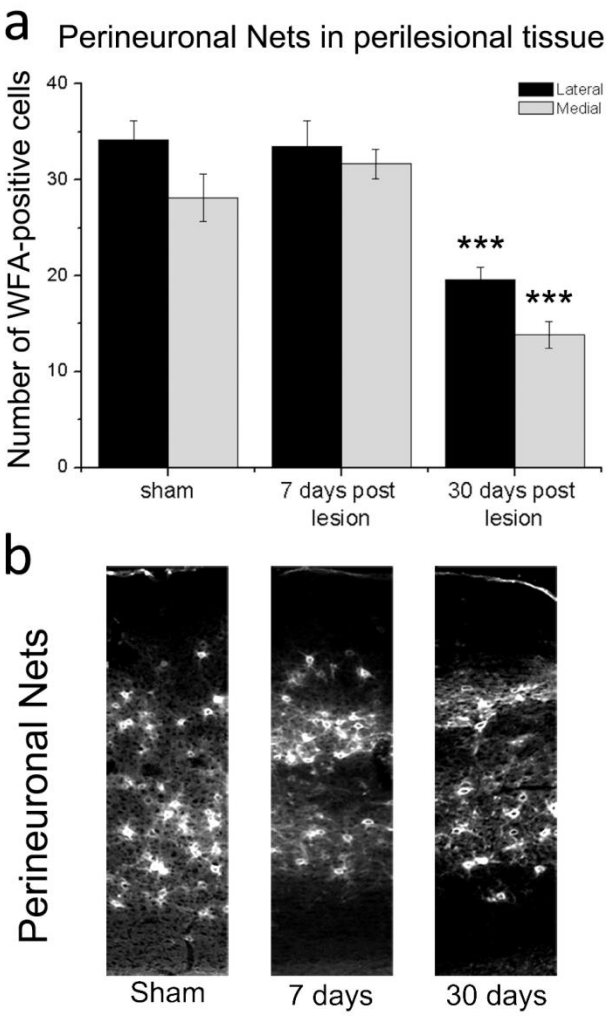

Figure 17 Reduced density of PNNs in peri-infarct areas. (a) Number of cells surrounded by PNNs in 200 µm wide cortical columns, lateral (black bars) and medial (grey bars) to the ischemic lesion, 7 (n=5) and 30 days post injury (n=8). Similar cortical regions were also sampled in controls (n=8). PNN density is significantly reduced at 30 but not 7 days after stroke (one Way ANOVA, post hoc Holm-Sidak test, ***, $p<0.001$ and refers to sham). Data are mean ± SE. (b) Representative images acquired from coronal sections of the motor cortex from sham and stroke mice at 7 and 30 days. Column width = 200 µm.

Another important class of inhibitory interneurons, namely SOM-positive cells, also showed a consistent downregulation following injury. In this case, a statistically significant decrease in cell density was already noted at day 7 (one way ANOVA, followed by Holm-Sidak test, medial $p=0.023$; lateral $p=0.017$), and further progressed at day 30 (medial $p=0.001$, lateral $p=0.003$; **Figure 18b**).

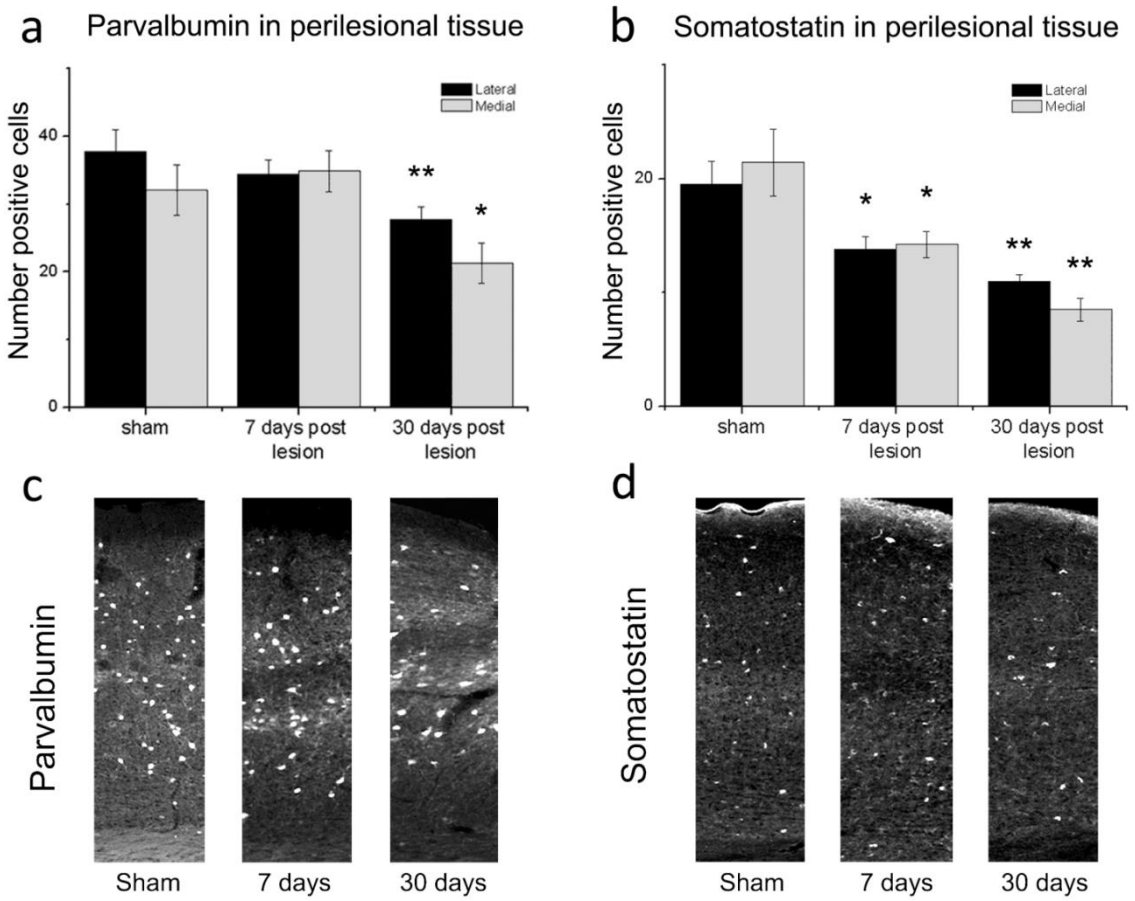

Figure 18 Reduced density of GABAergic interneurons in peri-infarct areas. (a, b) Number of PV-positive (a) and SOM-positive cells (b) in 200 µm wide cortical columns, lateral (black bars) and medial (grey bars) to the ischemic lesion, 7 (PV n=7; SOM n=6) and 30 days post injury (PV n=8; SOM n=4). Compared to controls (PV n=7; SOM n=6), density of PV-+ neurons is significantly dampened at 30 days (one Way ANOVA, post hoc Holm-Sidak test, $p<0.05$). SOM-+ cells are significantly reduced at 7 days and decrease further at 30 days. Data are mean ± SE. *, $p<0.05$; **, $p<0.01$ and refers to sham. (c, d) Representative low magnification images of PV (c) and SOM immunostaining (d) in the motor cortex. Images were taken from sham animals and from the perilesional areas of mice at 7 and 30 days post-infarct. Column width = 200 µm.

To study more precisely the excitation/inhibition ratio in perilesional cortex, I stained sections for vesicular transporter markers that label inhibitory and excitatory terminals impinging onto cortical neurons (Caleo et al., 2007; Vannini et al., 2015). Quantitative analysis of the immunostaining for the Vesicular GABA Transporter (V-GAT) indicated that the overall fluorescence of inhibitory terminals was unaffected at day 7, but robustly declined at day 30. This reduction was noted in superficial and deep layers on both sides of the infarct (one way ANOVA, followed by Holm-Sidak test, $p<0.01$ for all comparisons; **Figure 19a, c**). I also quantified perisomatic staining by measuring the mean V-GAT fluorescence in “puncta rings” surrounding cortical neurons (Di Cristo, 2007; Deidda et al., 2015). I detected a decrease of fluorescence 30 days after stroke that was significant in superficial layers (one way ANOVA, followed by Holm-Sidak test, medial $p<0.01$; lateral $p<0.05$; **Figure 19b, c**).

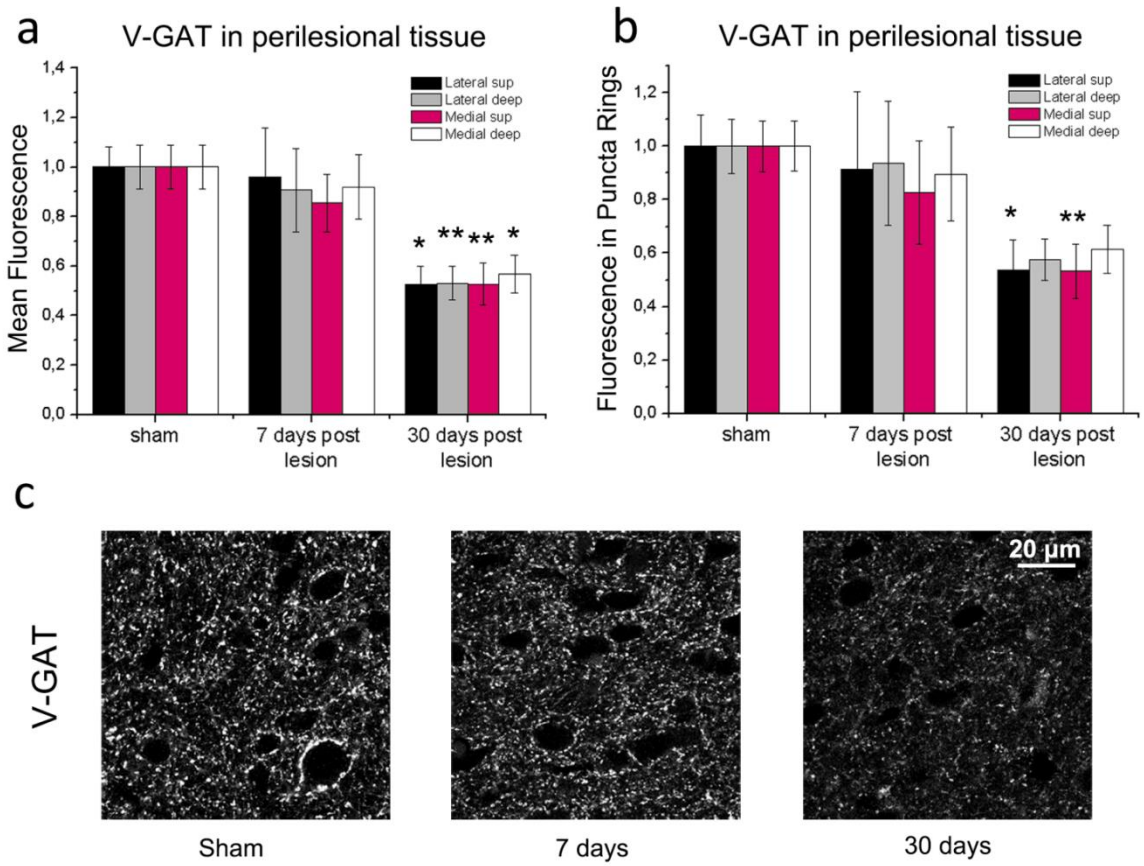

Figure 19 Late reduction of V-GAT-positive inhibitory terminals in perilesional cortex. (a, b) Mean fluorescence intensity of inhibitory, V-GAT-positive profiles in the neuropil (a) and in puncta rings surrounding the soma of pyramidal neurons (b). Measures were taken in superficial (sup) and deep layers, medial and lateral to the infarct. A consistent reduction in fluorescence is observed 30 but not 7 days after injury as compared to sham controls (one way ANOVA followed by Holm-Sidak test, $p<0.05$). Data are mean ± SE. *, $p<0.05$; **, $p<0.01$. (c) Representative V-GAT immunoreactivity in the motor cortex of sham animals and in perilesional tissues (7 and 30 days after the infarct). Note decreased staining at 30 days. Number of animals is as follows: control n=5, stroke 7 days n=5, stroke 30 days n=4. Scale bar = 20 µm.

To evaluate excitatory terminals, I quantified immunostaining for the Vesicular Glutamate Transporter 1 (V-GluT1) in lateral and medial perilesional cortex. I found no significant changes in the mean V-GluT1 fluorescence in the neuropil either at 7 or 30 days after stroke (one way ANOVA, $p>0.52$ for all peri-infarct regions; **Figure 20a-c**). Similarly, the intensity of perisomatic excitatory boutons showed no significant variation after stroke ($p>0.63$; **Figure 20b-c**).

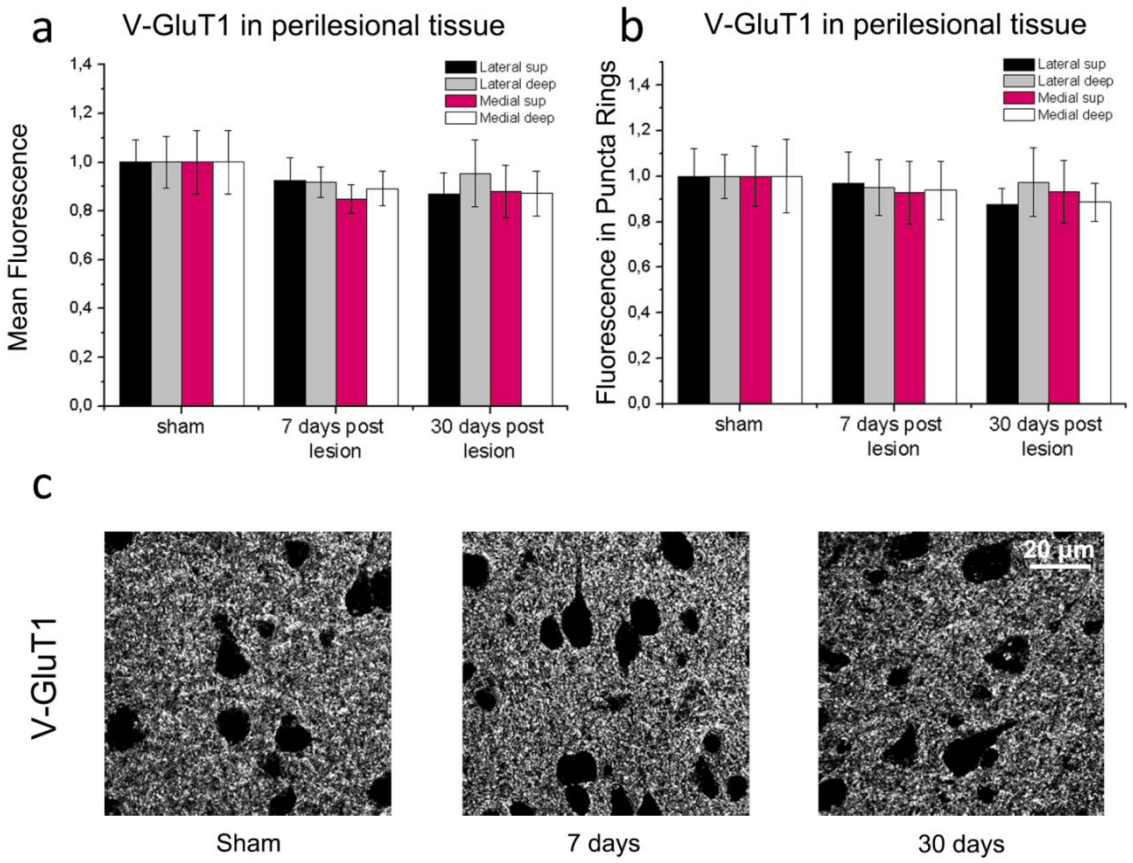

Figure 20. Quantitative analysis of V-GluT1 immunostaining. (a, b) Mean fluorescence intensity of excitatory, V-GluT1-positive presynaptic structures in the neuropil (a) and in puncta rings surrounding the soma of pyramidal neurons (b). Measures were taken in superficial (sup) and deep layers, medial and lateral to the infarct. There is no significant variation in staining in stroke animals as compared to sham controls (one Way ANOVA, followed by Holm-Sidak test, $p>0.52$). Data are mean ± SE. (c) Representative V-GluT1 staining in cortical sections from sham controls and stroke mice, 7 and 30 days following injury. Number of animals is as follows: control n=6, stroke 7days n=6, stroke 30 days n=5. Scale bar = 20 µm.

Overall, these data show a consistent downregulation of PNNs and several inhibitory markers in the peri-infarct cortex 30 days after stroke. Conversely, I found no detectable variation in V-GluT1 expression, indicating an overall shift of the excitation/inhibition ratio in favour of excitation. Increases in the excitation/inhibition balance are typically associated with an enhanced potential for plasticity in the adult cortex (Hensch, 2005; Maya Vetencourt et al., 2008; Harauzov et al., 2010), indicating their possible involvement in the spontaneous functional improvements occurring within the first weeks after stroke (van Meer et al., 2010; Starkey et al., 2012; Kerr et al., 2013; Lai et al., 2015b; Ng et al., 2015).

2. Strategies to improve motor function after stroke

2.1 Interfering with $GABA_A$ signalling

The post-stroke reduction of GABAergic markers prompted us to investigate the role of GABA signalling in motor improvements. I decided to hamper $GABA_A$ mediated neurotransmission during an early phase post-lesion (days 3-8) via systemic delivery of the benzodiazepine inverse agonist DMCM. I initially established doses of DMCM (1.5 mg/kg) that were well below those required to elicit epileptic seizures (Rägo et al., 1988; Volke et al., 2003; De Sarro et al., 2004), while at the same time impacting on GABA-mediated transmission as judged by a reduced path length in the open field (Volke et al., 2003) (**Figure 21**).

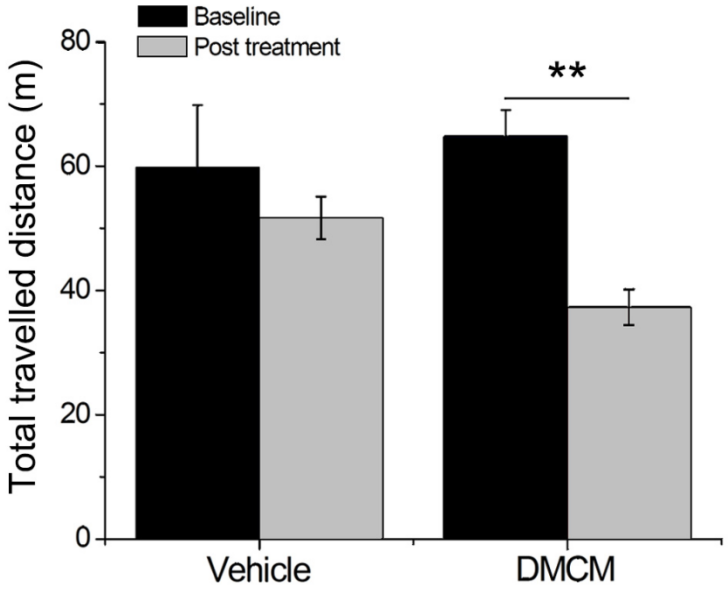

Figure 21. Effect of DMCM on exploratory activity in the open field. Total distance travelled by healthy animals treated with either DMCM (1.5 mg/kg) (n=3) or vehicle (n=3). Measurements were taken before (black) and after treatment (grey). DMCM produces a very significant reduction of locomotor activity (two way RM ANOVA, followed by Holm-Sidak test, $p<0.01$) while vehicle had no significant impact ($p=0.175$).

Mice were treated with either DMCM or vehicle starting from day 3 after stroke and following assessment of the initial deficit in the gridwalk task (**Figure 22a**).

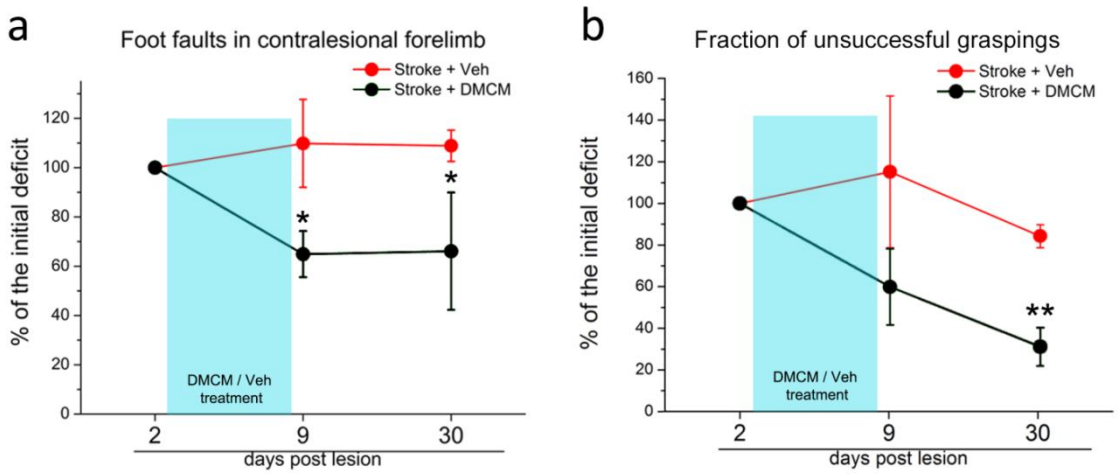

Figure 22. Long-lasting improvements in general motor outcome following DMCM treatment in stroke mice. Data are shown as percentage of the initial deficit, i.e. the difference in the fraction of foot faults/incorrect graspings between day 2 and baseline. Then, performances at day 9 and 30 have been normalized as a percentage of the initial deficit. Statistical analysis was performed on raw data and differences refer to day 2. (a) The number of foot faults in the gridwalk task decreases immediately after DMCM treatment and persists up to 30 days (two way RM ANOVA followed by Tukey test, $p<0.05$; n=10). Conversely, no significant improvements are detected in controls ($p>0.87$; n=3). (b) Performance in the single-pellet retrieval task. The fraction of incorrect graspings decreases after DMCM treatment, which rescues approximately 70% of the initial deficit 30 days post lesion (two way RM ANOVA, followed by Tukey test, $p<0.01$). Data are mean ± SE.*, $p<0.05$; **, $p<0.01$ and refers to baseline.

Injections were made daily until day 8 and motor function was again assessed at day 9 (i.e. immediately after treatment) and 30 (to probe persistence of the therapeutic effect). As expected, vehicle-treated mice showed no improvements in motor function in the gridwalk test. Importantly, a reduction in the number of foot faults was evident for DMCM-treated animals at day 9 and persisted at day 30 (two way RM ANOVA followed by Tukey test, day 9, p=0.039; day 30, p=0.038; **Figure 22a**). I also assessed the impact of DMCM treatment on skilled reaching (Lai et al., 2015b). The percentage of incorrect movements decreased at day 9 showing a trend for improvement in DMCM animals. This effect of DMCM became significant at day 30 (two way RM ANOVA followed by Tukey test, p=0.007; **Figure 22b**). Thus, performance in two motor tasks was consistently enhanced in the DMCM animals well beyond the completion of the treatment. This effect was not due to a difference in the initial deficit, since DMCM and vehicle groups had a comparable performance 2 days post lesion (two way RM ANOVA $p>0.095$). I also quantified the number of total attempts made during the tests (i.e. reaching attempts in the skilled reaching test and steps performed in the gridwalk test) and I found no significant differences with respect to vehicle controls at 30 days post lesion (total steps made in the gridwalk test: DMCM 619.7±96.46; Veh 635±19.22; t-test p=0.932; total attempts in the skilled reaching test: DMCM 63.6±6; Veh 56±7; t-test p=0.454).

In a subset of the animals employed for the pellet grasping task, I performed a kinematic analysis of reaching to address the issue of “true” recovery vs. compensation (Lai et al., 2015b). I found that DMCM treatment did not significantly improve trajectory kinematics, as they remained longer (ArcLen, Two way RM ANOVA, DMCM vs. vehicle, p=0.244; **Figure 23a**) and less smooth (i.e., with an increased number of trajectory adjustments; Two way RM ANOVA, DMCM vs. vehicle, p=0.330; **Figure 23b**) as compared to baseline, pre-stroke values. Overall, these data indicate that hampering $GABA_A$ signalling after stroke produces significant and long-lasting improvements in motor function, but compensatory adjustments appear to be required for task accomplishment.

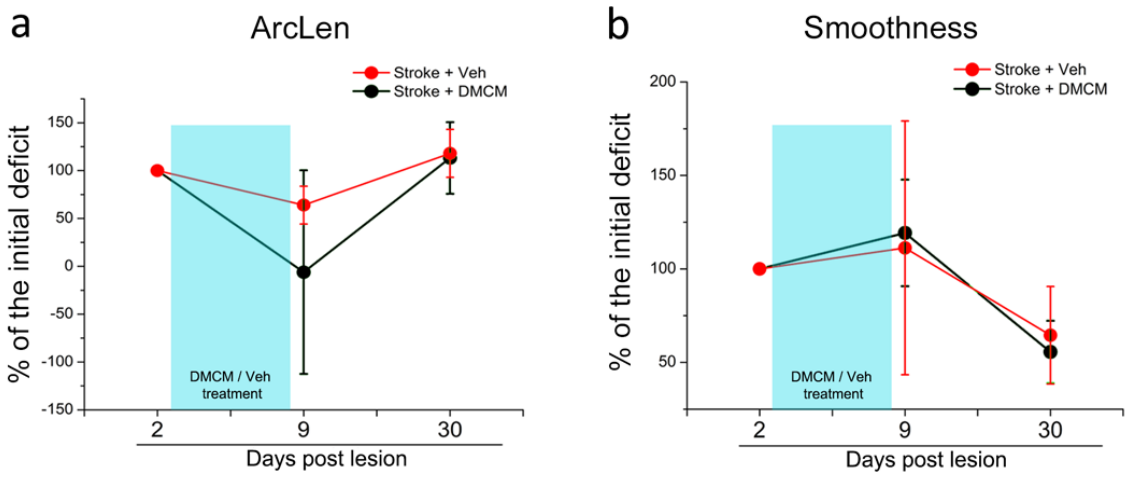

Figure 23. Kinematic analysis of pellet reaching indicates compensatory adjustments in DMCM-treated stroke mice. Data are expressed as percentage of the initial deficit. Post-stroke variation in the length of the whole trajectory (ArcLen; a) and in the smoothness of movement (b) during successful pellet retrievals in DMCM- (n=3) and vehicle-treated stroke mice (n=3). No significant differences are detected between the two groups (two way RM ANOVA, p>0.24).

2.2 Robotic rehabilitation: daily training in a retraction task promotes a specific motor recovery not generalized to other motor functions.

To stimulate motor recovery, I subjected the animals to daily controlled, repeatable and targeted exercises of forelimb retraction, guided by a robotic platform for mice, designed and characterized in our laboratory (Spalletti et al., 2014). The platform is a one-degree-of-freedom (DOF) robotic device that allows head-fixed mice to perform repeated sessions of retraction of the preferred forelimb (**Figure 24A)**. During each trial, the actuator extended the forelimb and the animal was trained to pull back the handle in order to receive a liquid reward on reaching the resting position (RP). Forces exerted during the task, time required for task execution (t-target), and number of sub-movements were quantified for each trial (**Figure 24B**). Mice rapidly learned the retraction task, as shown by the consistent decrease in t-target over training sessions (**Figure 24C**).

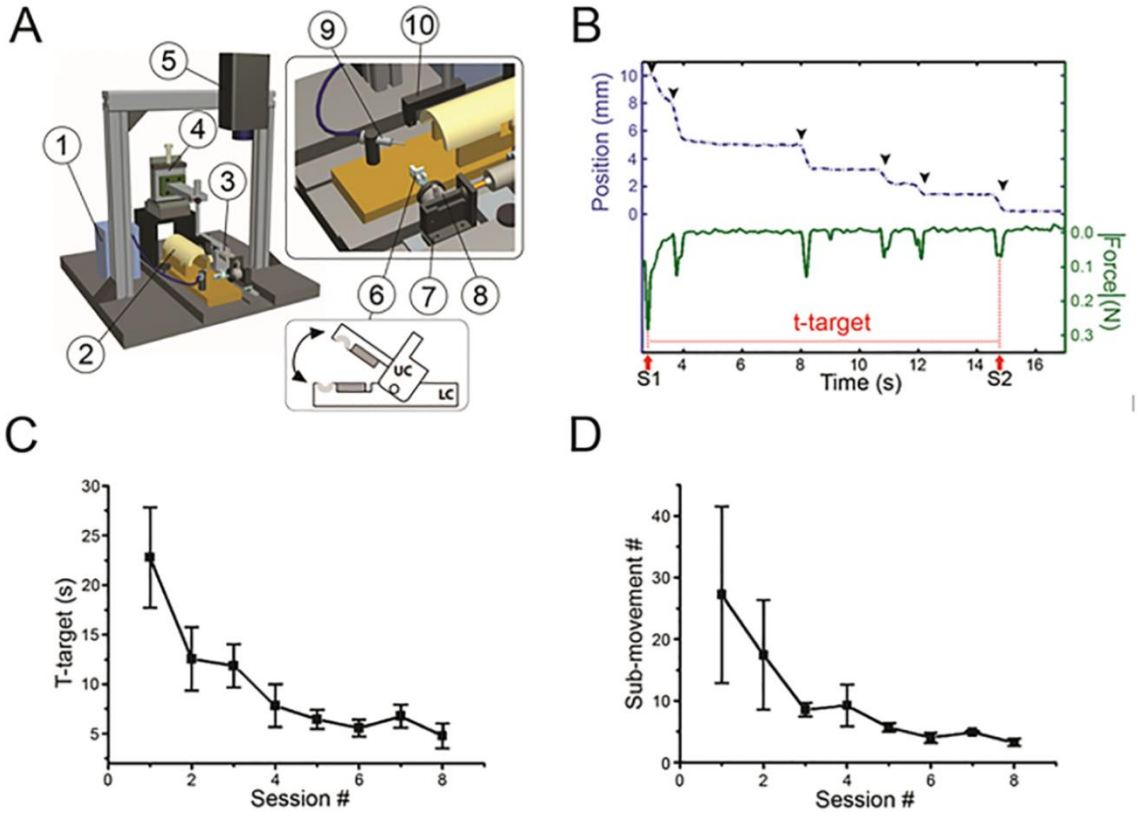

Figure 24. Learning of the retraction task in the robotic platform. (A) Schematic of the robotic interface. It consists of a peristaltic pump for reward delivery (1), mouse restrainer (2), linear actuator (3), micromanipulator (4) for precise positioning of the mouse head, camera (5), handle (6), slide (7), load cell (8), gavage-feeding needle (9), and head fixation system (10). A schematic of the handle is also shown: the upper and lower components (respectively UC and LC), the 2 magnets (gray) and the semicircular groove (light gray). (B) Representative example of a single retraction task (active phase) in the robotic platform. Blue dotted line, position of the handle over time; green continuous line, force over time. S1 and S2, tones indicating begin and end task. The offset of the force profile at S1 was because of the opposing force exerted by the animal during extension by the actuator. Arrowheads indicate single sub-movements; note force peaks in correspondence of each sub-movement. T-target was calculated as time S2 - time S1. Variation of t-target (C), and number of sub-movements (D) over the training sessions. Data are mean ± standard error.

In particular, a plateau was reached starting from the fifth session (Friedman test, $p < 0.001$, followed by Dunn's post hoc Method, $p < 0.05$). In parallel to the reduction of the t-target, Iobserved a significant increase of the mean force exerted by the mice (Friedman test, $p < 0.001$, followed by Dunn's post hoc Method, $p < 0.05$). This was also accompanied by a very consistent decrease in the number of sub-movements required to complete the task (Friedman test, $p < 0.001$, followed by Dunn's post hoc Method, $p < 0.05$ **Figure 24C**). In summary, these data show that mice can efficiently learn the retraction task and that forelimb performance can be accurately quantified by the robotic platform.

I next investigated whether (i) the parameters measured by the robotic platform are sensitive enough to detect deficits in performance after a localized cortical stroke and (ii) post-lesion training is effective in restoring performance on the robotic platform to baseline, pre-lesion values.

After stroke, both the ischemic and sham groups performed the task for at least three sessions (days 2, 4 and 6 following surgery). In the ischemic group the time required to complete the retraction task was significantly increased after the infarct (**Figure 25A**, "baseline" vs. "days 2-6" Dunn's test, P<0.0001). On the other hand, sham surgery had no statistically significant impact on performance (t-target pre- vs. post-injury, Mann Whitney Test, p = 0.472, data not shown).

In addition, the ischemic lesion led to a significant reduction in the force exerted by the forelimb contralateral to the cortical infarct (**Figure 25B**, "baseline" vs "days 2-6" Dunn's test, p < 0.0001).

Importantly, execution of movement was impaired following stroke, as there was a consistent increase in the number of sub-movements required to complete the task (**Figure 25C**; "baseline" vs "days 2-6" Dunn's test, p = 0.0013). Moreover, the number of force peaks (attempts) not resulting in a displacement of the handle, was significantly increased after lesion (**Figure 25D**; "baseline" vs "days 2-6" Dunn's test, p < 0.0001).

I continued the training of the ischemic group until day 14 post-lesion. I found a significant reduction of t-target to levels (**Figure 25A**, third column) that were comparable to those attained in the pre-lesion condition ("baseline" vs. "days 10-14", Dunn's test, p > 0.95; "days 2-6" vs. "days 10-14", p < 0.0001)

Similar results were observed for the mean force values, which showed a substantial increase during the course of post-stroke training (**Figure 25B**, "baseline" vs. "days 10-14", Dunn's test, p = 0.0516; "days 2-6" vs. "days 10-14", p < 0.0001).

Importantly, the number of both sub-movements and attempts were decreased after 14 days of post-lesion training and became comparable to pre-lesion values (sub-movements, **Figure 25C**, "baseline" vs. "days 10-14", Dunn's test, p = 0.0798; "days 2-6" vs. "days 10-14", p < 0.0001; attempts, Fig. 3D, "baseline" vs. "days 10-14", Dunn's test, p > 0.95; and "days 2-6" vs. "days 10-14", p = 0.0002).

Altogether, these data indicate that the robotic platform provides sensitive measures to probe deficits and recovery of forelimb function after a localized cortical infarct in mice.

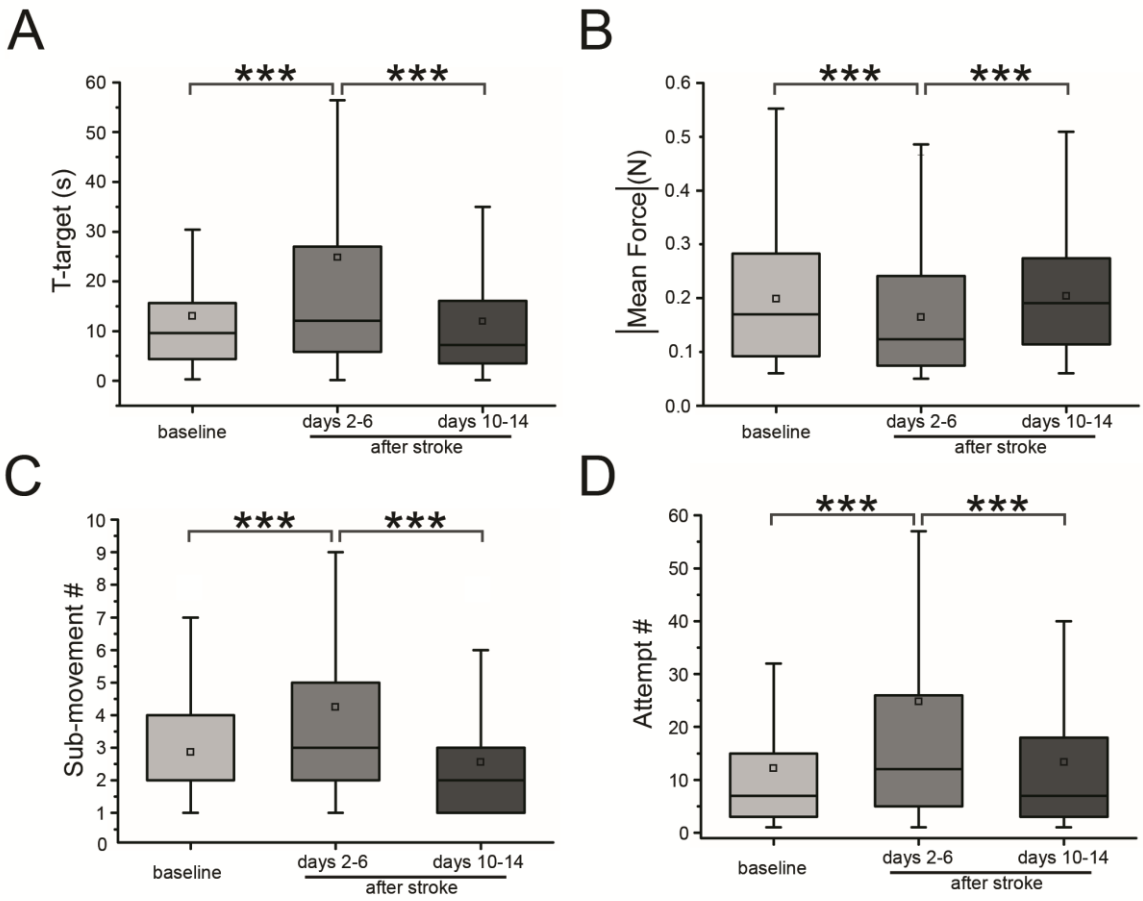

Figure 25 The robotic platform efficiently detects deficits and improvement of forelimb flexor performance following stroke. T-target (A), mean force exerted (B), number of sub-movements (C), and number of attempts (D) in baseline (pre-lesion) condition and either 2 to 6 days or 10 to 14 days after stroke. All animals were tested every other day in the robotic platform. Note the return to pre-lesion values of all parameters at the end of the training. Data are summarized by a box chart, in which the horizontal lines denote the 25th, 50th, and 75th percentile values, and the error bars denote the 5th and 95th percentile values; the square indicates the mean of the data set. ***P<0.001 (Friedman test, P<0.001, followed by Dunn's post hoc test).

Next, I was interested in evaluating whether the effect of the training could be generalized to other forelimb tasks. To this aim, 6 mice were first pre-habituated to be restrained on the robotic platform and to receive the liquid reward; moreover, baseline performances in Schallert and Gridwalk tests were recorded. Then the phototrombotic ischemic lesion was induced in the CFA and a metal post for head restraining was cemented over the skull. The acute effect of the lesion was evaluated 2 days after surgery with Schallert and Gridwalk tests while the daily robotic training started from day 5. The progression of the forelimb function was assessed once a week at day 9, 16, 23 and 30 post-lesion. I found that the improvement in the performance in the specific task on the platform was not generalized to other forelimb task, as demonstrated by the lack of recovery in Schallert and Gridwalk tests (**Figure 26**).

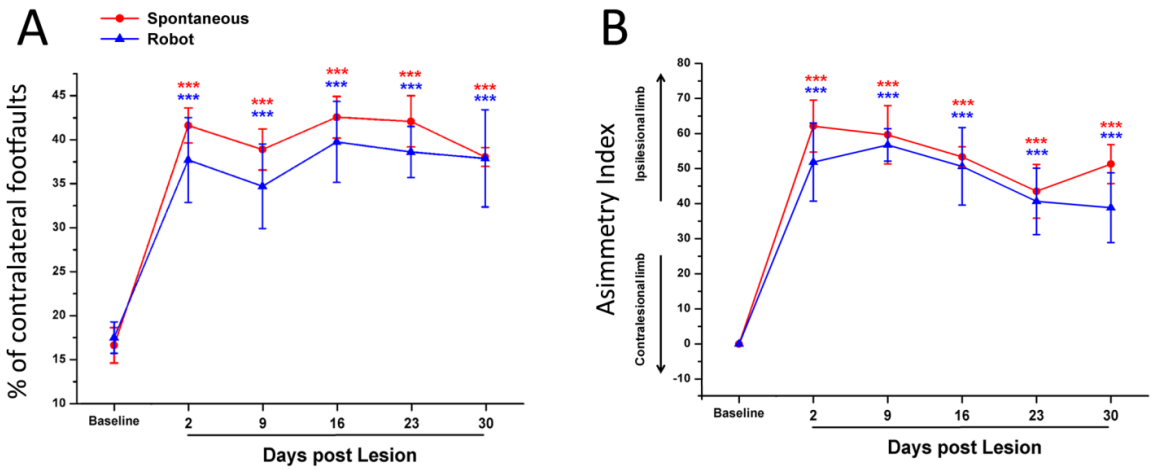

Figure 26. Motor deficit after rehabilitation on the robotic platform. After daily robotic platform rehabilitation (blue), animals showed a similar performance as control stroke animals (red) both in the Gridwalk (A) and in the Schallert Cylinder test. Data are mean ± SE. *, p<0.05; **, p<0.01; ***, p<0.001 and refers to baseline (Two Way RM ANOVA followed by Tukey test).

2.3 Re-establishing the balance between the hemispheres

In order to define possible changes in interhemispheric interactions between the two homotopic motor cortices after stroke, I focused on the spared ipsilesional and the contralesional Rostral Forelimb Areas (RFAs).

I used optogenetic stimulation in Thy1-ChR2 transgenic mice to record Local Field Potentials (LFPs) in RFA of chronic ischemic (30 days post lesion) and sham animals after 1ms of light stimulation in the contralateral homotopic area. Recordings were performed by means of 16 channel linear multielectrodes spanning all cortical layers. A schematic of the experimental protocol is shown in **Figure 27A**. In stroke animals I also switched the configuration and recorded the evoked response in the healthy RFA following stimulation of the contralateral, perilesional cortex. A representative FP recorded in layer V of the ipsilesional and contralesional RFA after single pulse stimulation in the other hemisphere in an ischemic animal is represented in **Figure 27B** (red and blue traces) and compared to a control animal (black trace). I identified two main components of the evoked FP: (i) an early negative component, peaking between 17 and 26 ms after stimulation (corresponding to a current sink) and (ii) a later positive component, peaking between 40 and 60 ms (corresponding to a source, i.e. outward, likely hyperpolarizing currents). The early negative-going FP likely reflects reduced direct transcallosal excitation, while the late positive component may be due to transcallosal, disynaptic inhibition of target neurons via local GABAergic cells. Both components were abolished by topical application over the cortex of

CNQX, a blocker of glutamatergic transmission, indicating the post-synaptic origin of the recorded FP.

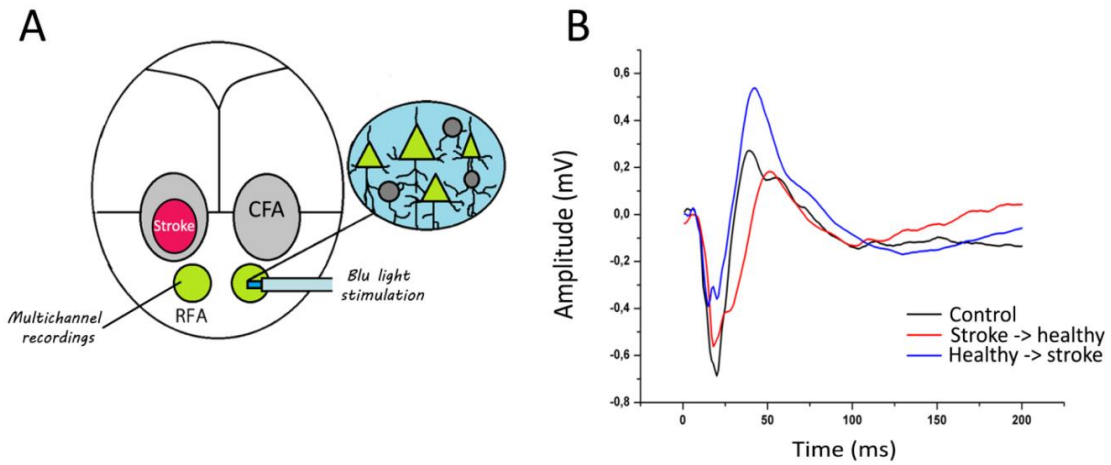

Figure 27. Optogenetic recordings in RFA after stroke. Schematic representation of the experimental setup for optogenetic recordings (A). Transgenic mice expressing Thy1-ChR2 (selectively pyramidal neurons were activated by the blue light) were used. The optic fiber was placed on the healthy RFA and the multichannel electrode in the perilesional RFA (or vice versa). (B) Representative field potential recorded in the ischemic RFA (blue line), healthy RFA (red line) of a healthy animal (black). Note the similarity between the red and black line (from a control animal).

The quantitative analysis revealed a clear asymmetry of interhemispheric communication in stroke animals. In particular, the negative and positive component were always lower and higher, respectively, in the healthy RFA than in the perilesional RFA of individual stroke mice (**Figure 28;** Paired t-test, negative component p=0.013 and positive component p=0.003).

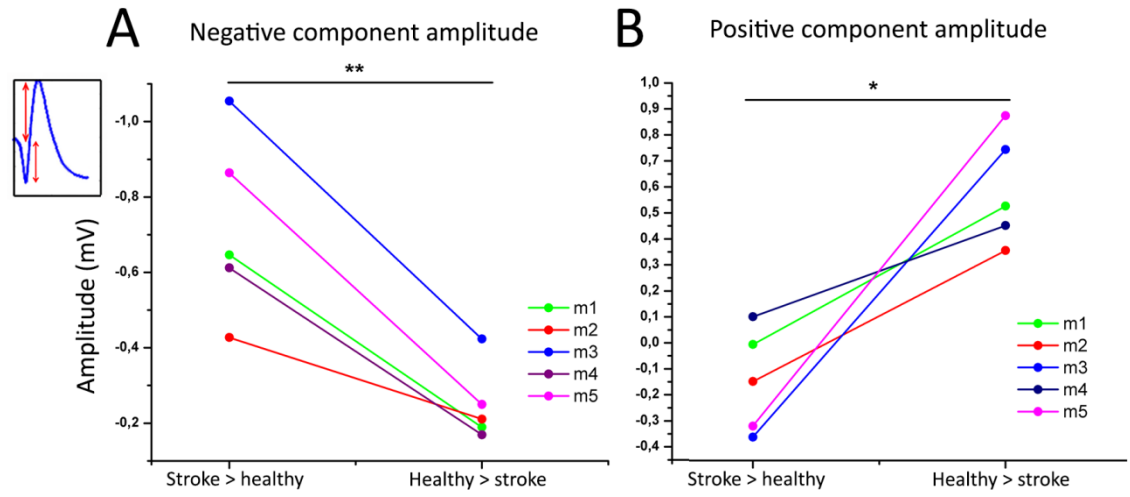

Figure 28. Quantitative analysis of the negative and positive components. Pre-post stroke differences in the amplitude of the early negative component (A, differences between baseline and the negative peak, see box on the left) and in the late positive component (B, basline - positive peak). Data are mean ± SE. *, p<0.05; **, p<0.01 and refers to baseline (Paired t-test).

These results can be interpreted as evidence of reduced excitation and enhanced inhibition through the transcallosal pathway from the intact to the stroke hemisphere, highlighting directional differences in the interhemispheric coupling of the two homotopic Premotor cortices after stroke.

On the basis of these results, I tried two different rehabilitative strategies to restore the correct interhemispheric balance: (i) transient inactivation of the contralesional motor cortex, (ii) a combination of healthy hemisphere silencing and robotic rehabilitation. All the statistical analyses were referred to the baseline pre-lesion values of each group; data of the sham group and spontaneous stroke group are also reported for comparison.

2.4 BoNT/E injection: the inhibition of the healthy hemisphere partially improves motor outcomes after stroke.

Based on my electrophysiological data and previous data from the literature (Vallone et al., 2016) I attempted to rebalance interhemispheric connectivity after stroke. To this aim, I performed a focused inactivation of the forelimb motor cortex in the hemisphere contralateral to the ischemic lesion by means of intracortical injections of the synaptic blocker Botulinum Neurotoxin E (BoNT/E). This neurotoxin is known to block the excitatory neurotransmission by cleaving the protein SNAP-25, a main component of the SNARE complex that is fundamental for neurotransmitter release and synaptic transmission.

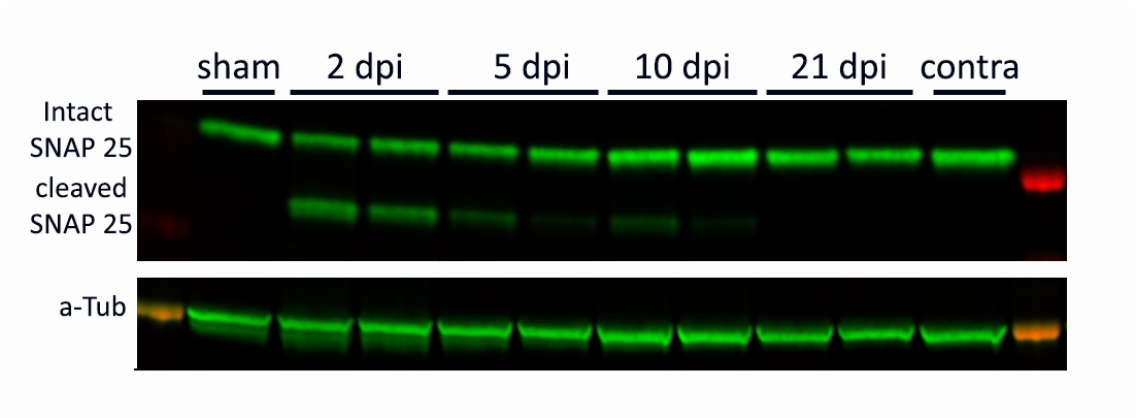

Figure 29. Time course of BoNT enzymatic effect in the cortex. Western blotting showing the duration of BoNT/E effects. BoNT/E activity was evaluated via expression of the intact and BoNT/E-truncated SNAP-25. I detected SNAP-25 cleavage up to 10 days post injection.

I first verified the effectiveness and the feasibility of this technique for my aim. Specifically I characterized the time course of BoNT/E action in the motor cortex by Western Blot analysis. I injected a group (n=5) of animals with the toxin in the CFA and I collected tissues from the injection site at different time from surgery. As controls, I collected also samples from motor cortex contralateral from the injection site and from the visual cortices. Western blotting

results are reported in **Figure 29** and show that BoNT/E is active for at least 10 days after injection, as shown by persistence of cleaved SNAP-25.

To evaluate the spread of toxin activity in the motor cortex, I injected a group of 5 mice with BoNT/E in the left CFA and I sacrificed animals 2 days post injection (when the activity of the toxin reaches its peak). I used 50 µm-thick brain slices for immunostaining of intact and cleaved SNAP-25 (**Figure 30A, C, D** and **B, E, F**, respectively). I found that SNAP-25 cleavage was evident along all the cortical layers and spanned the entire CFA. The RFA was less involved as I found low expression of cleaved SNAP-25 at its posterior border (+1.5mm from Bregma; data not shown).

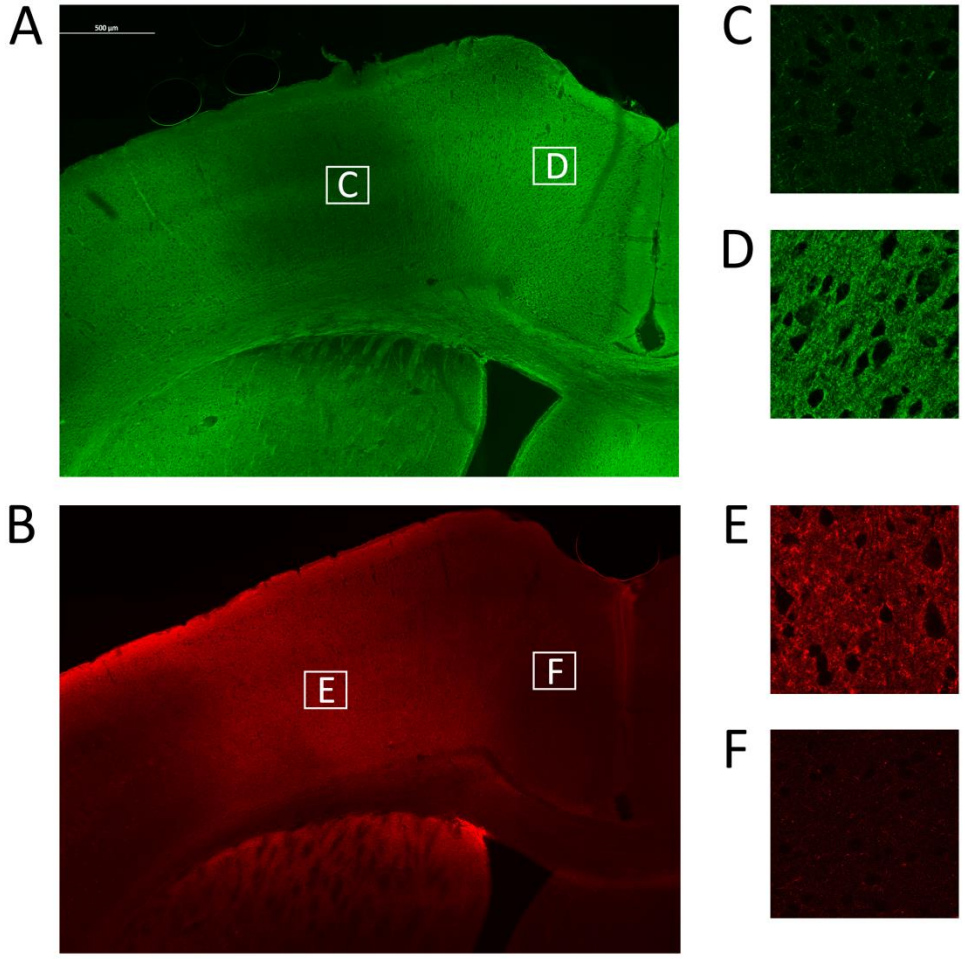

Figure 30. Representative micrographs of the BoNT/E injection site. immunofluorescence staining for intact (A) and cleaved SNAP-25 (B). Magnification of the injection site showed the nearly total absence of intact SNAP-25 (C) whereas the cleaved SNAP-25 signal is consistent (E). Conversely, in the peri-injection site there is a conspicuous amount of intact SNAP-25 (D), but no signal from cleaved SNAP-25 (F).

In order to assess the effect of inactivation of the contralesional hemisphere, a group (n=5) of animals subjected to phototrombosis were also intracortically injected, in the same surgery, with BoNT/E. I assessed motor performances of these animals once a week with behavioural tests up to 30 days post lesion. As shown in **Figure 31A and B**, the injection of BoNT/E appears to have an effect on the motor outcomes both in Schallert Cylinder Test and

in the Gridwalk test but it is not sufficient for inducing a complete recovery. In particular, in the Gridwalk Test, I found a robust deficit at day 9 followed by a slight improvement over time (**Figure 31A**). However, performance remained significantly worse than baseline at day 30 (two way RM ANOVA followed by Tukey test, Day 2 p<0.001; Day 30 P=0.017).

In the Schallert Cylinder test, the deficit measured at day 2 in BoNT/E-treated animals was lower than in controls (**Figure 31B**). Since the Schallert cylinder test measures the asymmetry in forelimb use, this acute effect may be due to the synaptic silencing of the contralesional cortex (with an impact on ipsilesional forelimb). However, over time the deficit in performance caught up with that measured in stroke controls and was significantly different from baseline (two way RM ANOVA followed by Tukey test, Day 9 P=0.024, Day 16 P=0.002, Day 23 and 30 P<0.001).

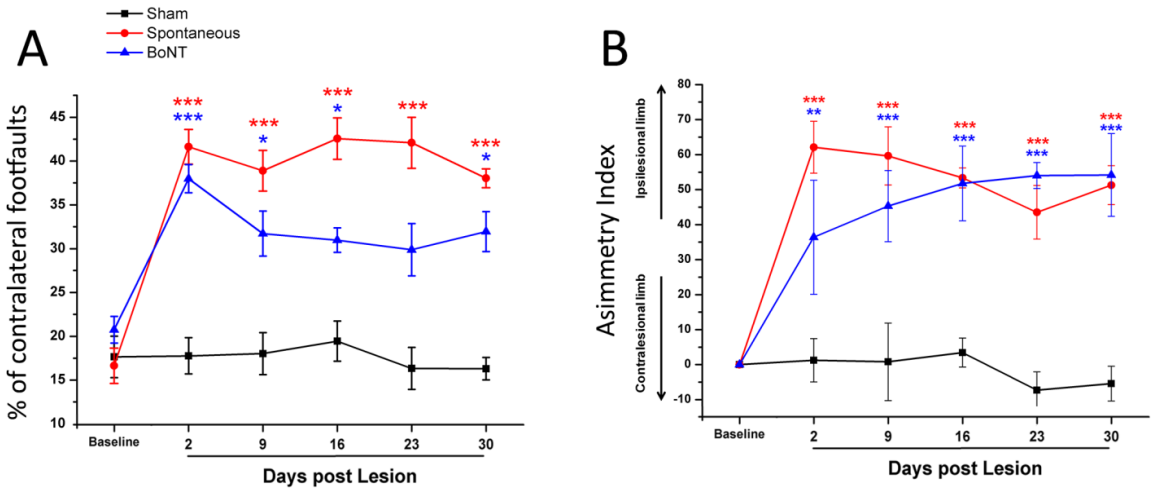

Figure 31. Performance in the general motor tests after BoNT/E injection in the contralesional CFA. After BoNT/E injection (blue line) there is a small improvement in the performance in the gridwalk test (A) respect to the spontaneous recovery (red line), that however remains statistically different from the baseline performance at 30 days post lesion. Moreover in the Schallert cylinder the use of the contralesional forelimb after BoNT/E injection (red) reflects the performance in the spontaneous time course (blue). Data are mean ± SE. *, p<0.05; **, p<0.01; ***, p<0.001 and refers to baseline (Two Way RM ANOVA followed by Tukey test).

2.5 Combined neurorehabilitation: robotic training combined with transient inactivation of contralesional hemisphere enhances motor recovery.

I decided to combine BoNT/E injection with daily robotic rehabilitation in the mechatronic platform. Motor improvements of the BoNT+Robot group (n=6) were evaluated with Schallert and Gridwalk tests once a week up to day 30. Moreover, in order to have a more specific measure of forelimb motor performance for the different groups, animals were also trained in the Skilled Reaching Test and kinematic analysis was also performed.

In **Figure 32A** and **B**, motor performances in the Gridwalk and the Schallert Cylinder Tests are reported: in both cases, a significant improvement was found, especially at day 30 post

lesion. In the Gridwalk, motor recovery started from day 16 post lesion, when error percentage with the impaired limb normalizes to baseline values, and remains steady up to day 30 (two way RM ANOVA followed by Tukey test, Day 16 P=0.067, Day 23 p=0.160 and 30 P=0.079). In the Schallert Cylinder test, the asymmetry index turns to be not different from baseline value at day 30 post lesion (two way RM ANOVA followed by Tukey test, p = 0.182).

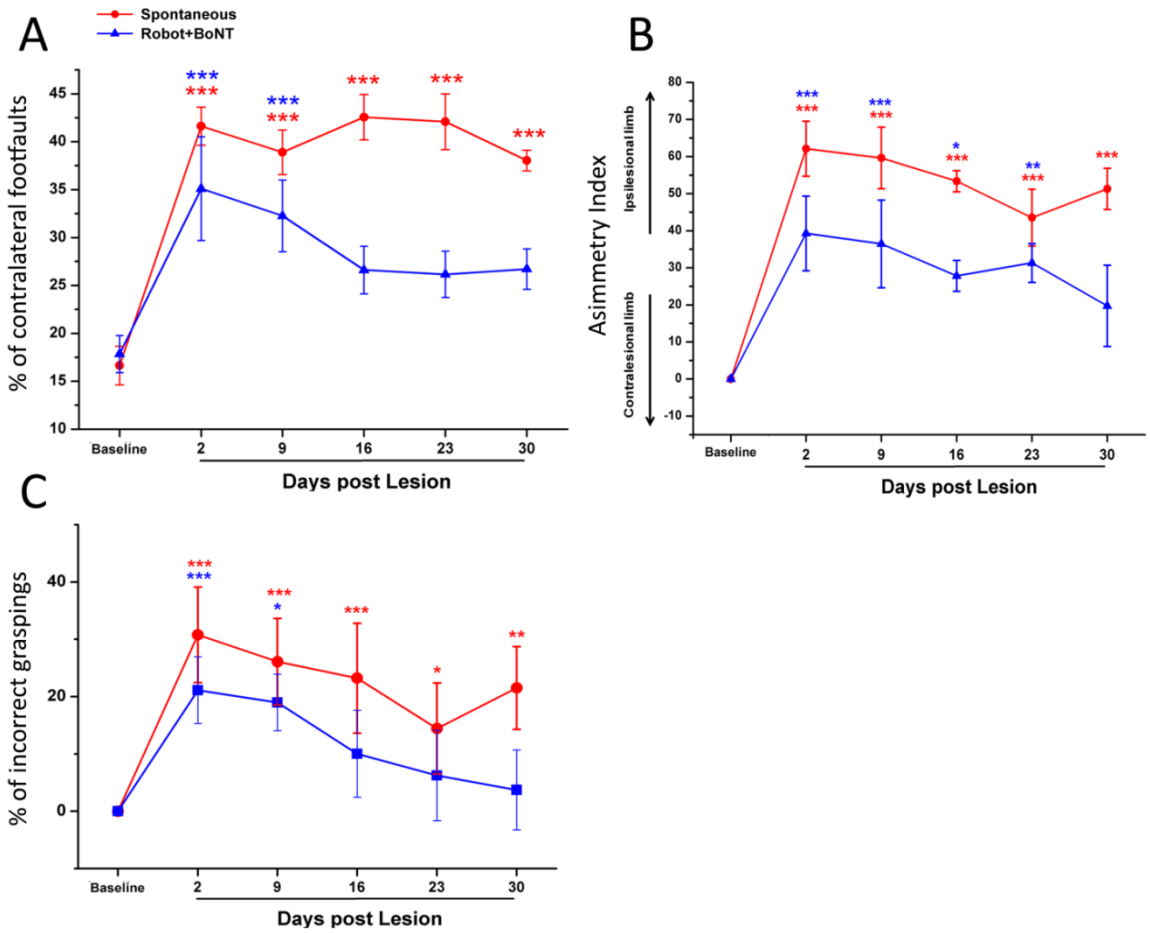

Figure 32. Combined treatment significantly improved motor recovery. Combining the inhibition of the healthy hemisphere with daily robotic rehabilitation significantly improved the post-stroke recovery in all tests used: in the Gridwalk test (A) from day 16 there is no significant difference to baseline values. In the Schallert Cylinder test (B) there is an early improvement and 30 days post stroke the performance is not different to baseline. Moreover, in the skilled reaching test (C) the percentage of incorrect graspings normalized after day 16. Data are mean ± SE. *, p<0.05; **, p<0.01; ***, p<0.001 and refers to baseline (Two Way RM ANOVA followed by Tukey test).

Interestingly, also the success rate in the Skilled Reaching Test, measured as the endpoint analysis of errors percentage, shows a marked improvement for the combined treatment group (**Figure 32**). In fact, while the spontaneous recovery is not sufficient to bring values back to baseline performance, the BoNT+Robot group improves starting from day 9 and from day 16 the motor outcome results undistinguishable from the baseline (two way RM ANOVA followed by Tukey test, Day 2 p=0.010; Day 9 p=0.027, Day 16 p=0.550, Day 23 p=0.901,

Day 30 p=0.989). More importantly, the motor recovery detected by generalized motor tests is reflected also by several parameters of reaching kinematic analysis, showed in **Figure 33**.

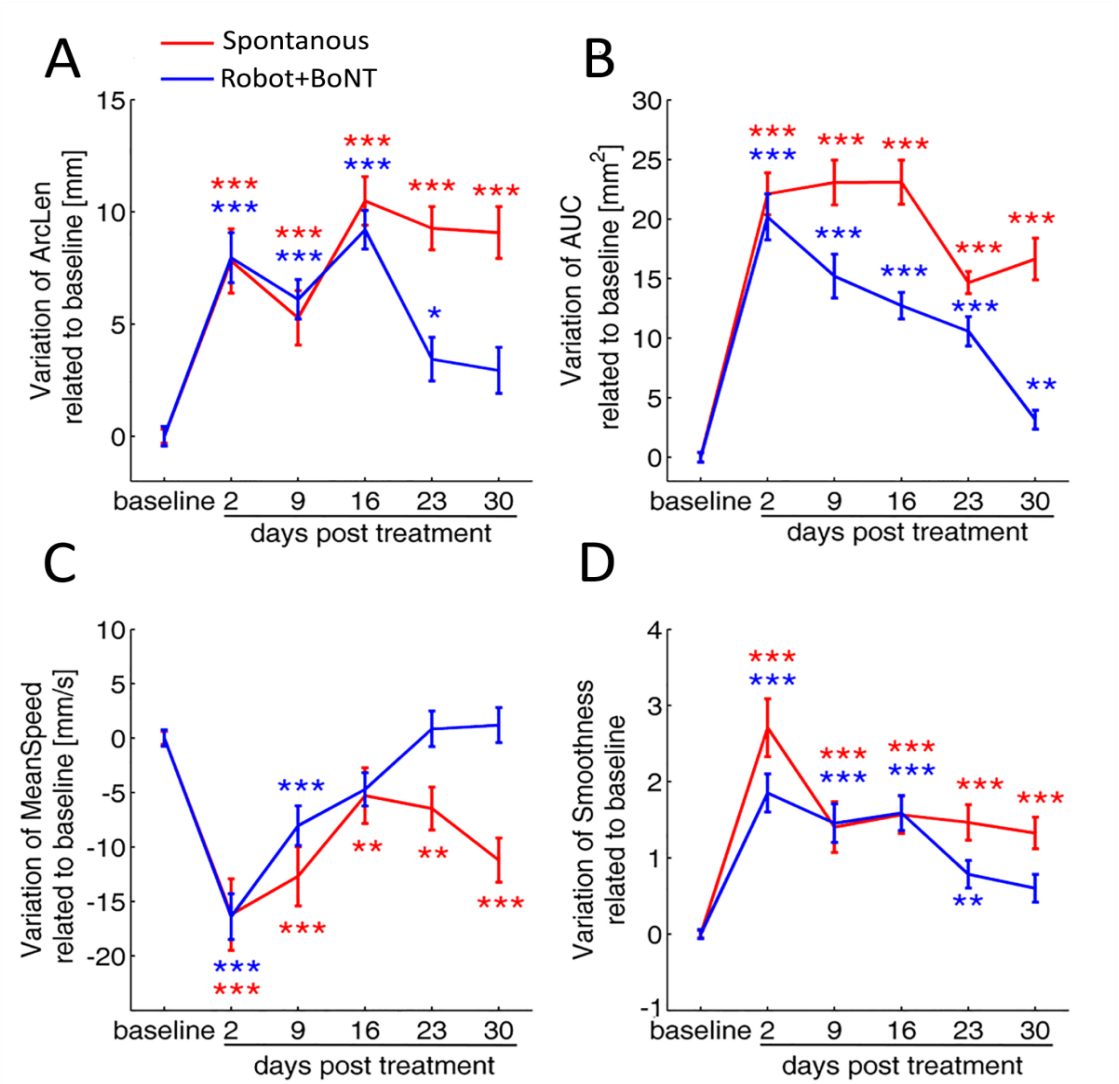

Figure 33. Kinematic analysis during the reaching movement after combined treatment. The kinematic analysis of the reaching showed that after combined therapy movement patterns returned similar to the pre-lesion conditions, especially at 30 days post-stroke as showed by the ArcLen (A), the Mean Speed (C) and the Smoothness (D). The Area under the Curve (AUC) remains significantly different from baseline at 30 days post-stroke, however a strong impact on the recovery is clearly visible (B). Data are mean ± SE. *, p<0.05; **, p<0.01; ***, p<0.001 and refers to baseline (One Way RM ANOVA followed by Tukey test).

In particular, the length of the movement improves at day 23 and completely recovers at day 30 post lesion while a positive trend is reported for the width of the trajectory (**Figure 33**A and B, one way RM ANOVA followed by Tukey test, ArcLen 23days p =0.022; 30days p=0.064; AUC 30days p=0.001). Of note, a significant restoration of pre-lesion values is also reported for the speed profile and for the smoothness of the reaching movement (**Figure 33**C and D, one way RM ANOVA followed by Tukey test, MeanSpeed 16days p=0.059; 23days p=0.998; 30days p=0.987; Smoothness 23days p=0.004; 30days p=0.099) (see Methods).

Altogether, these kinematic data are clear in indicating a substantial restoration of pre-lesion movement patterns in stroke animals subjected to combined robotic training and silencing of the healthy hemisphere.

2.6 Plasticity markers: combined treatment reduces the expression of "plasticity brakes" in the perilesional tissue

In order to identify possible mechanisms of the recovery induced by the combined treatment, I performed an immunohistochemical analysis looking for differences in the expression of plasticity markers between the spontaneous and the rehabilitated group. I counted the number of Parvalbumin- and Somatostatin-positive inhibitory interneurons in the perilesional tissue lateral and medial to the lesion in a group of stroke animals with and without rehabilitation and in a control group at 30 days post-surgery. I followed the same scheme depicted in **Figure 16** and then I pooled the values in a global perilesional measure. I found that the density of PV+ cells spontaneously decreased after stroke with respect to sham condition (t-test $p<0.001$). However, the BoNT+Robot treatment further accentuates this decline and the number of PV+ cells resulted to be significantly lower with respect to spontaneous condition (**Figure 34A, B**; t-test; $p=0.045$). The same trend was found for another important class of inhibitory interneurons, which is the SOM+ population. The number of these cells is significantly lower after stroke with respect to sham (t-test; $p<0.001$) but in the rehabilitated group is further diminished (**Figure 34C, D**; t-test; $p=0.014$).

Another important marker of the re-opening of cortical plasticity in the adult tissue is the myelin basic protein (MBP), which is one of the major components of the myelin sheath formed by oligodendrocytes (Bartholdi and Schwab, 1998; Kim et al., 2009). I compared MBP expression between spontaneous and BoNT+Robot group in 200 µm wide columns close to the lesion, 30 days after injury. I found a significant decrease in the protein expression in the rehabilitated group (**Figure 34E, F**; t-test; $p=0.045$), thus indicating a more plastic state of the perilesional tissue in the rehabilitated group.

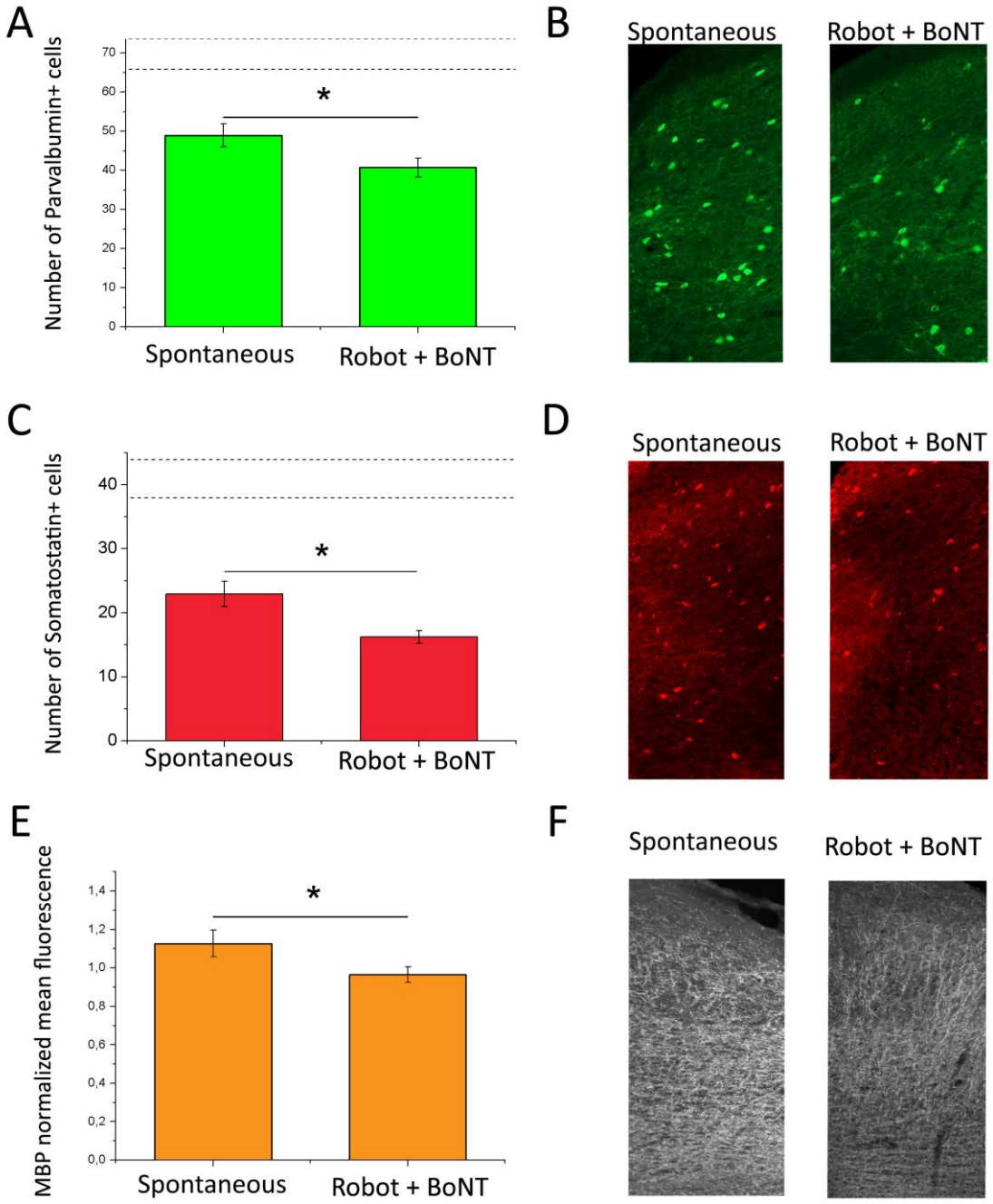

Figure 34. Plasticity markers after combined treatment. the number of Parvalbumin–positive cells decreased with rehabilitation (A) as shown by representative micrographs of the counting region (B, rehab n=6, spont n=8). Also the number of Somatostatin-positive cells in the perilesional tissue decreased after combined therapy (C and D, rehab n=6, spont n=4). The mean fluorescence of MBP staining indicated that the rehabilitated animals (n=4) have less MBP in the perilesional cortex with respect to non-rehabilitated group (n=3)(E and F). Data are mean ± SE. (t-test *, $p<0.05$).

3. Preliminary results: transplant of mouse embryonic stem cells (mESC) into the ischemic cortex

3.1 mESC in vitro differentiation protocol

Several groups have attempted transplant of stem cells in stroke to replace lost neurons and stimulate plasticity of spared pathways. I have collaborated with the laboratory of Federico Cremisi, which established a novel three steps protocol for the differentiation in a Chemically Defined Minimum Medium (CDMM) of mouse embryonic stem cells (mESC) into neurons of cortical identity (**Figure 35A**).

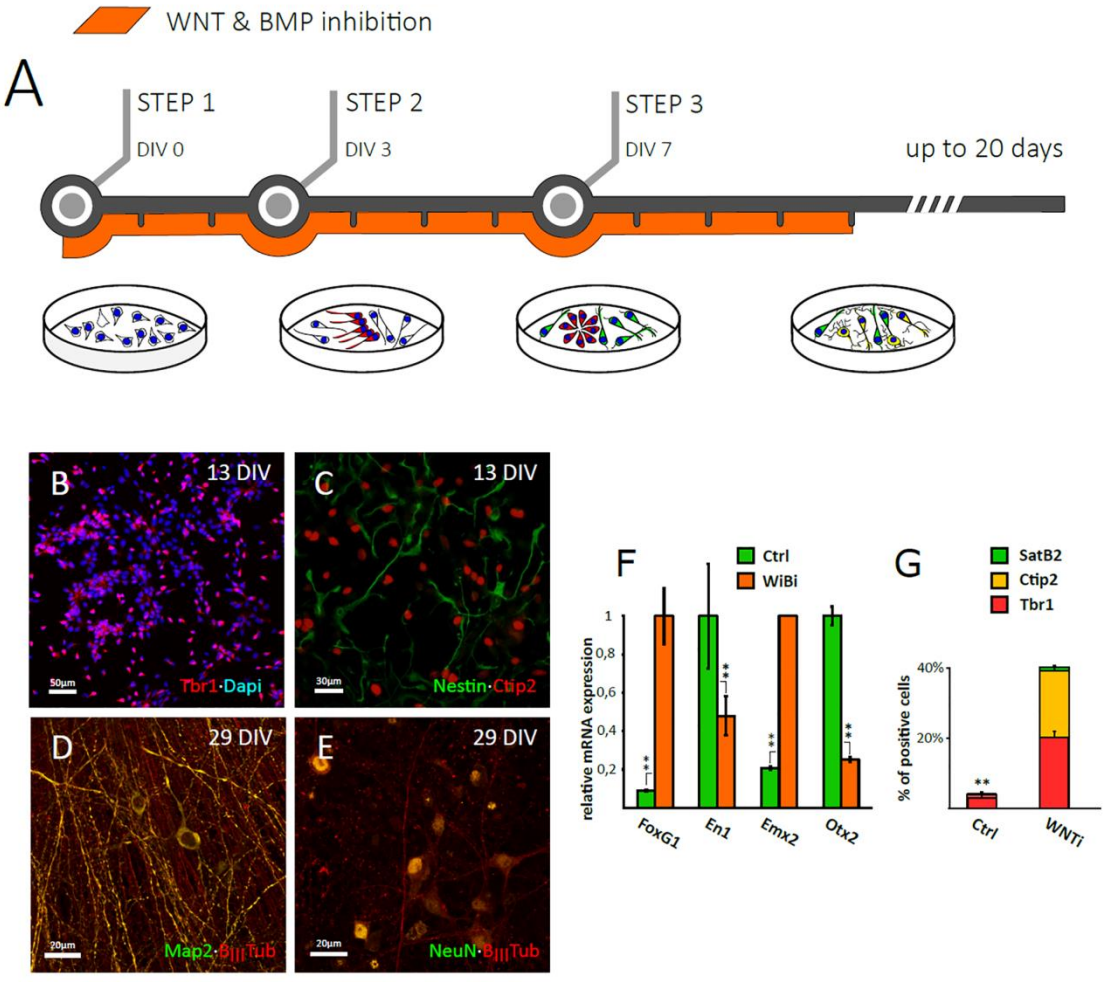

Figure 35. inhibition of the autologous Wnt and BMP signalling in differentiating mESC. Inhibiting Wnt and BMP pathways in a chemically defined medium (A) promotes the expression of the anterior forebrain marker FoxG1, the early telencephalic marker Emx2 (F) and the markers of cortical cell subtypes Tbr1, Ctip2 and Satb2 (B, G). Moreover, Wnt- and BMP-inhibited cells downregulate the expression of the more posterior neuronal markers Otx2 and En1 (F). Finally, at later stages of differentiation mature neural markers Map2 (D) and NeuN (E) are highly expressed in differentiated cells.

They found that the inhibition of the endogenous WNT and BMP signaling for 11 days promotes the expression of telencephalic and cortical genes, such as FoxG1 and Emx2, while it represses more posterior mesencephalic genes, such as Otx2 and En1 (**Figure 35F**). After 13 days of differentiation in vitro (DIV) these cells express the early cortical markers Tbr1 and Ctip2 (**Figure 35B-C**) at a higher level compared to control (**Figure 35G**).

Prox1, Wnt8b and Emx2 are highly expressed in the embryonic hippocampus compared to the surrounding cortical areas as shown by the specific expression of these three markers in the medial pallium embryonic after in situ hybridization experiments in E15.5 mice embryos (from Allen Brain Atlas and Fotaki et al., 2010, **Figure 36B**).

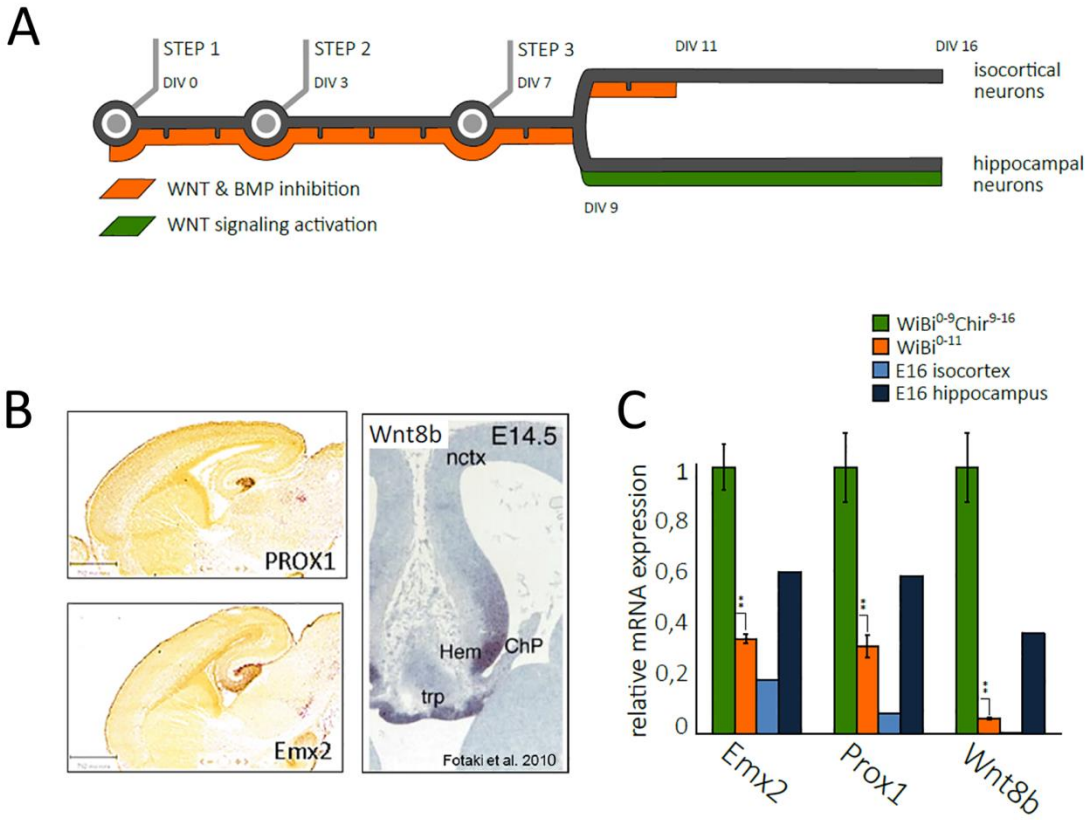

Figure 36. Hippocampal and isocortical differentiation. Layout of the differentiation protocol of mESC in isocrtical- and hippocampal-like neurons (A). Prox1, Wnt8b and Emx2 in situ hybridization from embryonic mouse show the expression in the developing hippocampal regions nctx = neocortex; Hem = cortical hem; ChP = choroid plexus; trp = telencephalic roof plate (B). (C) Expression analysis of embryonic hippocampal markers Emx2, Prox1 and Wnt8b in isocortical-like (WiBi treated) and in hippocampal-like (Wibi and Chir treated) mESC-derived neurons and E16 embryonic brain via RT-PCR.

The dorso-medial region of the telencephalon has a fundamental role as signaling center in cortical development. In fact, along the dorsal telencephalic midline there is a high expression of BMPs and WNTs (Hèbert et al., 2002; Shimogori et al., 2004), which are required for the hippocampal field specification (Lee et al., 2000; Yoshida et al., 2006).

Accordingly, the double inhibition of WNT and BMP signaling for the first 9 days of mESC differentiation, followed by activation of canonical WNT signaling with a Wnt agonist CHIR99021 (3uM, DBA) between DIV9 and DIV16 increase the expression of the embryonic hippocampal markers Prox1, Emx2 and Wnt8b (**Figure 36A, C**).

In conclusion, they were able to manipulate WNT and BMP signalling pathways in vitro in order to obtain isocortical and hippocampal neurons.

3.2 mESC derived neurons integrate and send projections in the adult brain, especially after stroke

In order to track transplanted cells in the host brain, cortical and hippocampal ESC-derived neurons were labelled with lentiviral vectors carrying membrane-bound forms of GFP and mCherry, respectively, which allowed to visualize long distance projections (see below). In order to evaluate survival and behavior of the cells in vivo, hippocampal (HIP) and isocortical (CRT) cells were pooled and transplanted into the motor cortex and hippocampus of adult mice (**Figure 37**). After two weeks I performed neuroanatomical analysis of the grafted cells and their projections.

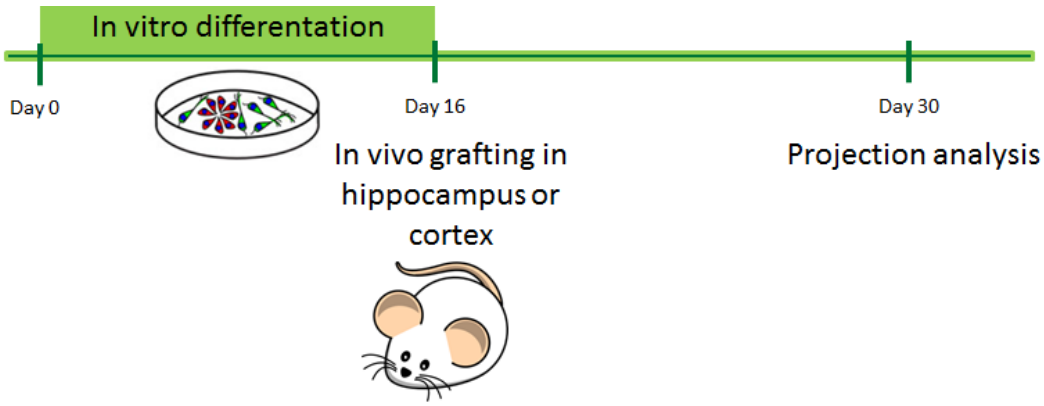

Figure 37. In vivo transplantation protocol. After 16 days of differentiation in vitro cells were differentially labelled with GFP (isocortical) and mCherry (hippocampal) and grafted into the motor cortex and hippocampus of healthy adult mice.

When the graft was centered in the dentate gyrus of the hippocampus, I found an extended projection pattern of HIP cells (red) mainly to hippocampal structures and to anterior brain areas. Conversely, cortical cells (green) showed a very poor arborisation that remained confined to the injection site (**Figure 38**).

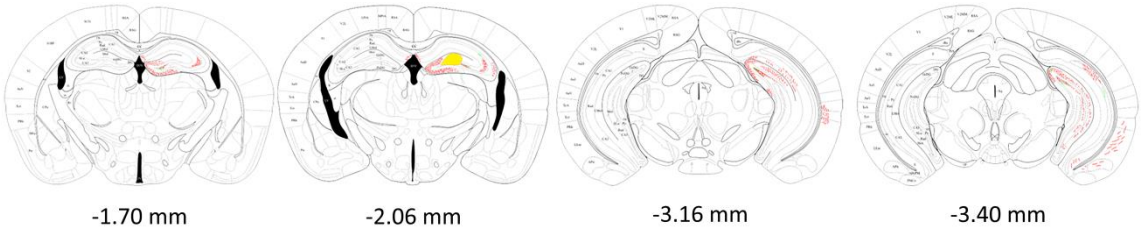

Figure 38. Projection pattern of hippocampal- and isocortical-like cells grafted in the hippocampus. Anteroposterior reconstruction of fibers elongated from hippocampal- (red) and isocortical-like (green) cells after double transplant in the dentate gyrus of hippocampus. The yellow spot represents the transplant composed by both green and red cells.

As in the previoous case, after grafting into the motor cortex, HIP neurons (red in **Figure 39**) sent very long projections from the injection site showing a preference for the agranular cortex, hippocampus and white matter. Conversely CRT grafted neurons (green) extended very short projections that remained in proximity of the transplant core.

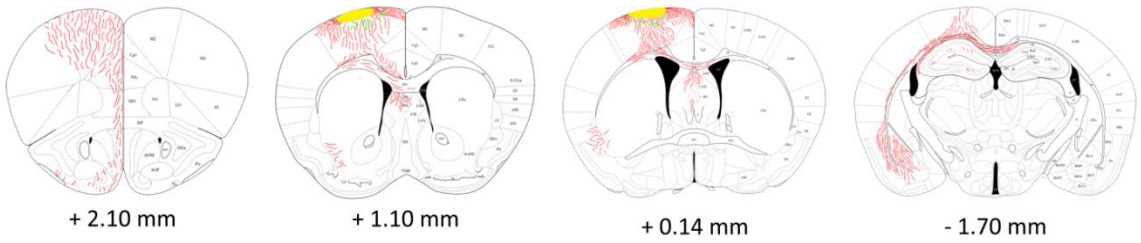

Figure 39 Projection pattern of hippocampal- and isocortical-like cells grafted in the cortex. Anteroposterior reconstruction of fibers elongated from hippocamapal- (red) and isocortical-like (green) cells after double transplant in the motor cortex. The yellow spot represents the transplant composed by both green and red cells.

Since I were interested in studying the behavior of mESC-derived cells in the ischemic brain, I grafted cortical and hippocampal cells at 3 days post-injury in the ischemic core and in the perilesional area and after 2 weeks I studied their projection patterns. HIP cells still elongated fibers in many cortical areas as in the healthy brain. Surprisingly, the projection patterns of CRT cells (green) grafted after stroke, are really different compared to the previous graftings in healthy animals. Indeed, I documented robust neurite extension from CRT cells both in the cortex surrounding the transplant and in other subcortical regions involved in the motor pathways such as the Internal Capsule (IC) (**Figure 40**).

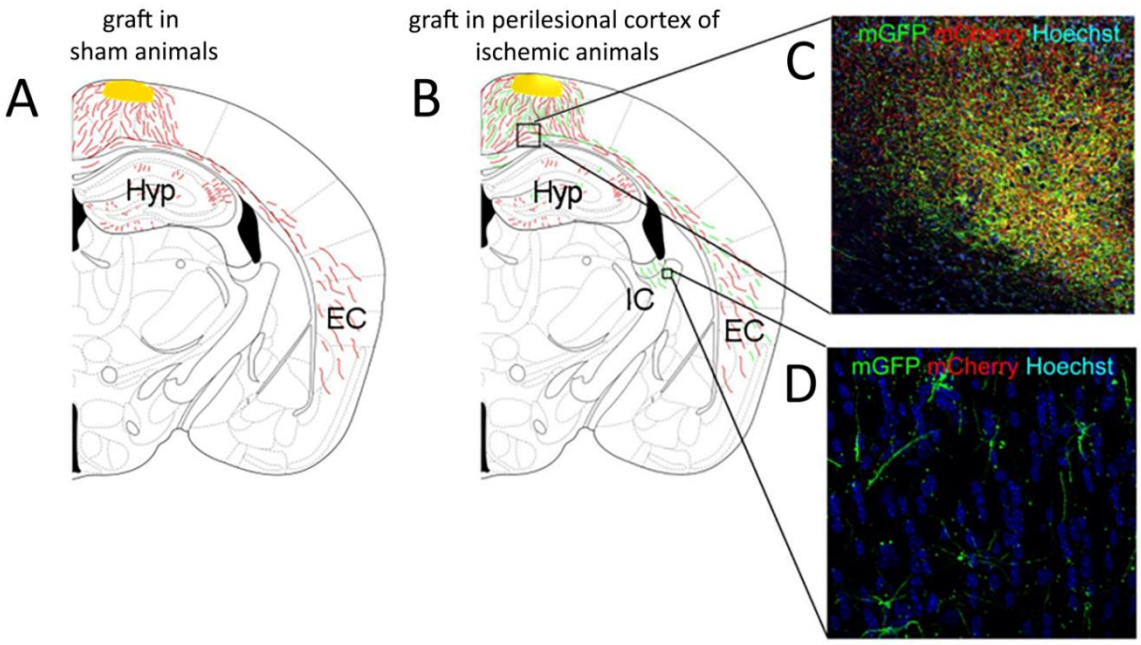

Figure 40. Projections after transplant of HIP and CRT cells in the host ischemic brain. After grafting cells in the perilesional cortex of the ischemic brain (B) CRT neurons extended many projections compared to graftings in healthy animals (A). Green fibers reached very long targets and extensively targeted the peri-injection site up to the Entorhinal Cortex together with red fibers (C) but only green fibers reached motor subcortical structure such as the Internal Capsule – IC (D).

Altogether, these data indicate that isocortical-like cells extend projections only when stimulated by the ischemic brain environment. I am currently investigating whether transplant of these cells may modulate functional recovery after stroke.

Discussion

Kinematic characterization of post-stroke reaching impairments

To objectively evaluate the effectiveness of a rehabilitative therapy, the training-induced motor improvement should be also detectable in other motor paradigms non-directly related to the exercised task. Concerning animal models, in the literature a battery of motor tests for rodents have been characterized and generally accepted for evaluating post-stroke forelimb motor function (Brooks and Dunnett, 2009). One of the most used motor tests is the Skilled Reaching Task: animals are trained to reach food pellets with their forepaw and bring them the mouth. The percentage of correct/incorrect grasps (including fallen pellets) is a relevant end-point measure for the assessment of the forelimb function during post-stroke recovery (Alaverdashvili & Whishaw, 2010; Klein et al., 2012; Moon et al., 2009; Whishaw et al., 2008). To better distinguish between "true recovery" and compensation, kinematics could provide useful information about the reaching movement strategy by means of the study of the paw trajectory. This kinematic approach has been already used in some reports, but the evaluation phase was always made manually by the experimenter, thus possibly introducing experimenter's bias and dramatically increasing the time required for analysis (Alaverdashvili & Whishaw, 2013; Braun et al., 2012).

Here, for the first time, kinematic impairments of mouse reaching movements have been quantitatively described by a set of measures computed from paw trajectories, instead of a time-consuming manual frame-by-frame video analysis. These findings demonstrate that in the mouse model, key kinematic measures are sensitive to detect differences in performance before vs. after stroke.

After stroke, reaching success by the forepaw contralateral to the lesion was impaired and partly recovered over the 4 postsurgical weeks (**Figure 10**). The photothrombotic lesion also caused distinct changes in forelimb preference (Schallert Cylinder), and important deficits in sensory-motor coordination (Gridwalk test) remaining defective up to 30 days after surgery. This is consistent with previous works on mice (Farr and Whishaw, 2002; O'Bryant et al., 2011) (**Figure 9**). It is worth noting that in my experiments, mice performed the grasping task only once a week, thus it is unlikely that such modest training be sufficient to achieve significant recovery in generalized motor tasks. Indeed, an intensive training regimen is necessary to produce functional gains that extend to dissimilar, untrained tasks. For example, in rats with spinal cord lesions, daily training in the single pellet grasping task leads

to a small but detectable improvement in performance on the horizontal ladder test (Gholamrezaei and Whishaw, 2009).

Rodent skilled reaching represents an ideal translational model and a powerful tool to generalize preclinical research to clinical conditions. In this work, kinematics of successful reaching movements was analyzed by a semi-automated tool that proved to be accurate, precise and robust. More interestingly, it allowed for a significant reduction of the total computational time required by a manual operator to perform a similar analysis. Impairments in kinematics of reaching movements were previously assessed in a mouse model of stroke (Farr and Whishaw, 2002; Klein et al., 2012), but only qualitatively and manually evaluated by an operator. Although that protocol allows for a more detailed analysis of reaching movement patterns, including digits flexion or extension, it is severely limited by inter-rater variability and by the need for time consuming frame-by-frame video analyses. On the other hand, the approach presented in this study is independent from operator's expertise and provides objective and prompt measures of kinematic impairments. These are desirable features, especially for studies envisaging multiple combined recording (and analysis) of kinematics and neurophysiological signals, or for rehabilitation protocols requiring continuous monitoring of performance to trigger appropriate modifications to foster motor improvement.

Several parameters were computed from the recorded trajectories, designed to describe both global and local features of the reaching movement. The kinematic analysis showed that, after stroke, mice displayed abnormal forepaw movements (**Figure 11 and Figure 12**). Compared to baseline, mice tended to move the paw higher before pellet grasping, and approached the pellet with a distorted curvature. Moreover, the whole movements were significantly longer, slower, irregular, and spanned a broader workspace. Finally, when retracting the paw towards the mouth to eat the pellet, dragging occurred more frequently and for a prolonged time interval. When compared to human studies (Cirstea and Levin, 2000; Rohrer et al., 2002; Subramanian et al., 2010; Alt Murphy et al., 2011, 2013; Panarese et al., 2012; Krebs et al., 2014; van Dokkum et al., 2014), important similarities were observed in the trajectories of the two species, summarized by the parameters *ArcLen*, *Mean Speed* and *Smoothness*: post-stroke reaching movements are longer, slower, and more segmented. No comparison, however, was possible on the other parameters, which have never - to my knowledge of the literature - investigated in humans. Nevertheless, they represent potentially interesting biomarkers of post-stroke impairment and deserve to be tested in future rehabilitation protocols for human subjects.

Thus, my results emphasizes the utility of the mouse model and the kinematic analysis as means to examine post-stroke functional impairments and, potentially, track motor improvements due to treatment effects that may ultimately generalize to patient populations.

Neuroplasticity changes after stroke

Understanding cellular mechanisms governing post-stroke cortical plasticity is critical to develop novel and more effective pharmacological therapies to improve outcome in stroke survivors.

I focused my analysis on peri-infarct regions since evidence in patients and animal models indicates that spared areas surrounding the lesion significantly contribute to functional recovery (Li et al., 2010; Starkey et al., 2012; Clarkson et al., 2013; Harrison et al., 2013; Grefkes and Ward, 2014). In ICMS experiments, I observed a reduction in the number of cortical sites that elicited movements of the lesioned forelimb 30 days after stroke. This was accompanied by a corresponding expansion of the hindlimb motor map, that in healthy animals is centered posterior to the CFA (Kleim et al., 1998; Pronichev and Lenkov, 1998). My results are consistent with previous reports indicating shrinkage of the cortical representation of affected forelimb in favour of other body parts (Castro-Alamancos and Borrel, 1995; Nudo and Milliken, 1996). These motor map reorganizations are reminiscent of activity-dependent competition in sensory cortices (Restani et al., 2009; Nahmani and Turrigiano, 2014; Deidda et al., 2015).

The current threshold to evoke movements also changed after stroke. Overall, a higher current intensity was required to evoke a forelimb movement post-stroke, while hindlimb movements were elicited with a slightly reduced current. In keeping with my results, previous studies in humans and rodents have shown an inverse correlation between the current threshold and the size of the motor map (Marconi et al., 2011; Young et al., 2011). Young and colleagues (2011) correlated GABAergic neurotransmission with cortical map properties, so that a shift in the balance between excitation and inhibition influenced both movement thresholds and map size. It has also been suggested that inhibitory neurotransmission is responsible for the stability and sharpening of motor and sensory maps (Hensch and Stryker, 2004; Foeller et al., 2005; Nudo, 2013). Specifically, local reduction of intracortical inhibition allows the unmasking of subthreshold inputs and the consequent expansion of adjacent motor maps (Jacobs and Donoghue, 1991). In this context, a reduction of GABAergic inhibition might allow plasticity of spared areas and pathways following stroke. Indeed, my neuroanatomical analyses revealed a significant reduction of two major populations of GABAergic cortical interneurons after the infarct. Somatostatin-containing interneurons represent a low-threshold inhibitory population involved in cortical plasticity (Cardin, 2012; Gentet et al., 2012; Stryker, 2014) whereas parvalbumin-positive fast-spiking interneurons play important roles in control of network firing due to their perisomatic synapses onto pyramidal cells (Di Cristo, 2007). My immunohistochemical data do not allow to distinguish between cell death of interneurons and down-regulation of the expression of their markers,

which are however potentially related to an impairment in the normal physiology of these cells. Reduction of GABAergic neurotransmission was confirmed by analysis of the number of V-GAT-positive inhibitory presynaptic terminals in the perilesional cortex, 30 but not 7 days after stroke. In order to quantify V-GAT- and V-GluT1-positive terminals in a more reliable way, I used a normalization method using a reference field for each analysed section (see methods) with the advantage of maintaining spatial information (compared to other quantification method e.g Western blotting). A reduced inhibitory tone is in keeping with the observation of a loss of selectivity in the motor maps, with a dramatic enhancement of the number of sites evoking simultaneous movement of different body parts, and a corresponding reduction in the percentage of cortical area evoking specific and unique movements (see **Figure 15a**). It is important to note that while synaptic GABA may be reduced, elevated tonic GABA currents have been clearly demonstrated after stroke (Clarkson et al., 2010).

Overall, my data point to a consistent downregulation of GABAergic markers that is initially detectable 7 days after stroke and becomes more widespread one month post-stroke, coupled with a reduction of PNNs. The role of the GABAergic system and PNNs in functional recovery after stroke has been suggested by previous reports. It has been shown that daily motor rehabilitation in stroke mice triggers an improvement of grasping abilities, which is associated with a reduction in parvalbumin, calretinin, and calbindin expression in the agranular cortex adjacent to the infarct in the first week after stroke (Zeiler et al., 2013). Similarly, removing PNNs from the perilesional tissue can be beneficial for motor recovery after injury (Soleman et al., 2012; Gherardini et al., 2015). Thus, the release of specific "neuroplasticity brakes" (such as GABAergic neurotransmission and PNNs) from the perilesional areas may trigger the reopening of a sensitive period for cortical remodelling that allows network reorganization and potentially some restoration of function. This interpretation fits well with the finding that, despite a global shrinkage of the affected forelimb representation, specific postero-medial sites of the motor cortex appear to gain forelimb responsiveness after stroke (blue "hot spots" in **Figure 15b**). This finding may indicate an initial attempt of the motor network to relocalize lost motor functions. Interestingly, Starkey et al. (2012) observed that in stroke rats with good functional outcome, neurons within the hindlimb motor cortex (posterior to the lesion site) acquire the ability of triggering forelimb movements, pointing to compensatory take-over by peri-lesional areas.

Several studies have reported a decreased intracortical inhibition in stroke patients (Liepert et al., 2000; Blicher et al., 2009). After unilateral stroke, Rossini and colleagues found a reduction of intracortical inhibition in the affected hemisphere and normal inhibitory levels in the contralesional one (Cicinelli et al., 2003). Kim et al. (2014) reported reduced $GABA_A$ receptor availability in the primary motor cortex of stroke patients and these changes in

GABA receptor availability were significantly related to motor recovery. Altogether, these data are consistent with the view that a reduction of the inhibitory tone generally facilitates the reinstatement of plasticity in the adult cortex (e.g. Harauzov et al., 2010).

Downregulating the GABAergic system to stimulate recovery

Based on these premises, I downregulated GABAergic signalling early after stroke in order to boost such spontaneous plastic phenomena. Increasing GABA signalling in post stroke patients and rodent models does not improve motor function (Madden et al., 2003). Rather, administering a benzodiazepine after rehabilitation leads to an acute loss of the regained function (Lazar et al., 2002, 2010). Finally, lowering tonic GABAergic inhibition improves motor recovery after stroke (Clarkson et al., 2010; Lake et al., 2015). Here, I targeted GABAergic signalling by using the benzodiazepine inverse agonist DMCM, which reduces inhibitory currents by binding predominantly to synaptic $GABA_A$ receptor subunits (DMCM binding affinity α1 > α2 = α3 > α5; Lüddens & Wisden, 1991). It should be noted, however, that some drugs with an effect α1-mediated of the $GABA_A$ receptor (usually synaptic) may also act extrasynaptically (Che Has et al., 2016). DMCM has been previously used to modulate plasticity in the visual cortex (Hensch and Stryker, 2004). My results show a significant improvement in behavioural readouts immediately after the treatment, i.e. day 9 post-stroke, which was maintained in the follow-up period up to 30 days after stroke. Improvements were seen both in general motor coordination and in skilled forelimb use, as shown by the gridwalk and pellet grasping task, respectively. Improvements were not due to the anxiogenic properties of the drug (Volke et al., 2003), as the motor performance was maintained or even enhanced at 30 days after termination of the treatment (see **Figure 22**).

I chose to administer DMCM during an early post-stroke phase (day 3 - day 8) corresponding to the period of maximal susceptibility to therapeutic interventions (Zeiler and Krakauer, 2013). Reducing GABA neurotransmission too early can have a detrimental effect on lesion size and motor outcome (Clarkson et al., 2010). Indeed, the inhibitory system is believed to dampen excitotoxic phenomena in the acute phase, thus limiting the extent of damage. On the other hand, previous studies have shown that an early therapeutic intervention appears to be critical for the motor outcome (Biernaskie et al., 2004; Ng et al., 2015). These data suggest the existence of a “critical period” during which intervention strategies are more effective. These post-stroke events are reminiscent of the sensitive periods in developing sensory cortices, determined by an optimal level of $GABA_A$ signalling (Hensch, 2005). In animal models, expression of $GABA_A$ receptor subunits shows a complex layer- and time-specific regulation after stroke. $GABA_A$ receptors generally decrease in

perilesional cortical areas (Neumann-Haefelin et al., 1998; Redecker et al., 2002; Jolkkonen et al., 2003; Kharlamov et al., 2008; Schmidt et al., 2012). One exception is a recent study by Hiu et al., (2016) who reported a transient increase in α1 receptor in layer V after stroke. In this context, it is possible that both increasing and reducing $GABA_A$ signalling (via zolpidem and picrotoxin/DMCM, respectively; Hiu et al., 2016 ; Clarkson et al., 2010 ; present data) results in a significant gain of forelimb function after stroke, possibly by restoring an optimal excitation/inhibition balance in specific cortical microcircuits (Hensch 2005). Whether DMCM acts at the level of the perilesional cortex, contralesional hemisphere or subcortical structures remains to be addressed. Overall, downregulation of $GABA_A$ signalling during an early post-stroke period appears to leave a persistent trace on post-stroke networks that translate into a long-lasting motor improvement.

Altogether, my data highlight a coordinated remodelling of GABAergic inhibitory networks that play an important role in post-stroke behavioural gains. Pharmacological therapies impacting on GABAergic signalling may accelerate and improve such spontaneous plastic adjustments resulting in significant, even if not complete, restoration of motor function. In fact, DMCM treatment was effective to improve general motor and skilled task but not the kinematics of reaching movements, possibly because of the lack of a specific rehabilitation that guides the re-establishment or pre-lesion motor patterns. It is possible that an appropriate combination of reduced GABAergic signalling and motor training leads to synergic effects resulting in a more complete post-stroke motor recovery (Wahl and Schwab, 2014). In keeping with this idea, recent studies have reported an additive or synergic effect of motor rehabilitation with plasticizing treatments, e.g. treatment with chondroitinase ABC was potentiated by task specific rehabilitation in spinalized rats (García-Alías et al., 2009). In this context our group recently introduced a robotic platform that allows animals to perform repeated controlled sessions of forelimb retraction and represents a promising tool for intensive and specific forepaw motor training (Spalletti et al., 2014).

Effects of robotic training and healthy hemisphere silencing on functional recovery

Previous studies reported that, not only the spared perilesional tissue but also the contralateral hemisphere is involved in functional changes after an ischemic insult in primary motor area. In fact, even if it is widely accepted that the healthy hemisphere plays a role in functional recovery, it is still not clear if it has an adaptive or maladaptive role. Previous findings showed that inhibition of the unaffected hemisphere decreases the interhemispheric inhibition toward the injured one and promotes motor recovery (Hummel and Cohen, 2006;

Zimerman et al., 2012). This effect was particularly evident in the case of small cortical lesions (Pino et al., 2014). To investigate this point, I transiently inhibited the contralesional CFA during the first two weeks post lesion (or at least up to 10 days, see **Figure 29**). I used Botulinum Neurotoxin E (BoNT/E) to reversibly block the excitatory neurotransmission by cleaving a main component of the SNARE complex thus impairing neurotransmitter release and synaptic transmission. I infused BoNT/E in the contralesional hemisphere at the same coordinates of the ischemic lesion and in the same surgery. This treatment partially improved general motor outcome in the gridwalk test (**Figure 31A**), but did not increase the spontaneous use of the impaired forelimb (Schallert Cylinder test, **Figure 31B**). Thus, this treatment alone is not able to guarantee stable, long-lasting recovery. It is possible that silencing the contralesional motor area favours plastic events in the perilesional tissue and enhance cortical reorganization, thus opening the way for a functional recovery, that however, needs to be appropriately guided. Consistently, even after DMCM treatment the kinematic analysis failed to demonstrate a return to pre-lesion movement patterns. Thus, a plasticizing treatment alone may increase success in completing a task (i.e. end points), but if not guided by rehabilitation, the motor improvements appear to be associated with the development of compensatory strategies.

To supply motor training in my project, I used an innovative robotic platform as a rehabilitative device to restore motor function. To make the rehabilitative protocol more similar to human patients situation, the robotic treatment was applied in the sub-acute and not in the acute phase. Repetitive training on the robotic platform (from day 5 up to 30 post-injury, once a day, 5 days per week) was not sufficient to improve motor outcome in both Gridwalk and Schallert Cylinder test. It has been reported that physical exercise is able to induce activity dependent plasticity and to model neural circuits both in normal conditions and after a brain injury (Griesbach et al., 2004; Vaynman and Gomez-Pinilla, 2005; Ding et al., 2006). However, most of the studies that assessed the effect of motor training, especially in animal models, had the problem of circularity, i.e. the same skilled motor test was used both as a rehabilitative treatment and to quantify motor performance. On this aspect my findings are in accordance with literature since I found that motor training alone, despite ameliorating performances in the specific task used for rehabilitation (**Figure 25**), is not effective enough to extend motor improvements to other motor tasks (**Figure 26**).

Finally I coupled the previous plasticizing treatment (BoNT/E cortical infusion) with a daily rehabilitative training 5 days a week for 30 days post lesion after a first assessment of forelimb motor deficit in classical behavioral tests and in the kinematic parameters during the skilled reaching. The results of these experiments showed an improvement in general motor function in Gridwalk and Schallert Cylinder test that in both cases showed a final performance not different from baseline (**Figure 32A, B**). Of note, the motor improvement

interested also skilled forelimb abilities in the reaching test, not only in terms of end-point measures (**Figure 32C**) but, more importantly, in terms of kinematic features (**Figure 33**). In fact, a highly significant improvement was detected in the Mean Speed and smoothness of the reaching movement. However, not all the kinematic parameters were improved by the treatment: in fact, the reaching trajectory continued to be slightly higher and to cover a wider space compared to baseline performances.

These results are in keeping with the idea that a combination of motor training and "plasticizing" treatment can provide an additional synergic therapeutic effect. In fact, it is known from other animal studies that exposure to Environmental Enrichment (EE) improves cognitive skills, induces marked increase in synapse number and in dendritic branching and that after an ischemic injury could lead to an improvement in several sensorimotor tasks (Hebb, 1949; Diamond et al., 1976; Johansson and Ohlsson, 1996; Kleim et al., 1996). However, more specific investigations have demonstrated that for recovery of proximal and distal forelimb function, the exposure to enriched conditions was not effective (Grabowski et al., 1993b) while the combination of EE with skilled reaching training effectively improved forelimb motor performances and increased dendritic arborization complexity in the healthy hemisphere (Biernaskie and Corbett, 2001b). Moreover, combining the delivery of anti-Nogo-A antibodies, with motor training in forelimb reaching strongly improved motor recovery (Wahl and Schwab, 2014) Specifically, the authors reported a time-dependent effect in the coupling of these two approaches, in fact, the best recovery has been obtained when administration of anti-Nogo-A antibody precedes motor training (Wahl and Schwab, 2014).

Another example of sequential administration of different therapies shows that intracerebral delivery of epidermal growth factors, followed by EE and training accelerates the recovery process in pellet retrieval – a recovery which is already complete 4 weeks from stroke (Jeffers et al., 2014). In a similar way, rehabilitation has been administered in combination with perturbation of ephrin-A5 signalling and CSPGs degradation (Hill et al., 2012; Overman et al., 2012; Gherardini et al., 2015).

Many of the published studies found a reorganization of the neural tissue together with sprouting phenomena. Consistently I found a decrease in "plasticity brakes" in the perilesional area after the combined treatment. This decrease was evident also in the spontaneous, untreated stroke group, suggesting an attempt to allow motor recovery. Interestingly, after combined treatment the extent of this decrease is even more evident with respect to non-rehabilitated animals (see **Figure 34**). Overall, these data indicate that the increased recovery is accompanied by modulation of well-known plasticity markers, such as GABAergic neurotransmission and myelin. Thus the combined treatment renders the perilesional environment more plastic and optimizes motor recovery driven by focused motor training.

Cell-based therapy for ischemic stroke

A different approach for brain repair is the use of neurons grafted in the host brain with the idea to reconstruct the lost circuitry. It is possible to transplant different type of cells, using different delivery systems. Initial studies in this field have used immature neurons or neuron precursors of embryonic or fetal origin. For example immature dopaminergic neurons, deriving from ventral midbrain during fetal development, and grafted in the striatum, ameliorate symptoms in Parkinson disease in animal models (Herman and Abrous, 1994) and patients (Kordower et al., 1998). However these cells have the drawbacks to be difficultly reachable for ethical and technical reasons.

More accessible cells are Mesenchymal stem cells (MSCs), that can be taken from bone marrow, placenta and umbilical cord blood, and they usually have a really low immunogenic effect. These have been used for stroke treatment after either direct injection in the brain parenchyma or in the blood circulation (Eckert et al., 2013; Zhang and Chopp, 2013). It is likely that their beneficial effect is based on a trophic support mechanism instead of a cell replacement process. In fact, delivery of MSCs medium is sufficient to have a similar therapeutic effect in stroke recovery (Eckert et al., 2013). The neurotrophic effect of stem cells has been proved also in clinical trials where the product of an immortalized cell line has been stereotaxically injected in the brain parenchyma of stroke patients (Kalladka et al., 2016).

The use of Induced pluripotent cells (iPSCs) for cell grafting is very desirable because of the advantage of autologous transplant, avoiding immune rejection problems. Moreover, they are easily accessible, since they can be reprogrammed starting from fibroblasts, using a cocktail of viral vectors that target specific master genes in keeping pluripotency. In a recent study, iPSCs have been transplanted in the striatum and cortex of stroke rodents, inducing an improved recovery in the reaching task (Tatarishvili et al., 2014). However, the use of vectors limits so far, the large-scale use of these cells in clinical trials because of their tumorigenic potentiality.

In my thesis I reported some preliminary results regarding the grafts of in vitro differentiated mouse stem cells (mESCs) in normal and ischemic animals. The group of Federico Cremisi (Scuola Normale Superiore, Pisa) set up a novel differentiation protocol in order to obtain two different cell types resembling, in terms of expressed markers, hippocampal and cortical neurons. I found that cells grafted in the brain of adult mice survive and integrate in the host tissue, extending even long projections from the injection site (in the case of hippocampal cells) when transplanted both at the cortical and hippocampal level. Specifically, when grafted into the dentate gyrus of the hippocampus, hippocampal cells direct they projections towards the CA3 subfield, following the normal course of the mossy fiber pathway and

densely arborize within the CA3 stratum radiatum (**Figure 38**). Concerning the cortical cells, they survive in the host tissue, but do not send projections around. In fact, quite short and few green protrusions are detectable in the tissue immediately around the transplant core (**Figure 38** and **Figure 39**). This difference could be due to intrinsic molecular features characterizing these two different populations. It is possible that hippocampal cells, since they look like cell of the dentate gyrus, a zone with an high intrinsic neurogenic potential, are more prone to extend projections and make new connections in a healthy and structured neural circuitry. Conversely, cortical cells seem less able to weave new connections in a pre-existing intact and functional network.

Interestingly, if the same cells are transplanted in stroke animals, the resulting scenario appears different. In fact, while hippocampal cells showed a similar behavior in respect to transplants in healthy animals, cortical cells showed a really different projections pattern, now extending long protrusions reaching lateral cortical regions and subcortical structures. In particular I found fibers from cortical, but not hippocampal, cells within the Internal Capsule region, suggesting integration of cortical cells in the motor pathway (**Figure 40**). In accordance with these results, Vanderhaeghen and collaborators, found that pluripotent stem-cell-derived neurons re-establish damaged pathways including long-range, reciprocal axonal projections and synaptic connections with targets of the damaged cortex, after a lesion of the adult mouse visual cortex. Moreover the success of the integration after the transplant depends on the state of the tissue, in fact if the same cell are grafted in a healthy visual cortex, no axonal projections were observed except in the immediate vicinity of the graft (Michelsen et al., 2015).

An attractive hypothesis is that in vitro differentiated cortical neurons are sensitive to inflammatory molecules that in some way trigger their ability to protrude long-distant projections. In keeping with this idea, reactive gliosis results to be important for motor recovery (Hayakawa et al., 2010). It is possible that a bridge connects inflammatory processes with the induction of a “growth-promoting zone” in the vicinity of the infarct characterized by a facilitating context for axonal sprouting (Carmichael et al., 2005).

Bibliography

Abramowitz M, Stegun IA (1964) Handbook of Mathematical Functions with Formulas, Graphs, and Mathematical Tables.

Aisen ML, Krebs HI, Hogan N, McDowell F, Volpe BT (1997) The effect of robot-assisted therapy and rehabilitative training on motor recovery following stroke. Arch Neurol 54:443–446.

Alaverdashvili M, Whishaw IQ (2010) Compensation aids skilled reaching in aging and in recovery from forelimb motor cortex stroke in the rat. Neuroscience 167:21–30.

Alaverdashvili M, Whishaw IQ (2013) A behavioral method for identifying recovery and compensation: hand use in a preclinical stroke model using the single pellet reaching task. Neurosci Biobehav Rev 37:950–967.

Alilain WJ, Horn KP, Hu H, Dick TE, Silver J (2011) Functional regeneration of respiratory pathways after spinal cord injury. Nature 475:196–200.

Allman C, Amadi U, Winkler AM, Wilkins L, Filippini N, Kischka U, Stagg CJ, Johansen-Berg H (2016) Ipsilesional anodal tDCS enhances the functional benefits of rehabilitation in patients after stroke. Sci Transl Med 8.

Allred RP, Cappellini CH, Jones T a (2010) The “good” limb makes the “bad” limb worse: experience-dependent interhemispheric disruption of functional outcome after cortical infarcts in rats. Behav Neurosci 124:124–132.

Alt Murphy M, Willén C, Sunnerhagen KS (2011) Kinematic variables quantifying upper-extremity performance after stroke during reaching and drinking from a glass. Neurorehabil Neural Repair 25:71–80.

Alt Murphy M, Willén C, Sunnerhagen KS (2013) Responsiveness of upper extremity kinematic measures and clinical improvement during the first three months after stroke. Neurorehabil Neural Repair 27:844–853.

Altman J (1962) Are New Neurons Formed in the Brains of Adult Mammals? Science (80-) 135:1127–1128.

Anon (2009) ASTM E691 - 99 Standard Practice for Conducting an Interlaboratory Study to Determine the Precision of a Test Method.

Anon (n.d.) World Heart Day: New European statistics released on heart disease and stroke.

Antonucci F, Cerri C, Vetencourt JFM, Caleo M (2010) Acute neuroprotection by the synaptic blocker botulinum neurotoxin E in a rat model of focal cerebral ischaemia. Neuroscience 169:395–401.

Assenza G, Zappasodi F, Pasqualetti P, Vernieri F, Tecchio F (2013) A contralesional EEG

power increase mediated by interhemispheric disconnection provides negative prognosis in acute stroke. Restor Neurol Neurosci 31:177–188.

Barker AT, Jalinous R, Freeston IL (1985) Non-invasive magnetic stimulation of human motor cortex. Lancet 1:1106–1107.

Baroncelli L, Sale A, Viegi A, Maya Vetencourt JF, De Pasquale R, Baldini S, Maffei L (2010) Experience-dependent reactivation of ocular dominance plasticity in the adult visual cortex. Exp Neurol 226:100–109.

Barreca S, Wolf SL, Fasoli S, Bohannon R (2003) Treatment interventions for the paretic upper limb of stroke survivors: a critical review. Neurorehabil Neural Repair 17:220–226.

Bartholdi D, Schwab ME (1998) Oligodendroglial reaction following spinal cord injury in rat: transient upregulation of MBP mRNA. Glia 23:278–284.

Bavelier D, Levi DM, Li RW, Dan Y, Hensch TK (2010) Removing brakes on adult brain plasticity: from molecular to behavioral interventions. J Neurosci 30:14964–14971.

Bembenek JP, Kurczych K, Karli Nski M, Czlonkowska A (2012) The prognostic value of motor-evoked potentials in motor recovery and functional outcome after stroke − a systematic review of the literature. Funct Neurol 27:79–84.

Berkhemer OA et al. (2014) A Randomized Trial of Intraarterial Treatment for Acute Ischemic Stroke. N Engl J Med 372:141217070022009.

Berlucchi G (2011) Brain plasticity and cognitive neurorehabilitation. Neuropsychol Rehabil 21:560–578.

Biernaskie J, Chernenko G, Corbett D (2004) Efficacy of rehabilitative experience declines with time after focal ischemic brain injury. J Neurosci 24:1245–1254.

Biernaskie J, Corbett D (2001a) Enriched rehabilitative training promotes improved forelimb motor function and enhanced dendritic growth after focal ischemic injury. J Neurosci 21:5272–5280.

Biernaskie J, Corbett D (2001b) Enriched Rehabilitative Training Promotes Improved Forelimb Motor Function and Enhanced Dendritic Growth after Focal Ischemic Injury. J Neurosci 21:5272–5280.

Biernaskie J, Szymanska A, Windle V, Corbett D (2005) Bi-hemispheric contribution to functional motor recovery of the affected forelimb following focal ischemic brain injury in rats. Eur J Neurosci 21:989–999.

Binkofski F, Seitz RJ, Arnold S, Classen J, Benecke R, Freund HJ (1996) Thalamic metbolism and corticospinal tract integrity determine motor recovery in stroke. Ann Neurol 39:460–470.

Blicher JU, Jakobsen J, Andersen G, Nielsen JF (2009) Cortical excitability in chronic stroke and modulation by training: a TMS study. Neurorehabil Neural Repair 23:486–493.

Bradbury EJ, Moon LDF, Popat RJ, King VR, Bennett GS, Patel PN, Fawcett JW, McMahon

SB (2002) Chondroitinase ABC promotes functional recovery after spinal cord injury. Nature 416:636–640.

Braun RG, Andrews EM, Kartje GL (2012) Kinematic analysis of motor recovery with human adult bone marrow-derived somatic cell therapy in a rat model of stroke. Neurorehabil Neural Repair 26:898–906.

Brewer L, Horgan F, Hickey a, Williams D (2013) Stroke rehabilitation: recent advances and future therapies. QJM 106:11–25.

Brooks SP, Dunnett SB (2009) Tests to assess motor phenotype in mice: a user's guide. Nat Rev Neurosci 10:519–529.

Brown JA, Lutsep H, Cramer SC, Weinand M (2003) Motor cortex stimulation for enhancement of recovery after stroke: case report.

Buchkremer-Ratzmann I, Witte OW (1997) Extended brain disinhibition following small photothrombotic lesions in rat frontal cortex. Neuroreport 8:519–522.

Bütefisch C, Weßling M, Netz J, Seitz R, Hömberg V (2008) Relationship Between Interhemispheric Inhibition and Motor Cortex Excitability in Subacute Stroke Patients. Neurorehabil Neural Repair.

Calautti C, Baron J-C (2003) Functional neuroimaging studies of motor recovery after stroke in adults: a review. Stroke 34:1553–1566.

Caleo M, Restani L, Gianfranceschi L, Costantin L, Rossi C, Rossetto O, Montecucco C, Maffei L (2007) Transient synaptic silencing of developing striate cortex has persistent effects on visual function and plasticity. J Neurosci 27:4530–4540.

Cao Y, D'Olhaberriague L, Vikingstad EM, Levine SR, Welch KMA (1998) Pilot Study of Functional MRI to Assess Cerebral Activation of Motor Function After Poststroke Hemiparesis. Stroke 29:112–122.

Cardin JA (2012) Dissecting local circuits in vivo: integrated optogenetic and electrophysiology approaches for exploring inhibitory regulation of cortical activity. J Physiol Paris 106:104–111.

Carmichael ST (2005) Rodent models of focal stroke: size, mechanism, and purpose. NeuroRx 2:396–409.

Carmichael ST, Archibeque I, Luke L, Nolan T, Momiy J, Li S (2005) Growth-associated gene expression after stroke: Evidence for a growth-promoting region in peri-infarct cortex. Exp Neurol 193:291–311.

Carmichael ST, Wei L, Rovainen CM, Woolsey T a (2001) New patterns of intracortical projections after focal cortical stroke. Neurobiol Dis 8:910–922.

Castro-Alamancos MA, Borrel J (1995) Functional recovery of forelimb response capacity after forelimb primary motor cortex damage in the rat is due to the reorganization of adjacent areas of cortex. Neuroscience 68:793–805.

Cerri C, Fabbri A, Vannini E, Spolidoro M, Costa M, Maffei L, Fiorentini C, Caleo M (2011) Activation of Rho GTPases triggers structural remodeling and functional plasticity in the adult rat visual cortex. J Neurosci 31:15163–15172.

Che Has AT, Absalom N, van Nieuwenhuijzen PS, Clarkson AN, Ahring PK, Chebib M (2016) Zolpidem is a potent stoichiometry-selective modulator of α1β3 GABAA receptors: evidence of a novel benzodiazepine site in the α1-α1 interface. Sci Rep 6:28674.

Cheng YD, Al-Khoury L, Zivin JA (2004) Neuroprotection for ischemic stroke: Two decades of success and failure. NeuroRX 1:36–45.

Cherubini E (2012) Phasic GABAA-Mediated Inhibition. In: Jasper's Basic Mechanisms of the Epilepsies (Noebels J, Avoli M, Rogawski M, Olsen R, Delgado-Escueta A, eds). National Center for Biotechnology Information (US).

Choi EY, Yeo BTT, Buckner RL (2012) The organization of the human striatum estimated by intrinsic functional connectivity. J Neurophysiol 108:2242–2263.

Cicinelli P, Pasqualetti P, Zaccagnini M, Traversa R, Oliveri M, Rossini PM (2003) Interhemispheric asymmetries of motor cortex excitability in the postacute stroke stage: a paired-pulse transcranial magnetic stimulation study. Stroke 34:2653–2658.

Cicinelli P, Traversa R, Rossini PM (1997) Post-stroke reorganization of brain motor output to the hand: a 2-4 month follow-up with focal magnetic transcranial stimulation. Electroencephalogr Clin Neurophysiol 105:438–450.

Cirstea MC, Levin MF (2000) Compensatory strategies for reaching in stroke. Brain 123 (Pt 5:940–953.

Clarkson AN, Huang BS, Macisaac SE, Mody I, Carmichael ST (2010) Reducing excessive GABA-mediated tonic inhibition promotes functional recovery after stroke. Nature 468:305–309.

Clarkson AN, López-Valdés HE, Overman JJ, Charles AC, Brennan KC, Thomas Carmichael S (2013) Multimodal examination of structural and functional remapping in the mouse photothrombotic stroke model. J Cereb Blood Flow Metab 33:716–723.

Classen J, Schnitzler A, Binkofski F, Werhahn KJ, Kim YS, Kessler KR, Benecke R (1997) The motor syndrome associated with exaggerated inhibition within the primary motor cortex of patients with hemiparetic stroke. Brain 120:605–619.

Combs HL, Jones TA, Kozlowski DA, Adkins DL (2015) Combinatorial Motor Training Results In Functional Reorganization Of Remaining Motor Cortex After Controlled Cortical Impact In Rats. J Neurotrauma.

Cramer SC, Nelles G, Benson RR, Kaplan JD, Parker RA, Kwong KK, Kennedy DN, Finklestein SP, Rosen BR (1997) A Functional MRI Study of Subjects Recovered From Hemiparetic Stroke. Stroke 28:2518–2527.

Currà A, Modugno N, Inghilleri M, Manfredi M, Hallett M, Berardelli A (2002) Transcranial magnetic stimulation techniques in clinical investigation. Neurology 59:1851–1859.

Dancause N (2006) Vicarious function of remote cortex following stroke: recent evidence from human and animal studies. Neuroscientist 12:489–499.

Dancause N, Nudo RJ (2011) Shaping plasticity to enhance recovery after injury.

Dancause N, Touvykine B, Mansoori BK (2015) Inhibition of the contralesional hemisphere after stroke. In, pp 361–387.

Davis SM, Lees KR, Albers GW, Diener HC, Markabi S, Karlsson G, Norris J (2000) Selfotel in Acute Ischemic Stroke : Possible Neurotoxic Effects of an NMDA Antagonist. Stroke 31:347–354.

De Sarro G, Ibbadu GF, Marra R, Rotiroti D, Loiacono A, Donato Di Paola E, Russo E (2004) Seizure susceptibility to various convulsant stimuli in dystrophin-deficient mdx mice. Neurosci Res 50:37–44.

De Weerd AW, Veldhuizen RJ, Veering MM, Poortvliet DC, Jonkman EJ (1988) Recovery from cerebral ischaemia. EEG, cerebral blood flow and clinical symptomatology in the first three years after a stroke. Electroencephalogr Clin Neurophysiol 70:197–204.

Deidda G, Allegra M, Cerri C, Naskar S, Bony G, Zunino G, Bozzi Y, Caleo M, Cancedda L (2015) Early depolarizing GABA controls critical-period plasticity in the rat visual cortex. Nat Neurosci 18:87–96.

Di Cristo G (2007) Development of cortical GABAergic circuits and its implications for neurodevelopmental disorders. Clin Genet 72:1–8.

Diamond MC, Ingham CA, Johnson RE, Bennett EL, Rosenzweig MR (1976) Effects of environment on morphology of rat cerebral cortex and hippocampus. J Neurobiol 7:75–85.

Dickstein R (2008) Rehabilitation of Gait Speed After Stroke:\nA Critical Review of Intervention Approaches. Neurorehabil Neural Repair.

Dietrich WD, Ginsberg MD, Busto R, Watson BD (1986) Photochemically induced cortical infarction in the rat. 1. Time course of hemodynamic consequences. J Cereb Blood Flow Metab 6:184–194.

Dijkhuizen RM, Ren J, Mandeville JB, Wu O, Ozdag FM, Moskowitz MA, Rosen BR, Finklestein SP (2001) Functional magnetic resonance imaging of reorganization in rat brain after stroke. Proc Natl Acad Sci U S A 98:12766–12771.

Ding Q, Vaynman S, Akhavan M, Ying Z, Gomez-Pinilla F (2006) Insulin-like growth factor I interfaces with brain-derived neurotrophic factor-mediated synaptic plasticity to modulate aspects of exercise-induced cognitive function. Neuroscience 140:823–833.

Dominici N, Keller U, Vallery H, Friedli L, van den Brand R, Starkey ML, Musienko P, Riener R, Courtine G (2012) Versatile robotic interface to evaluate, enable and train locomotion

and balance after neuromotor disorders. Nat Med 18:1142–1147.

Duncan PW, Zorowitz R, Bates B, Choi JY, Glasberg JJ, Graham GD, Katz RC, Lamberty K, Reker D (2005) Management of Adult Stroke Rehabilitation Care: a clinical practice guideline. Stroke 36:e100-43.

Durukan A, Tatlisumak T (2007) Acute ischemic stroke: Overview of major experimental rodent models, pathophysiology, and therapy of focal cerebral ischemia. Pharmacol Biochem Behav 87:179–197.

Eckert MA, Vu Q, Xie K, Yu J, Liao W, Cramer SC, Zhao W (2013) Evidence for high translational potential of mesenchymal stromal cell therapy to improve recovery from ischemic stroke. J Cereb Blood Flow Metab 33:1322–1334.

Edwards DJ, Krebs HI, Rykman A, Zipse J, Thickbroom GW, Mastaglia FL, Pascual-Leone A, Volpe BT (2009) Raised corticomotor excitability of M1 forearm area following anodal tDCS is sustained during robotic wrist therapy in chronic stroke. Restor Neurol Neurosci 27:199–207.

Eriksson PS, Perfilieva E, Björk-Eriksson T, Alborn AM, Nordborg C, Peterson DA, Gage FH (1998) Neurogenesis in the adult human hippocampus. Nat Med 4:1313–1317.

Escudero J V., Sancho J, Bautista D, Escudero M, Lopez-Trigo J (1998) Prognostic Value of Motor Evoked Potential Obtained by Transcranial Magnetic Brain Stimulation in Motor Function Recovery in Patients With Acute Ischemic Stroke. Stroke 29:1854–1859.

Fagiolini M, Leblanc JJ (2011) Autism: A critical period disorder? Neural Plast 2011.

Farr TD, Whishaw IQ (2002) Quantitative and qualitative impairments in skilled reaching in the mouse (Mus musculus) after a focal motor cortex stroke. Stroke 33:1869–1875.

Farrant M, Nusser Z (2005) Variations on an inhibitory theme: phasic and tonic activation of GABA(A) receptors. Nat Rev Neurosci 6:215–229.

Fasoli SE, Krebs HI, Stein J, Frontera WR, Hogan N (2003) Effects of robotic therapy on motor impairment and recovery in chronic stroke. Arch Phys Med Rehabil 84:477–482.

Fawcett JW (2015) The extracellular matrix in plasticity and regeneration after CNS injury and neurodegenerative disease. Prog Brain Res 218:213–226.

Ferrante S, Pedrocchi A, Ferrigno G, Molteni F (2008) Cycling induced by functional electrical stimulation improves the muscular strength and the motor control of individuals with post-acute stroke. Europa Medicophysica-SIMFER 2007 Award Winner. Eur J Phys Rehabil Med 44:159–167.

Finnigan S, van Putten MJAM (2013) EEG in ischaemic stroke: Quantitative EEG can uniquely inform (sub-)acute prognoses and clinical management. Clin Neurophysiol 124:10–19.

Finnigan SP, Rose SE, Walsh M, Griffin M, Janke AL, McMahon KL, Gillies R, Strudwick MW, Pettigrew CM, Semple J, Brown J, Brown P, Chalk JB (2004) Correlation of

Quantitative EEG in Acute Ischemic Stroke with 30-Day NIHSS Score: Comparison with Diffusion and Perfusion MRI. Stroke 35:899–903.

Finnigan SP, Walsh M, Rose SE, Chalk JB (2007) Quantitative EEG indices of sub-acute ischaemic stroke correlate with clinical outcomes. Clin Neurophysiol 118:2525–2532.

Fisher M (1997) Characterizing the target of acute stroke therapy. Stroke 28:866–872.

Foeller E, Celikel T, Feldman DE (2005) Inhibitory sharpening of receptive fields contributes to whisker map plasticity in rat somatosensory cortex. J Neurophysiol 94:4387–4400.

Fotaki V, Larralde O, Zeng S, McLaughlin D, Nichols J, Price DJ, Theil T, Mason JO (2010) Loss of Wnt8b has no overt effect on hippocampus development but leads to altered Wnt gene expression levels in dorsomedial telencephalon. Dev Dyn 239:284–296.

Fregni F, Pascual-Leone A (2007) Technology insight: noninvasive brain stimulation in neurology-perspectives on the therapeutic potential of rTMS and tDCS. Nat Clin Pract Neurol 3:383–393.

Freund P, Schmidlin E, Wannier T, Bloch J, Mir A, Schwab ME, Rouiller EM (2006) Nogo-A-specific antibody treatment enhances sprouting and functional recovery after cervical lesion in adult primates. Nat Med 12:790–792.

Fritschy J-M, Panzanelli P (2014) GABAA receptors and plasticity of inhibitory neurotransmission in the central nervous system. Eur J Neurosci 39:1845–1865.

Froehler MT, Ovbiagele B (2010) Therapeutic hypothermia for acute ischemic stroke. Expert Rev Cardiovasc Ther 8:593–603.

Frost SB, Barbay S, Friel KM, Plautz EJ, Nudo RJ (2003) Reorganization of remote cortical regions after ischemic brain injury: a potential substrate for stroke recovery. J Neurophysiol 89:3205–3214.

Gage FH (2002) Neurogenesis in the Adult Brain. J Neurosci 22:612–613.

García-Alías G, Barkhuysen S, Buckle M, Fawcett JW (2009) Chondroitinase ABC treatment opens a window of opportunity for task-specific rehabilitation. Nat Neurosci 12:1145–1151.

Gentet LJ, Kremer Y, Taniguchi H, Huang ZJ, Staiger JF, Petersen CCH (2012) Unique functional properties of somatostatin-expressing GABAergic neurons in mouse barrel cortex. Nat Neurosci 15:607–612.

Gerloff C, Bushara K, Sailer A, Wassermann EM, Chen R, Matsuoka T, Waldvogel D, Wittenberg GF, Ishii K, Cohen LG, Hallett M (2006) Multimodal imaging of brain reorganization in motor areas of the contralesional hemisphere of well recovered patients after capsular stroke. Brain 129:791–808.

Gherardini L, Gennaro M, Pizzorusso T (2015) Perilesional treatment with chondroitinase ABC and motor training promote functional recovery after stroke in rats. Cereb Cortex 25:202–212.

Gholamrezaei G, Whishaw IQ (2009) Individual differences in skilled reaching for food related to increased number of gestures: Evidence for goal and habit learning of skilled reaching. Behav Neurosci 123:863–874.

Ginsberg MD (2008) Neuroprotection for ischemic stroke: Past, present and future. Neuropharmacology 55:363–389.

Ginsberg MD, Busto R (1989) Rodent models of cerebral ischemia. Stroke 20:1627–1642.

Glenberg AM, Lopez-Mobilia G, McBeath M, Toma M, Sato M, Cattaneo L (2010) Knowing beans: human mirror mechanisms revealed through motor adaptation. Front Hum Neurosci 4:206.

Gonzalez CLR, Gharbawie OA, Williams PT, Kleim JA, Kolb B, Whishaw IQ (2004) Evidence for bilateral control of skilled movements: Ipsilateral skilled forelimb reaching deficits and functional recovery in rats follow motor cortex and lateral frontal cortex lesions. Eur J Neurosci 20:3442–3452.

Gordon JA, Stryker MP (1996) Experience-dependent plasticity of binocular responses in the primary visual cortex of the mouse. J Neurosci 16:3274–3286.

Grabowski M, Brundin P, Johansson BB (1993a) Paw-reaching, sensorimotor, and rotational behavior after brain infarction in rats. Stroke 24:889–895.

Grabowski M, Brundin P, Johansson BB (1993b) Paw-reaching, sensorimotor, and rotational behavior after brain infarction in rats. Stroke 24:889–895.

Green AR (2004) Protecting the brain: the search for a clinically effective neuroprotective drug for stroke. Crit Rev Neurobiol 16:91–97.

Grefkes C, Ward NS (2014) Cortical reorganization after stroke: how much and how functional? Neuroscientist 20:56–70.

Gresham GE, Duncan PW SW (1995) Post-Stroke Rehabilitation Guideline Panel. Post-Stroke Rehabil Clin Pract Guidel 16.

Griesbach GS, Hovda DA, Molteni R, Wu A, Gomez-Pinilla F (2004) Voluntary exercise following traumatic brain injury: Brain-derived neurotrophic factor upregulation and recovery of function. Neuroscience 125:129–139.

Harauzov A, Spolidoro M, DiCristo G, De Pasquale R, Cancedda L, Pizzorusso T, Viegi A, Berardi N, Maffei L (2010) Reducing intracortical inhibition in the adult visual cortex promotes ocular dominance plasticity. J Neurosci 30:361–371.

Harel NY, Song K-H, Tang X, Strittmatter SM (2010) Nogo receptor deletion and multimodal exercise improve distinct aspects of recovery in cervical spinal cord injury. J Neurotrauma 27:2055–2066.

Harrison TC, Silasi G, Boyd JD, Murphy TH (2013) Displacement of sensory maps and disorganization of motor cortex after targeted stroke in mice. Stroke 44:2300–2306.

Hayakawa K, Nakano T, Irie K, Higuchi S, Fujioka M, Orito K, Iwasaki K, Jin G, Lo EH,

Mishima K, Fujiwara M (2010) Inhibition of reactive astrocytes with fluorocitrate retards neurovascular remodeling and recovery after focal cerebral ischemia in mice. J Cereb Blood Flow Metab 30:871–882.

Hebb DO (1949) The organization of behavior: a neuropsychological theory. Sci Educ 44:335.

Hendricks HT, Van Limbeek J, Geurts AC, Zwarts MJ (2002) Motor recovery after stroke: A systematic review of the literature. Arch Phys Med Rehabil 83:1629–1637.

Hensch TK (2005) Critical period plasticity in local cortical circuits. Nat Rev Neurosci 6:877–888.

Hensch TK, Stryker MP (2004) Columnar architecture sculpted by GABA circuits in developing cat visual cortex. Science 303:1678–1681.

Herman J-P, Abrous ND (1994) Dopaminergic neural grafts after fifteen years: results and perspectives. Prog Neurobiol 44:1–35.

Hill JJ, Jin K, Mao XO, Xie L, Greenberg DA (2012) Intracerebral chondroitinase ABC and heparan sulfate proteoglycan glypican improve outcome from chronic stroke in rats. Proc Natl Acad Sci U S A 109:9155–9160.

Hiu T, Farzampour Z, Paz JT, Wang EHJ, Badgely C, Olson A, Micheva KD, Wang G, Lemmens R, Tran K V, Nishiyama Y, Liang X, Hamilton SA, O'Rourke N, Smith SJ, Huguenard JR, Bliss TM, Steinberg GK (2015) Enhanced phasic GABA inhibition during the repair phase of stroke: a novel therapeutic target. Brain 139:468–480.

Hofmeijer J, Van Putten MJAM (2012) Ischemic cerebral damage: An appraisal of synaptic failure. Stroke 43:607–615.

Hogan N, Krebs HI (2011) Physically interactive robotic technology for neuromotor rehabilitation.

Holtmaat AJGD, Trachtenberg JT, Wilbrecht L, Shepherd GM, Zhang X, Knott GW, Svoboda K (2005) Transient and persistent dendritic spines in the neocortex in vivo. Neuron 45:279–291.

Hong JM, Lee JS, Song H-J, Jeong HS, Jung H-S, Choi HA, Lee K (2014) Therapeutic hypothermia after recanalization in patients with acute ischemic stroke. Stroke 45:134–140.

Huber D, Gutnisky D a., Peron S, O'Connor DH, Wiegert JS, Tian L, Oertner TG, Looger LL, Svoboda K (2012) Multiple dynamic representations in the motor cortex during sensorimotor learning. Nature 484:473–478.

Hummel FC, Cohen LG (2006) Non-invasive brain stimulation: a new strategy to improve neurorehabilitation after stroke? Lancet Neurol 5:708–712.

Jacobs KM, Donoghue JP (1991) Reshaping the cortical motor map by unmasking latent intracortical connections. Science 251:944–947.

James GA, Lu Z-L, VanMeter JW, Sathian K, Hu XP, Butler AJ (2009) Changes in resting state effective connectivity in the motor network following rehabilitation of upper extremity poststroke paresis. Top Stroke Rehabil 16:270–281.

Jang SH, Kim Y-H, Cho S-H, Lee J-H, Park J-W, Kwon Y-H (2003) Cortical reorganization induced by task-oriented training in chronic hemiplegic stroke patients. Neuroreport 14:137–141.

Jeffers MS, Hoyles A, Morshead C, Corbett D (2014) Epidermal growth factor and erythropoietin infusion accelerate functional recovery in combination with rehabilitation. Stroke 45:1856–1858.

Johansson BB (2000) Brain plasticity and stroke rehabilitation. The Willis lecture. Stroke 31:223–230.

Johansson BB, Ohlsson AL (1996) Environment, social interaction, and physical activity as determinants of functional outcome after cerebral infarction in the rat. Exp Neurol 139:322–327.

Jolkkonen J, Gallagher NP, Zilles K, Sivenius J (2003) Behavioral deficits and recovery following transient focal cerebral ischemia in rats: glutamatergic and GABAergic receptor densities. Behav Brain Res 138:187–200.

Jørgensen HS, Nakayama H, Raaschou HO, Larsen K, Hübbe P, Olsen TS (1995) The effect of a stroke unit: reductions in mortality, discharge rate to nursing home, length of hospital stay, and cost. A community-based study. Stroke 26:1178–1182.

Kajikawa Y, Schroeder CE (2011) How local is the local field potential? Neuron 72:847–858.

Kalladka D, Sinden J, Pollock K, Haig C, McLean J, Smith W, McConnachie A, Santosh C, Bath PM, Dunn L, Muir KW (2016) Human neural stem cells in patients with chronic ischaemic stroke (PISCES): a phase 1, first-in-man study. Lancet 388:787–796.

Kerr AL, Wolke ML, Bell JA, Jones TA (2013) Post-stroke protection from maladaptive effects of learning with the non-paretic forelimb by bimanual home cage experience in C57BL/6 mice. Behav Brain Res 252:180–187.

Kharlamov EA, Downey KL, Jukkola PI, Grayson DR, Kelly KM (2008) Expression of GABA A receptor alpha1 subunit mRNA and protein in rat neocortex following photothrombotic infarction. Brain Res 1210:29–38.

Kim J, Zhang R, Strittmatter EF, Smith RD, Zand R, Kim J, Zhang ÁR, Strittmatter EF, Smith ÁRD, Zand R (2009) Post-translational Modifications of Chicken Myelin Basic Protein Charge Components. Neurochem Res 34:360–372.

Kim YK, Yang EJ, Cho K, Lim JY, Paik N-J (2014) Functional Recovery After Ischemic Stroke Is Associated With Reduced GABAergic Inhibition in the Cerebral Cortex: A GABA PET Study. Neurorehabil Neural Repair 28:576–583.

Kinsbourne M (1974) Lateral interactions in the brain.

Kitago T, Liang J, Huang VS, Hayes S, Simon P, Tenteromano L, Lazar RM, Marshall RS, Mazzoni P, Lennihan L, Krakauer JW (2013) Improvement After Constraint-Induced Movement Therapy: Recovery of Normal Motor Control or Task-Specific Compensation? Neurorehabil Neural Repair 27:99–109.

Klamroth-Marganska V, Blanco J, Campen K, Curt A, Dietz V, Ettlin T, Felder M, Fellinghauer B, Guidali M, Kollmar A, Luft A, Nef T, Schuster-Amft C, Stahel W, Riener R (2014) Three-dimensional, task-specific robot therapy of the arm after stroke: a multicentre, parallel-group randomised trial. Lancet Neurol 13:159–166.

Kleim JA et al. (1998) Functional reorganization of the rat motor cortex following motor skill learning. J Neurophysiol 80:3321–3325.

Kleim J a., Lussnig E, Schwarz ER, Comery T a., Greenough WT (1996) Synaptogenesis and Fos expression in the motor cortex of the adult rat after motor skill learning. JNeurosci 16:4529–4535.

Kleim JA, Boychuk JA, Adkins DL (2007) Rat models of upper extremity impairment in stroke. ILAR J 48:374–384.

Kleim JA, Jones TA (2008) Principles of experience-dependent neural plasticity: implications for rehabilitation after brain damage. In: Journal of speech, language, and hearing research : JSLHR, pp S225–S239.

Klein A, Dunnett SB (2012) Analysis of skilled forelimb movement in rats: The single pellet reaching test and staircase test. Curr Protoc Neurosci 1.

Klein A, Sacrey L-AR, Whishaw IQ, Dunnett SB (2012) The use of rodent skilled reaching as a translational model for investigating brain damage and disease. Neurosci Biobehav Rev 36:1030–1042.

Kobayashi M, Pascual-Leone A (2003) Transcranial magnetic stimulation in neurology. Lancet Neurol 2:145–156.

Kordower JH, Freeman TB, Chen EY, Mufson EJ, Sanberg PR, Hauser RA, Snow B, Olanow CW (1998) Fetal nigral grafts survive and mediate clinical benefit in a patient with Parkinson's disease. Mov Disord 13:383–393.

Krebs HI, Krams M, Agrafiotis DK, DiBernardo A, Chavez JC, Littman GS, Yang E, Byttebier G, Dipietro L, Rykman A, McArthur K, Hajjar K, Lees KR, Volpe BT (2014) Robotic Measurement of Arm Movements After Stroke Establishes Biomarkers of Motor Recovery. Stroke 45.

Krnjević K (2008) Electrophysiology of cerebral ischemia. Neuropharmacology 55:319–333.

Kwakkel G, Wagenaar RC, Koelman TW, Lankhorst GJ, Koetsier JC (1997) Effects of intensity of rehabilitation after stroke. A research synthesis. Stroke 28:1550–1556.

Lai C-J, Wang C-P, Tsai P-Y, Chan R-C, Lin S-H, Lin F-G, Hsieh C-Y (2015a) Corticospinal integrity and motor impairment predict outcomes after excitatory repetitive transcranial

magnetic stimulation: a preliminary study. Arch Phys Med Rehabil 96:69–75.

Lai S, Panarese A, Spalletti C, Alia C, Ghionzoli A, Caleo M, Micera S (2015b) Quantitative Kinematic Characterization of Reaching Impairments in Mice After a Stroke. Neurorehabil Neural Repair 29:382–392.

Lai TW, Zhang S, Wang YT (2014) Excitotoxicity and stroke: identifying novel targets for neuroprotection. Prog Neurobiol 115:157–188.

Lake EMR, Chaudhuri J, Thomason L, Janik R, Ganguly M, Brown M, McLaurin J, Corbett D, Stanisz GJ, Stefanovic B (2015) The effects of delayed reduction of tonic inhibition on ischemic lesion and sensorimotor function. J Cereb Blood Flow Metab 35:1601–1609.

Lazar RM, Berman MF, Festa JR, Geller AE, Matejovsky TG, Marshall RS (2010) GABAergic but not anti-cholinergic agents re-induce clinical deficits after stroke. J Neurol Sci 292:72–76.

Lazar RM, Fitzsimmons B-F, Marshall RS, Berman MF, Bustillo MA, Young WL, Mohr JP, Shah J, Robinson J V (2002) Reemergence of stroke deficits with midazolam challenge. Stroke 33:283–285.

Lees KR (1997) Cerestat and other NMDA antagonists in ischemic stroke. Neurology 49:S66–S69.

Li P, Murphy TH (2008) Two-photon imaging during prolonged middle cerebral artery occlusion in mice reveals recovery of dendritic structure after reperfusion. J Neurosci 28:11970–11979.

Li S, Carmichael ST (2006) Growth-associated gene and protein expression in the region of axonal sprouting in the aged brain after stroke. Neurobiol Dis 23:362–373.

Li S, Overman JJ, Katsman D, Kozlov S V, Donnelly CJ, Twiss JL, Giger RJ, Coppola G, Geschwind DH, Carmichael ST (2010) An age-related sprouting transcriptome provides molecular control of axonal sprouting after stroke. Nat Neurosci 13:1496–1504.

Liepert J, Miltner WH, Bauder H, Sommer M, Dettmers C, Taub E, Weiller C (1998) Motor cortex plasticity during constraint-induced movement therapy in stroke patients. Neurosci Lett 250:5–8.

Liepert J, Storch P, Fritsch A, Weiller C (2000) Motor cortex disinhibition in acute stroke. Clin Neurophysiol 111:671–676.

Lim DH, Mohajerani MH, LeDue J, Boyd J, Chen S, Murphy TH (2012) In vivo Large-Scale Cortical Mapping Using Channelrhodopsin-2 Stimulation in Transgenic Mice Reveals Asymmetric and Reciprocal Relationships between Cortical Areas. Front Neural Circuits 6:1–19.

Liu Y, Rouiller EM (1999) Mechanisms of recovery of dexterity following unilateral lesion of the sensorimotor cortex in adult monkeys. In: Experimental Brain Research, pp 149–159.

Lo AC et al. (2010) Robot-assisted therapy for long-term upper-limb impairment after stroke. N Engl J Med 362:1772–1783.

Lodder J, van Raak L, Hilton A, Hardy E, Kessels A (2006) Diazepam to improve acute stroke outcome: results of the early GABA-Ergic activation study in stroke trial. a randomized double-blind placebo-controlled trial. Cerebrovasc Dis 21:120–127.

Lotze M, Markert J, Sauseng P, Hoppe J, Plewnia C, Gerloff C (2006) The role of multiple contralesional motor areas for complex hand movements after internal capsular lesion. J Neurosci 26:6096–6102.

Loubinoux I (2003) Correlation between cerebral reorganization and motor recovery after subcortical infarcts. Neuroimage 20:2166–2180.

Lüddens H, Wisden W (1991) Function and pharmacology of multiple GABAA receptor subunits. Trends Pharmacol Sci 12:49–51.

Luu P, Tucker DM, Englander R, Lockfeld A, Lutsep H, Oken B (2001) Localizing acute stroke-related EEG changes: assessing the effects of spatial undersampling.

Mackay J, Mensah GA (2004) The Atlas of Heart Disease and Stroke.

Macrae IM, Robinson MJ, Graham DI, Reid JL, McCulloch J (1993) Endothelin-1-induced reductions in cerebral blood flow: dose dependency, time course, and neuropathological consequences. J Cereb Blood Flow Metab 13:276–284.

Madden K, Clark W, Lessov N (2003) Failure of ischemic neuroprotection by potentiators of gamma-aminobutyric acid. Clin Med Res 1:119–124.

Maier IC, Ichiyama RM, Courtine G, Schnell L, Lavrov I, Edgerton VR, Schwab ME (2009) Differential effects of anti-Nogo-A antibody treatment and treadmill training in rats with incomplete spinal cord injury. Brain 132:1426–1440.

Mansoori B, Jean-Charles L, Touvykine B, A L, S Q, Dancause N (2014) Acute inactivation of the contralesional hemisphere for longer durations improves recovery after cortical injury. - PubMed - NCBI. Available at: https://www.ncbi.nlm.nih.gov/pubmed/?term=mansoori+2014+stroke.

Marconi B, Filippi GM, Koch G, Giacobbe V, Pecchioli C, Versace V, Camerota F, Saraceni VM, Caltagirone C (2011) Long-term effects on cortical excitability and motor recovery induced by repeated muscle vibration in chronic stroke patients. Neurorehabil Neural Repair 25:48–60.

Marshall RS, Perera GM, Lazar RM, Krakauer JW, Constantine RC, DeLaPaz RL (2000) Evolution of Cortical Activation During Recovery From Corticospinal Tract Infarction. Stroke 31.

Maya Vetencourt JF, Sale A, Viegi A, Baroncelli L, De Pasquale R, O'Leary OF, Castrén E, Maffei L (2008) The antidepressant fluoxetine restores plasticity in the adult visual cortex. Science 320:385–388.

Merton PA, Morton HB (1980) Stimulation of the cerebral cortex in the intact human subject. Nature 285:227.

Meyer BU, Röricht S, Gräfin von Einsiedel H, Kruggel F, Weindl A (1995) Inhibitory and excitatory interhemispheric transfers between motor cortical areas in normal humans and patients with abnormalities of the corpus callosum. Brain 118 (Pt 2:429–440.

Micera S, Carrozza MC, Guglielmelli E, Cappiello G, Zaccone F, Freschi C, Colombo R, Mazzone A, Delconte C, Pisano F, Minuco G, Dario P (2005) A simple robotic system for neurorehabilitation. Auton Robots 19:271–284.

Michelsen KA, Acosta-Verdugo S, Benoit-Marand M, Espuny-Camacho I, Gaspard N, Saha B, Gaillard A, Vanderhaeghen P (2015) Area-Specific Reestablishment of Damaged Circuits in the Adult Cerebral Cortex by Cortical Neurons Derived from Mouse Embryonic Stem Cells. Neuron 85:982–997.

Mohajerani MH, Aminoltejari K, Murphy TH (2011) Targeted mini-strokes produce changes in interhemispheric sensory signal processing that are indicative of disinhibition within minutes. Proc Natl Acad Sci U S A 108:E183-91.

Moon SK, Alaverdashvili M, Cross AR, Whishaw IQ (2009) Both compensation and recovery of skilled reaching following small photothrombotic stroke to motor cortex in the rat. Exp Neurol 218:145–153.

Mozaffarian D et al. (2014) Heart Disease and Stroke Statistics--2015 Update: A Report From the American Heart Association.

Mundkur N (2005) Neuroplasticity in children. Indian J Pediatr 72:855–857.

Murase N, Duque J, Mazzocchio R, Cohen LG (2004) Influence of Interhemispheric Interactions on Motor Function in Chronic Stroke. Ann Neurol 55:400–409.

Murphy TH, Corbett D (2009) Plasticity during stroke recovery: from synapse to behaviour. Nat Rev Neurosci 10:861–872.

Murphy TH, Li P, Betts K, Liu R (2008) Two-photon imaging of stroke onset in vivo reveals that NMDA-receptor independent ischemic depolarization is the major cause of rapid reversible damage to dendrites and spines. J Neurosci 28:1756–1772.

Murri L, Gori S, Massetani R, Bonanni E, Marcella F, Milani S (1998) Evaluation of acute ischemic stroke using quantitative EEG: a comparison with conventional EEG and CT scan.

Nahmani M, Turrigiano GG (2014) Adult cortical plasticity following injury: Recapitulation of critical period mechanisms? Neuroscience 283:4–16.

Nair DG, Hutchinson S, Fregni F, Alexander M, Pascual-Leone A, Schlaug G (2007) Imaging correlates of motor recovery from cerebral infarction and their physiological significance in well-recovered patients. Neuroimage 34:253–263.

Nakayama H, Jørgensen HS, Raaschou HO, Olsen TS (1994) The influence of age on stroke

outcome. The Copenhagen Stroke Study. Stroke 25:808–813.

Napieralski JA, Butler AK, Chesselet MF (1996) Anatomical and functional evidence for lesion-specific sprouting of corticostriatal input in the adult rat. J Comp Neurol 373:484–497.

Nascimbeni A, Gaffuri A, Granella L, Colli M, Imazio P (2005) Prognostic value of motor evoked potentials in stroke motor outcome. Eura Medicophys 41:125–130.

Neumann-Haefelin T, Staiger JF, Redecker C, Zilles K, Fritschy JM, Möhler H, Witte OW (1998) Immunohistochemical evidence for dysregulation of the GABAergic system ipsilateral to photochemically induced cortical infarcts in rats. Neuroscience 87:871–879.

Ng KL, Gibson EM, Hubbard R, Yang J, Caffo B, O'Brien RJ, Krakauer JW, Zeiler SR (2015) Fluoxetine Maintains a State of Heightened Responsiveness to Motor Training Early After Stroke in a Mouse Model. Stroke 46:2951–2960.

Nishibe M, Barbay S, Guggenmos D, Nudo RJ (2010) Reorganization of motor cortex after controlled cortical impact in rats and implications for functional recovery. J Neurotrauma 27:2221–2232.

Nishibe M, Urban ETR, Barbay S, Nudo RJ (2015) Rehabilitative training promotes rapid motor recovery but delayed motor map reorganization in a rat cortical ischemic infarct model. Neurorehabil Neural Repair 29:472–482.

Nitsche MA, Cohen LG, Wassermann EM, Priori A, Lang N, Antal A, Paulus W, Hummel F, Boggio PS, Fregni F, Pascual-Leone A (2008) Transcranial direct current stimulation: State of the art 2008. Brain Stimul 1:206–223.

Nudo RJ (2006) Mechanisms for recovery of motor function following cortical damage. Curr Opin Neurobiol 16:638–644.

Nudo RJ (2007) Postinfarct cortical plasticity and behavioral recovery. Stroke 38:840–845.

Nudo RJ (2013) Recovery after brain injury: mechanisms and principles. Front Hum Neurosci 7:887.

Nudo RJ, Milliken GW (1996) Reorganization of movement representations in primary motor cortex following focal ischemic infarcts in adult squirrel monkeys. J Neurophysiol 75:2144–2149.

O'Bryant AJ, Allred RP, Maldonado M a., Cormack LK, Jones T a. (2011) Breeder and batch-dependent variability in the acquisition and performance of a motor skill in adult Long-Evans rats. Behav Brain Res 224:112–120.

Overman JJ, Clarkson a. N, Wanner IB, Overman WT, Eckstein I, Maguire JL, Dinov ID, Toga a. W, Carmichael ST (2012) PNAS Plus: A role for ephrin-A5 in axonal sprouting, recovery, and activity-dependent plasticity after stroke. Proc Natl Acad Sci 109:E2230–E2239.

Paciaroni M, Caso V, Agnelli G (2009) The concept of ischemic penumbra in acute stroke

and therapeutic opportunities. Eur Neurol 61:321–330.

Panarese A, Colombo R, Sterpi I, Pisano F, Micera S (2012) Tracking Motor Improvement at the Subtask Level During Robot-Aided Neurorehabilitation of Stroke Patients. Neurorehabil Neural Repair 26:822–833.

Pearson-Fuhrhop KM, Kleim JA, Cramer SC (2009) Brain Plasticity and Genetic Factors. Top Stroke Rehabil 16:282–299.

Pino G Di, Pellegrino G, Assenza G, Capone F, Ferreri F, Formica D, Ranieri F, Tombini M, Ziemann U, Rothwell JC, Lazzaro V Di, Pino D (2014) Modulation of brain plasticity in stroke: a novel model for neurorehabilitation. Rev Neurol 10.

Pizzorusso T, Medini P, Berardi N, Chierzi S, Fawcett JW, Maffei L (2002) Reactivation of ocular dominance plasticity in the adult visual cortex. Science 298:1248–1251.

Poli P, Morone G, Rosati G, Masiero S (2013) Robotic technologies and rehabilitation: New tools for stroke patients' therapy. Biomed Res Int 2013.

Posteraro F, Mazzoleni S, Aliboni S, Cesqui B, Battaglia A, Carrozza MC, Dario P, Micera S (2010) Upper limb spasticity reduction following active training: A robot-mediated study in patients with chronic hemiparesis. J Rehabil Med 42:279–281.

Posteraro F, Mazzoleni S, Aliboni S, Cesqui B, Battaglia A, Dario P, Micera S (2009) Robot-mediated therapy for paretic upper limb of chronic patients following neurological injury. In: Journal of Rehabilitation Medicine, pp 976–980.

Prange GB, Jannink MJA, Groothuis-Oudshoorn CGM, Hermens HJ, Ijzerman MJ (2006) Systematic review of the effect of robot-aided therapy on recovery of the hemiparetic arm after stroke. J Rehabil Res Dev 43:171–184.

Pronichev I V., Lenkov DN (1998) Functional mapping of the motor cortex of the white mouse by a microstimulation method. Neurosci Behav Physiol 28:80–85.

Rägo L, Kiivet RA, Harro J, Põld M (1988) Behavioral differences in an elevated plus-maze: correlation between anxiety and decreased number of GABA and benzodiazepine receptors in mouse cerebral cortex. Naunyn Schmiedebergs Arch Pharmacol 337:675–678.

Redecker C, Wang W, Fritschy J-M, Witte OW (2002) Widespread and long-lasting alterations in GABA(A)-receptor subtypes after focal cortical infarcts in rats: mediation by NMDA-dependent processes. J Cereb Blood Flow Metab 22:1463–1475.

Reis J, Swayne OB, Vandermeeren Y, Camus M, Dimyan MA, Harris-Love M, Perez MA, Ragert P, Rothwell JC, Cohen LG (2008) Contribution of transcranial magnetic stimulation to the understanding of cortical mechanisms involved in motor control. J Physiol 586:325–351.

Restani L, Antonucci F, Gianfranceschi L, Rossi C, Rossetto O, Caleo M (2011) Evidence for anterograde transport and transcytosis of botulinum neurotoxin A (BoNT/A). J Neurosci

31:15650–15659.

Restani L, Cerri C, Pietrasanta M, Gianfranceschi L, Maffei L, Caleo M (2009) Functional masking of deprived eye responses by callosal input during ocular dominance plasticity. Neuron 64:707–718.

Rohrer B, Fasoli S, Krebs HI, Hughes R, Volpe B, Frontera WR, Stein J, Hogan N (2002) Movement smoothness changes during stroke recovery.

Rossini PM, Tecchio F, Pizzella V, Lupoi D, Cassetta E, Pasqualetti P, Paqualetti P (2001) Interhemispheric differences of sensory hand areas after monohemispheric stroke: MEG/MRI integrative study. Neuroimage 14:474–485.

Sacrey L-AR, Alaverdashvili M, Whishaw IQ (2009) Similar hand shaping in reaching-for-food (skilled reaching) in rats and humans provides evidence of homology in release, collection, and manipulation movements. Behav Brain Res 204:153–161.

Saletti A, Morghen I, Finessi L, Fainardi E (2011) Angioplasty in acute middle cerebral artery stroke due to atrial fibrillation selected by CT perfusion: a case report. Int J Emerg Med 4:23.

Saver JL (2010) Targeting the Brain: Neuroprotection and Neurorestoration in Ischemic Stroke. Pharmacotherapy 30:62S–69S.

Schaechter JD (2004) Motor rehabilitation and brain plasticity after hemiparetic stroke. Prog Neurobiol 73:61–72.

Schiene K, Bruehl C, Zilles K, Qü M, Hagemann G, Kraemer M, Witte OW (1996) Neuronal hyperexcitability and reduction of GABAA-receptor expression in the surround of cerebral photothrombosis. J Cereb Blood Flow Metab 16:906–914.

Schmid-Elsaesser R, Zausinger S, Hungerhuber E, Baethmann A, Reulen HJ (1998) A critical reevaluation of the intraluminal thread model of focal cerebral ischemia: evidence of inadvertent premature reperfusion and subarachnoid hemorrhage in rats by laser-Doppler flowmetry. Stroke 29:2162–2170.

Schmidt S, Bruehl C, Frahm C, Redecker C, Witte OW (2012) Age dependence of excitatory-inhibitory balance following stroke. Neurobiol Aging 33:1356–1363.

Schroeter M, Jander S, Stoll G (2002) Non-invasive induction of focal cerebral ischemia in mice by photothrombosis of cortical microvessels: Characterization of inflammatory responses. J Neurosci Methods 117:43–49.

Seniow J, Bilik M, Lesniak M, Waldowski K, Iwanski S, Czlonkowska A (2012) Transcranial Magnetic Stimulation Combined With Physiotherapy in Rehabilitation of Poststroke Hemiparesis: A Randomized, Double-Blind, Placebo-Controlled Study. Neurorehabil Neural Repair 26:1072–1079.

Sheorajpanday RVA, Nagels G, Weeren AJTM, van Putten MJAM, De Deyn PP (2011) Quantitative EEG in ischemic stroke: correlation with functional status after 6 months.

Clin Neurophysiol 122:874–883.

Shimizu T (2002) Motor cortical disinhibition in the unaffected hemisphere after unilateral cortical stroke. Brain 125:1896–1907.

Shintani Y, Terao Y, Ohta H (2010) Molecular mechanisms underlying hypothermia-induced neuroprotection. Stroke Res Treat 2011:809874.

Sicuri C, Porcellini G, Merolla G, Merolla G, Rimini T, Beethoven L V (2014) Robotics in shoulder rehabilitation Corresponding author : Muscles Ligaments Tendons J 4:207–213.

Soleman S, Yip PK, Duricki DA, Moon LDF (2012) Delayed treatment with chondroitinase ABC promotes sensorimotor recovery and plasticity after stroke in aged rats. Brain 135:1210–1223.

Spalletti C, Lai S, Mainardi M, Panarese A, Ghionzoli A, Alia C, Gianfranceschi L, Chisari C, Micera S, Caleo M (2014) A robotic system for quantitative assessment and poststroke training of forelimb retraction in mice. Neurorehabil Neural Repair 28:188–196.

Starkey ML, Bleul C, Zörner B, Lindau NT, Mueggler T, Rudin M, Schwab ME (2012) Back seat driving: Hindlimb corticospinal neurons assume forelimb control following ischaemic stroke. Brain 135:3265–3281.

Starkey ML, Schwab ME (2012) Anti-Nogo-A and training: Can one plus one equal three? Exp Neurol 235:53–61.

Steultjens EMJ, Dekker J, Bouter LM, van de Nes JCM, Cup EHC, van den Ende CHM (2003) Occupational therapy for stroke patients: a systematic review. Stroke 34:676–687.

Stewart KC, Cauraugh JH, Summers JJ (2006) Bilateral movement training and stroke rehabilitation: A systematic review and meta-analysis. J Neurol Sci 244:89–95.

Stinear CM, Barber PA, Smale PR, Coxon JP, Fleming MK, Byblow WD (2007) Functional potential in chronic stroke patients depends on corticospinal tract integrity. Brain 130:170–180.

Stroemer RP, Kent TA, Hulsebosch CE (1993) Acute increase in expression of growth associated protein GAP-43 following cortical ischemia in rat. Neurosci Lett 162:51–54.

Stryker MP (2014) A Neural Circuit That Controls Cortical State, Plasticity, and the Gain of Sensory Responses in Mouse. Cold Spring Harb Symp Quant Biol 79:1–9.

Subramanian SK, Yamanaka J, Chilingaryan G, Levin MF (2010) Validity of movement pattern kinematics as measures of arm motor impairment poststroke. Stroke 41:2303–2308.

Takatsuru Y, Fukumoto D, Yoshitomo M, Nemoto T, Tsukada H, Nabekura J (2009) Neuronal circuit remodeling in the contralateral cortical hemisphere during functional recovery from cerebral infarction. J Neurosci 29:10081–10086.

Tatarishvili J, Oki K, Monni E, Koch P, Memanishvili T, Buga A-M, Verma V, Popa-Wagner A, Brüstle O, Lindvall O, Kokaia Z (2014) Human induced pluripotent stem cells improve recovery in stroke-injured aged rats. Restor Neurol Neurosci 32:547–558.

Taub E, Miller NE, Novack TA, Cook EW, Fleming WC, Nepomuceno CS, Connell JS, Crago JE (1993) Technique to improve chronic motor deficit after stroke. Arch Phys Med Rehabil 74:347–354.

Taub E, Uswatte G, Mark VW, Morris DMM (2006) The learned nonuse phenomenon: implications for rehabilitation. Eura Medicophys 42:241–256.

Teasell RW, Foley NC, Bhogal SK, Speechley MR (2003) An evidence-based review of stroke rehabilitation. Top Stroke Rehabil 10:29–58.

Tennant KA, Adkins DL, Donlan NA, Asay AL, Thomas N, Kleim JA, Jones TA (2011) The organization of the forelimb representation of the C57BL/6 mouse motor cortex as defined by intracortical microstimulation and cytoarchitecture. Cereb Cortex 21:865–876.

Theodore WH (2002) Handbook of Transcranial Magnetic Stimulation. Edited by A. Pascual-Leone, N.J. Davey, J. Rothwell, E.M. Wasseran, B.K. Puri, Arnold, London, 2001. pound 110 sterling, ISBN 0340720093. Epilepsy Behav 3:404.

Traversa R, Cicinelli P, Bassi A, Rossini PM, Bernardi G (1997) Mapping of motor cortical reorganization after stroke. A brain stimulation study with focal magnetic pulses. Stroke 28:110–117.

Tzvetanov P, Rousseff RT, Atanassova P (2005) Prognostic value of median and tibial somatosensory evoked potentials in acute stroke. Neurosci Lett 380:99–104.

Vallone F, Lai S, Spalletti C, Panarese A, Alia C, Micera S, Caleo M, Di Garbo A (2016) Post-Stroke Longitudinal Alterations of Inter-Hemispheric Correlation and Hemispheric Dominance in Mouse Pre-Motor Cortex. PLoS One 11:e0146858.

van den Brand R, Heutschi J, Barraud Q, DiGiovanna J, Bartholdi K, Huerlimann M, Friedli L, Vollenweider I, Moraud EM, Duis S, Dominici N, Micera S, Musienko P, Courtine G (2012) Restoring Voluntary Control of Locomotion after Paralyzing Spinal Cord Injury. Science (80-) 336:1182–1185.

van Dokkum L, Hauret I, Mottet D, Froger J, Métrot J, Laffont I (2014) The contribution of kinematics in the assessment of upper limb motor recovery early after stroke. Neurorehabil Neural Repair 28:4–12.

van Meer MPA, van der Marel K, Wang K, Otte WM, El Bouazati S, Roeling TAP, Viergever MA, Berkelbach van der Sprenkel JW, Dijkhuizen RM (2010) Recovery of sensorimotor function after experimental stroke correlates with restoration of resting-state interhemispheric functional connectivity. J Neurosci 30:3964–3972.

Vannini E, Restani L, Pietrasanta M, Panarese A, Mazzoni A, Rossetto O, Middei S, Micera

S, Caleo M (2015) Altered sensory processing and dendritic remodeling in hyperexcitable visual cortical networks. Brain Struct Funct.

Vaynman S, Gomez-Pinilla F (2005) License to run: exercise impacts functional plasticity in the intact and injured central nervous system by using neurotrophins. Neurorehabil Neural Repair 19:283–295.

Volke V, Wegener G, Vasar E (2003) Augmentation of the NO-cGMP cascade induces anxiogenic-like effect in mice. J Physiol Pharmacol 54:653–660.

Volpe BT, Krebs HI, Hogan N, Edelstein OTR L, Diels C, Aisen M (2000) A novel approach to stroke rehabilitation: robot-aided sensorimotor stimulation.

Wahl A-S, Schwab ME (2014) Finding an optimal rehabilitation paradigm after stroke: enhancing fiber growth and training of the brain at the right moment. Front Hum Neurosci 8:381.

Wang T, Cui W, Xie Y, Zhang W, Ding S (2010) Controlling the Volume of the Focal Cerebral Ischemic Lesion through Photothrombosis. Am J Biomed Sci 2:33–42.

Wang Y, Jin K, Greenberg DA (2007) Neurogenesis associated with endothelin-induced cortical infarction in the mouse. Brain Res 1167:118–122.

Ward NS, Brown MM, Thompson a. J, Frackowiak RSJ (2003) Neural correlates of motor recovery after stroke: A longitudinal fMRI study. Brain 126:2476–2496.

Wassermann EM, Samii A, Mercuri B, Ikoma K, Oddo D, Grill SE, Hallett M (1996) Responses to paired transcranial magnetic stimuli in resting, active, and recently activated muscles. Exp Brain Res 109:158–163.

Watson BD, Dietrich WD, Busto R, Wachtel MS, Ginsberg MD (1985) Induction of reproducible brain infarction by photochemically initiated thrombosis. Ann Neurol 17:497–504.

Whishaw IQ, Pellis SM, Gorny BP, Pellis VC (1991) The impairments in reaching and the movements of compensation in rats with motor cortex lesions: an endpoint, videorecording, and movement notation analysis. Behav Brain Res 42:77–91.

Whishaw IQ, Whishaw P, Gorny B (2008) The structure of skilled forelimb reaching in the rat: a movement rating scale. J Vis Exp.

Wiesel TN, Hubel DH (1963) EFFECTS OF VISUAL DEPRIVATION ON MORPHOLOGY AND PHYSIOLOGY OF CELLS IN THE CATS LATERAL GENICULATE BODY. J Neurophysiol 26:978–993.

Wise SP, Boussaoud D, Johnson PB, Caminiti R (1997) Premotor and parietal cortex: corticocortical connectivity and combinatorial computations. Annu Rev Neurosci 20:25–42.

Wittenberg GF (2010) Experience, cortical remapping, and recovery in brain disease. Neurobiol Dis 37:252–258.

Young NA, Vuong J, Flynn C, Teskey GC (2011) Optimal parameters for microstimulation derived forelimb movement thresholds and motor maps in rats and mice. J Neurosci Methods 196:60–69.

Zangwill OL (1947) Psychological aspects of rehabilitation in cases of brain injury. Br J Psychol Gen Sect 37:60–69.

Zappasodi F, Tombini M, Milazzo D, Rossini PM, Tecchio F (2007) Delta dipole density and strength in acute monohemispheric stroke. Neurosci Lett 416:310–314.

Zeiler SR, Gibson EM, Hoesch RE, Li MY, Worley PF, O'Brien RJ, Krakauer JW (2013) Medial premotor cortex shows a reduction in inhibitory markers and mediates recovery in a mouse model of focal stroke. Stroke 44:483–489.

Zeiler SR, Krakauer JW (2013) The interaction between training and plasticity in the poststroke brain. Curr Opin Neurol 26:609–616.

Zemke AC, Heagerty PJ, Lee C, Cramer SC (2003) Motor cortex organization after stroke is related to side of stroke and level of recovery. Stroke 34:e23–e28.

Zhang J, Chopp M (2013) Cell-based therapy for ischemic stroke. Expert Opin Biol Ther 13:1229–1240.

Zhao S, Zhao M, Xiao T, Jolkkonen J, Zhao C (2013) Constraint-induced movement therapy overcomes the intrinsic axonal growth-inhibitory signals in stroke rats. Stroke 44:1698–1705.

Ziemann U, Ishii K, Borgheresi A, Yaseen Z, Battaglia F, Hallett M, Cincotta M, Wassermann EM (1999) Dissociation of the pathways mediating ipsilateral and contralateral motor-evoked potentials in human hand and arm muscles. J Physiol 518:895–906.

Zimerman M, Heise KF, Hoppe J, Cohen LG, Gerloff C, Hummel FC (2012) Modulation of training by single-session transcranial direct current stimulation to the intact motor cortex enhances motor skill acquisition of the paretic hand. Stroke 43:2185–2191.

Acknowledgments

First, a large thanks to Scuola Normale Superiore to give me the possibility to earn the PhD in one of the best Italian University. Thanks to prof. Antonino Cattaneo for the supervision of my work in all these years.

The results obtained in this thesis have been collected at the Neuroscience Institute of the CNR of Pisa. I would like to thank all the people from IN for their help, support and suggestions. Especially, I have to thank my supervisor Matteo Caleo, that always with large kindness and great scientific knowledge, gave me valuable scientific and non-scientific suggestions. A special thanks to old and new Caleo's lab members, for their help and their friendship, particularly to Laura R that coached me a lot of lab and "non-lab" teachings; Cristina, whom divided with me many of the experiments shown in this thesis and with whom I shared joy and sorrow of the research life. Thanks for your help and your kind attentions with me. Stefano, my personal engineer specialist whom saved me in robotic/programming problems, my mentor in Matlab, informatics and mathematical issues. Thanks to Alessandro and people from the group of prof. Silvestro Micera from Scuola Superiore Sant'Anna for the precious collaboration.

Thanks to Federico Cremisi and Marco, for their work with cell differentiation and for the precious flow of ideas. Thank you to Irene for the lively help with the in vivo part of the cell-transplant project.

Thanks to Francesca, for her attention and dedication in the animal care, and for helping me with the animal housing.

Thanks to people I met during my PhD in the lab that made my work more pleasant, sharing funny launch- and coffee-brakes: Laura B, Marta, Gabriele, Eleonora, Viviana, Davide, Michele, Caterina, Giovanna, Sara, Nadia and many others.

Finally I would like to thank all my friends and my family, my parents and particularly Simone with whom I shared my life and I am building my future.